TECHNISCHE UNIVERSITÄT DARMSTADT

Identification of cellular and molecular signals involved in neural retina specification in the developing chick embryo

Vom Fachbereich Biologie der Technischen Universität Darmstadt

zur

Erlangung des akademischen Grades

eines Doctor rerum naturalium

genehmigte Dissertation von

Dipl. - Biologe Nicola Coronato

aus Darmstadt

1. Referent: Prof. Dr. Paul G. Layer

2. Referent: Prof. Dr. Bodo Laube

Tag der Einreichung: 09.11.2016

Tag der mündlichen Prüfung: 20.12.2016

Darmstadt 2017

D 17

Table of contents

List of abbreviations

%	Percentage
(v/v)	Volume for volume
(w/v)	Weight for volume
x g	Gravitational force
°C	Degree Celsius
ActRII	Activin receptor type II
ALK	Activin receptor-like kinase
AMHR	Anti-Müllerian hormone receptor
BCIP	5-Bromo-4-chloro-3-indolyl phosphate
bHLH	Basic helix-loop-helix
BMP	Bone morphogenetic protein
BMPR	Bone morphogenetic protein receptor
BSA	Bovine serum albumin
CA-hSMAD1-EVEMM	Constitutive activated human SMAD1, mutations in MAPK phosphorylation site
ChAT	Choline acetyl-transferase
CHO	Chinese hamster ovary
Chx10	ceh-10 homeodomain-containing homolog homeobox gene; see also *Vsx2*
DAPI	2-(4-Amidinophenyl)-1*H*-indole-6-carboxamidine
DEPC	Diethyl dicarbonate
DIG	Digoxigenin
DMSO	Dimethyl sulfoxide
DNA	Deoxyribonucleic acid
DTT	Dithiothreitol
EDTA	Ethylenediamine-tetraacetic acid
ERK	Extracellular-signal related kinase
FGF	Fibroblast growth factor
FGFR	Fibroblast growth factor receptor
FRS2	Fibroblast growth factor receptor substrate 2
GRB2	Growth factor receptor-bound 2
GFP	Green fluorescent protein
HH	Hamburger & Hamilton stage
h	Hour
IGF	Insulin-like growth factor
ISH	*in situ* hybridization
Islet-1	Insulin gene enhancer protein ISL-1
LB	Luria-Bertani
M	Molar concentration
MAPK / ERK	Mitogen activated protein kinase / extra-cellular-signal related kinase pathway
min	Minute
Mitf	Microphthalmia-associated transcription factor
MEK1/2	Mitogen activated protein kinase kinase
mm	Millimetres
mL	Millilitres

mRNA	Messenger ribonucleic acid
ms	Millisecond
mV	Millivolt
µm	Micrometre
µL	Microlitre
NBA	Nile Blue Sulfate A
NBT	Nitro blue tetrazolium chloride
NR	Neural retina
PBS	Phosphate buffer saline
PCR	Polymerase chain reaction
PFA	Paraformaldehyde
pH	potentia hydrogenii
PLCγ	Phospholipase C γ
pSMAD	Phosphorylated mothers against decapentaplegic homolog protein
RAS	Rat sarcoma
RAF	v-raf-leukemia viral oncogene homologue 1
RNA	Ribonucleic acid
RPE	Retinal pigment epithelium
rpm	Rotations per minute
SHH	Sonic hedgehog
Shp2	SH2 domain-containing tyrosine phosphatase 2
SMAD	Mothers against decapentaplegic homolog protein
SOS	Son of sevenless
Src	Sarcoma proto-oncogene tyrosine kinase
TGF-β	Transforming growth factor-β
TβRII	Transforming growth factor-β receptor type II
UV / VIS	Ultraviolet / visible spectrum
V	Volt
Vsx2	Visual system homeobox gene 2, formerly known as *Chx10*
WNT	Wingless-type family member

Danksagung / Acknowledgement

Ich habe eine sehr schöne und prägende Zeit als Doktorand in der AG Layer verbringen dürfen. Dies lag nicht nur am spannenden Thema meiner Arbeit, sondern auch an den tollen Menschen, die mich während dieser Zeit begleitet haben.

Hierfür möchte ich mich an erster Stelle bei Herrn Prof. Dr. Paul G. Layer bedanken. Lieber Paul, vielen Dank, dass Du in mir die Begeisterung für die Entwicklungsbiologie entfacht hast. Dies war mit Sicherheit der wichtigste Schritt während meiner Studienzeit. Ich möchte Dir auch für das entgegengebrachte Vertrauen, für die immer offenstehende Tür und für die gemeinsamen Diskussionen danken. Zudem möchte ich mich nochmals für die tolle Zeit in den USA und für die Möglichkeit, meine Forschungsdaten dort präsentieren zu dürfen, bedanken. In diesem Zusammenhang vielen Dank auch an Kristiana Layer.

Meine Begeisterung für die Entwicklungsbiologie ist von Frau PD Dr. Astrid Vogel-Höpker weiter gefördert worden. Liebe Astrid, Dir gilt mein besonderer Dank, denn ohne Dich hätte es diese Arbeit in dieser Form nicht gegeben. Ich danke Dir für Dein Vertrauen, für Deine ansteckende Begeisterung für die Wissenschaft und für diese Arbeit (insbesondere in Momenten, in denen es nicht lief). Ich danke Dir für die Freiheit, die ich bei der Planung und Umsetzung der Arbeit genießen durfte. Aber besonders möchte ich mich bei Dir für Dein immer offenes Ohr, das oft keine Uhrzeit kannte, bedanken. Hierfür danke ich auch Deiner Familie für das Verständnis.

Ich möchte mich bei Herrn Prof. Dr. Laube für die Übernahme des Zweitgutachtens bedanken.

Ein ganz großes Dankeschön an Ulrike Hoppe, Jutta Smidek-Huhn, Meike Stotz-Reimers, Michaela Becker-Röck und Wolfgang Schäfer. Vielen Dank für Eure geduldige und freundliche Unterstützung. Ohne Euch wäre einiges im Labor nicht gelaufen!

Ich möchte mich bei Frau Prof. Dr. Ulrike Nuber für die Möglichkeit, meine Arbeit in Ihrer Arbeitsgruppe fertig stellen zu können, bedanken.

Für eine sehr kollegiale und freundschaftliche Zusammenarbeit möchte ich mich bei allen Mitgliedern und ehemaligen Mitgliedern der AG Layer bedanken. Insbesondere danke ich Frau Dr. Gesine Bachmann, Frau und Herrn Dr. Antonia und Dr. Florian Frohns, Frau Dr. Anja Heselich, Frau Johanna Kramer, Frau Dr. Anke König und Frau Dr. Laura Sperling.

Ein ganz besonderer Dank gilt meinen Kollegen und Freunden Frau Meggi-Lee Hampel, Frau Ichie Steinfeld, Herrn Dr. Jörg Steinfeld, Herrn Thomas Mudersbach und Herrn Dr. Gopenath Thangaraj. Danke für die tolle Zeit mit Euch im Labor, sie wird mir in bester Erinnerung bleiben.

Ich möchte auch meinen Freunden Philipp, Sabi, Flo, Simon, Felix, Mini und Philipp danken. Danke für Eure ehrliche Freundschaft, sie ist mir sehr viel wert.
Aus tiefstem Herzen möchte ich jedoch den wichtigsten Personen in meinem Leben danken: meiner Familie. Diese Arbeit ist Euch gewidmet.
Liebe Mama und lieber Papa, ich danke Euch aus tiefstem Herzen für all das was Ihr für uns getan habt. Danke für Eure Liebe, dafür dass Ihr immer an mich glaubt und mir immer eine große Hilfe in allen Belangen des Lebens seid. Ich wäre niemals ohne Euch so weit gekommen. Ihr seid für mich einzigartige Vorbilder!
Ich möchte meinem Bruder Domenico und seiner kleinen Familie danken. Lieber Domenico, Deine Unterstützung und Deine motivierenden Worte haben immer geholfen. Die Zeit mit Dir, Carla und Antonio bringt mich immer wieder zur Ruhe.
Ganz besonders möchte ich jedoch meiner lieben Frau Giovanna danken. Danke für all das, was ich in meinem Leben wirklich brauche: Deine Liebe, Deine Geduld und Dein Vertrauen. Dipinti l'uno per l'altra!

Abstract

The current proximo-distal model of vertebrate eye development proposes that signals released from the distally located surface ectoderm induce neural retina (NR) development, while signals released from the proximally located mesenchyme induce the development of the retinal pigment epithelium (RPE). In this model, fibroblast growth factors (FGFs) released from the overlying surface ectoderm are considered to induce a NR cell fate in optic vesicle cells. However, recent studies implicate bone morphogenetic proteins (BMPs) in NR specification. For example, in conditional BMP receptor I (BMPRI) knockout mice the earliest known retinal progenitor cell marker gene, *Vsx2*, is downregulated, suggesting an involvement of BMP signaling pathway in NR specification. Moreover, BMP4 released from the surface ectoderm appears to induce a NR cell fate in underlying optic vesicle cells in the chick. On the other hand, our recent data show that BMPs and WNTs released from the surface ectoderm pattern the optic vesicle into a dorsal RPE domain. In this thesis I show, that following tissue ablation experiments in the developing chick embryo, the inductive signals, which initiate NR development, are derived from the ventral midline and not as previously assumed from the surface ectoderm. By carrying out loss-of-function and rescue experiments *in vivo*, I show that both the sonic hedgehog (SHH) and BMP signaling pathways are involved in inducing *Vsx2*-expressing retinal progenitor cells. Based on these results and together with our previous study, I propose a new dorso-ventral model of vertebrate eye development. While the dorsal optic vesicle is patterned by BMPs and WNTs into RPE, BMP and SHH signals originating from the ventral midline induce retinal progenitor cells in the ventral part of the optic vesicle. These findings could be of major interest for stem cell research and might help to develop new approaches for stem cell-based retinal tissue generation.

Zusammenfassung

Das aktuelle proximodistale Modell der embryonalen Augenentwicklung bei Vertebraten sieht die Beteiligung unterschiedlicher Gewebearten bei der Musterbildung des optischen Vesikels vor. Hierbei werden vom distal liegenden Oberflächenektoderm Fibroblastenwachstumsfaktoren (FGFs) sezerniert, die für die Bildung der Netzhaut (NR) verantwortlich sind, während Signale aus dem proximal liegenden Mesenchym die Bildung des retinalen Pigmentepithels (RPE) induzieren. Neuere Studien zeigen jedoch, dass auch Knochenwachstumsfaktoren (BMP) an der Entwicklung der Netzhaut beteiligt sind. So werden zum Beispiel in BMP Rezeptor-1 knockout Mäusen keine *Vsx2*-exprimierenden Vorläuferzellen gebildet. Des Weiteren scheint BMP4 aus dem Oberflächenektoderm die Bildung der Netzhaut in den Zellen des optischen Vesikels im Hühnerembryo zu initiieren. Dagegen deuten unsere bereits veröffentlichten Forschungsergebnisse daraufhin, dass BMP und WNT Signale aus dem Oberflächenektoderm das optische Vesikel polarisieren und dorsal RPE induzieren. In dieser Arbeit wird durch die Entfernung unterschiedlicher Gewebearten gezeigt, dass Netzhaut-induzierende Signale nicht wie bisher angenommen vom Oberflächenektoderm, sondern von der ventralen Mittellinie des Vorderhirnbereichs stammen. Weiterhin konnte *in vivo* durch sogenannte „loss-of-function“ und „rescue“ Versuche gezeigt werden, dass sowohl der BMP- als auch der SHH-Signalweg an der Induktion *Vsx2*-exprimierender Vorläuferzellen der Netzhaut beteiligt sind. Basierend auf den Ergebnissen dieser Arbeit und auf den von uns zuvor veröffentlichten Beobachtungen postuliere ich ein neues dorsoventrales Modell für die embryonale Augenentwicklung in Wirbeltieren. Dieses dorsoventrale Modell sieht die Unterteilung des optischen Vesikels in einer dorsalen und ventralen Domäne vor, wobei BMPs und WNTs aus dem Oberflächenektoderm dorsal zur Spezifizierung des RPEs, und ventral SHH und BMPs aus der ventralen Mittellinie zur Spezifizierung der Netzhaut Domäne beitragen. Diese Erkenntnisse könnten für die Stammzellforschung von großem Interesse sein und zur Entwicklung von patientenspezifischem Netzhautgewebe führen.

1 Introduction

The early organogenesis of the vertebrate eye is a spatio-temporally highly coordinated process. Initially an eye field forms in the anterior neural plate, which subsequently becomes split into two molecularly identical eye field regions. Once the neural tube has formed, these regions give rise to the optic vesicles that subsequently will develop into the optic cups. The result of all these developmental processes is the generation of two eyes, consisting of the light sensitive retina in the inner and the retinal pigment epithelium in the outer layer of the optic cup. Environmental and genetic disturbances during early eye development lead to several eye disorders such as cyclopia, anophthalmia, microphthalmia and coloboma. These disorders display malformations of the retina and for this purpose, elucidation of the cellular and molecular interplay involved in retinogenesis may help to develop new approaches in stem cell-based regenerative medicine.

1.1 The eye field is split into two domains

Based on observations of cyclopia in newborns in the late 19th century, it has been proposed that during the initial stages of embryonic development a single eye field is initially specified (reviewed in Chow and Lang, 2001). This long-standing hypothesis of the existence of a single eye field and its separation at the early developmental stages of the embryo has been confirmed in newts, frog and chick embryos (Mangold, 1931; Li et al., 1997; Pera and Kessel, 1997). Indeed, during embryonic development, before any morphological signs of eye development are evident, specific cells in the forebrain region are determined to form the eye primordium (Chow and Lang, 2001). In the chick for example, fate mapping studies during the early neurula stages identified specific cells in the anterior neural plate as the source of eye forming cells (reviewed in Esteve and Bovolenta, 2006). The eye field itself is then split into two regions of cells competent to contribute to eye development, which are arranged on both sides of the midline in all vertebrate species (Chow and Lang, 2001). It has been proposed that a signal from the ventral midline, the prechordal plate, emanates factors that are involved in the splitting of the eye field into two eye field regions. Ablation of the prechordal plate at early neurula stages prevented the splitting of the eye field and led to cyclopia in newts, frog and chick embryos (Mangold, 1931; Li et al., 1997; Pera and Kessel, 1997). A gene expressed in the prechordal plate and the ventral forebrain region prior to eye formation is *Sonic hedgehog* (*Shh*) (Echelard et al., 1993; Ekker et al., 1995; Zhang and Yang, 2001). Indeed, in humans and mice, loss of SHH signaling results in malformations of

brain structures and cyclopia (Belloni et al., 1996; Chiang et al., 1996). Taken together, these studies confirm the existence of one single eye field during embryonic development, which is subsequently split by the influence of midline-derived SHH into two eye field regions.

1.2 The formation of the optic vesicle and optic cup

During the process of neurulation, the neural plate forms the neural tube. The neural tube gives rise at its anterior portion to the three primary brain vesicles, namely the prosencephalon (forebrain), mesencephalon (midbrain) and rhombencephalon (hindbrain). The optic vesicles are the first morphological signs of eye development and are formed through the evagination of the neuroepithelium from the diencephalon (Figure 1 A). The interaction between the neuroepithelium of the optic vesicles with the overlying surface ectoderm induces lens development. Signals released from the distal region of the optic vesicle lead to a thickening of the overlying surface ectoderm, the so-called lens placode (Figure 1 B). The lens placode and the optic vesicle invaginate simultaneously and this coordinated event results in the formation of a lens vesicle and the formation of a bilayered optic cup (Figure 1 C and D). The inner layer of the optic cup is facing the lens vesicle and gives rise to the multilayered neural retina (NR), whereas the outer layer will form the retinal pigment epithelium (RPE). The connection between the optic cup and the diencephalon persists proximally through the optic stalk and projecting axons. Due to the invagination of the optic vesicle and the overlying surface ectoderm, a narrow groove is formed which is called optic or choroid fissure (Figure 1 E). This groove forms a channel for projecting axons and blood vessels, required for nourishing the different eye tissues, and forms during the process of development the optic nerve (reviewed in Chow and Lang, 2001; Adler and Canto-Soler, 2007).

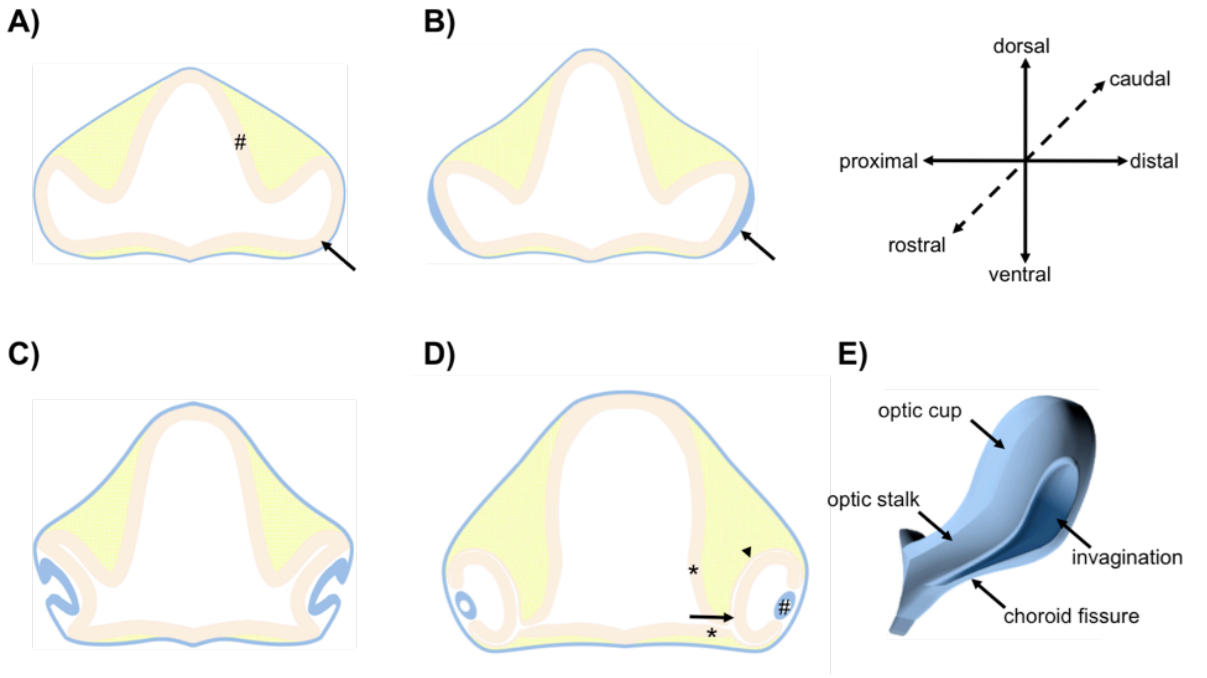

Figure 1: The formation of the optic vesicle and optic cup. **(A)** The optic vesicles (arrow) arise from the outgrowth of the diencephalon (hash key). **(B)** Interactions between the neuroepithelium of the optic vesicle and the surface ectoderm induce a lens placode, a thickening of the surface ectoderm (arrow). **(C)** The lens placode and the optic vesicle invaginates contemporaneously to form an optic cup. During this process, a groove called optic or choroid fissure is formed. The choroid fissure will form the future optic nerve. **(D)** The optic cup consists of an inner and an outer layer, which will form the multilayered neural retina (arrow) and the single-layered retinal pigment epithelium (arrowhead), respectively. The lens vesicle (hash key) detaches from the surface ectoderm and will form the lens. Through the optic stalks (asterisks) the optic vesicles are still connected to the diencephalon **(E)** 3-D view of the optic vesicle during the formation of the choroid fissure. Surface ectoderm and lens vesicle (light blue), mesenchymal cells (yellow), neuroepithelium (light orange).

1.3 Patterning of the optic vesicle in vertebrates

The neuroepithelial cells of the optic vesicles in vertebrates are initially morphologically and molecularly indistinguishable, expressing the same transcription factors which are initially expressed in the single eye field. A polarity of the optic vesicle is established by extrinsic signals released from the surrounding extraocular tissues. These signals pattern the optic vesicle into three distinct domains, namely the RPE domain, the NR domain and the optic stalk/nerve (reviewed in Chow and Lang, 2001; Fuhrmann, 2010; Layer et al., 2010; Venters et al., 2015). Molecularly, the RPE and NR domains differ in the expression of tissue specific genes. The earliest expressed specific genes in neuroepithelial cells of the optic vesicles are the basic helix-loop-helix (bHLH) *microphthalmia-associated transcription factor* (*Mitf*) which is required for specifying an RPE cell fate, whereas the *visual system homeobox 2* gene (*Vsx2*, formerly known as *Chx10*) is restricted to cells that will develop into cells of the NR (Liu et al., 1994, Burmeister et al., 1996; Nguyen and Arnheiter, 2000; Green et al., 2003; Müller et al., 2007). Thus, expression of these two genes patterns the optic vesicle into a NR and an RPE domain during embryonic development in vertebrates (see below).

1.4 The classical proximo-distal model of optic vesicle patterning

1.4.1 The surface ectoderm is involved in NR specification

Since the 1930's the surface ectoderm has been attributed a fundamental role in NR specification (reviewed in Lopashov and Stroeva, 1964; Chow and Lang, 2001). Early insights were provided by explantation studies of the surface ectoderm using optic vesicles of amphibians. Theses optic vesicles arrested their differentiation into a proper optic cup with a normal RPE and NR (Holtfreter, 1939). A further indication of the involvement of the surface ectoderm in specifying the NR was provided by rotation experiments of optic cups in amphibians. When the optic cups were inverted, so that the RPE came into contact with the surface ectoderm, the RPE lost its commitment and developed into a second retina (Dragomirov, 1937; Mikami, 1939). *In vitro* and *in vivo* studies in chick and mouse confirmed an involvement of the surface ectoderm in NR specification (Hyer et al., 1998; Nguyen and Arnheiter, 2000). For example, following ablation of the surface ectoderm, a fully pigmented optic vesicle developed and expression of neuronal markers were only sparsely observed (Hyer et al., 1998; Nguyen and Arnheiter, 2000). Thus, the surface ectoderm appears to release extrinsic factors required for NR specification.

1.4.2 FGF signaling appears to be involved in NR specification

Possible signals that might be involved in inducing a NR cell fate are members of the fibroblast growth factor (FGF) (reviewed in Venters et al., 2015; Fuhrmann, 2010). In vertebrates, 22 members grouped in 7 subfamilies have been identified (reviewed in Dorey and Amaya, 2010). The transduction of the FGF signal occurs mainly by the activation of several pathways such as the MAPK/ERK pathway, which is associated with proliferation and differentiation and seems to be involved in NR specification (Dorey and Amaya, 2010; Fuhrmann, 2010). Following the ligand-dependent dimerization and conformational shift of the transmembrane tyrosine kinase receptors, the intracellular kinase domains of the FGF receptors (FGFR) are activated by phosphorylation of tyrosine residues (Figure 2). These activated residues form a docking site on the receptors for adaptor proteins like PLCγ, FRS2 and Src family members and are necessary for further signal transduction. A key adaptor protein is the FGFR specific FGFR substrate 2 (FRS2). This adaptor protein binds to the juxtamembrane region of the FGFR, where it is phosphorylated by the FGFR on several phosphorylation sites. The activated FRS2 recruits two further adaptor proteins, growth factor receptor-bound 2 (GRB2) and son of sevenless (SOS). This recruitment allows the initiation

of a phosphorylation cascade by activating the kinase RAS and other downstream kinases like RAF, MEK and ERK (reviewed in Turner and Grose, 2010; Dorey and Amaya, 2010).

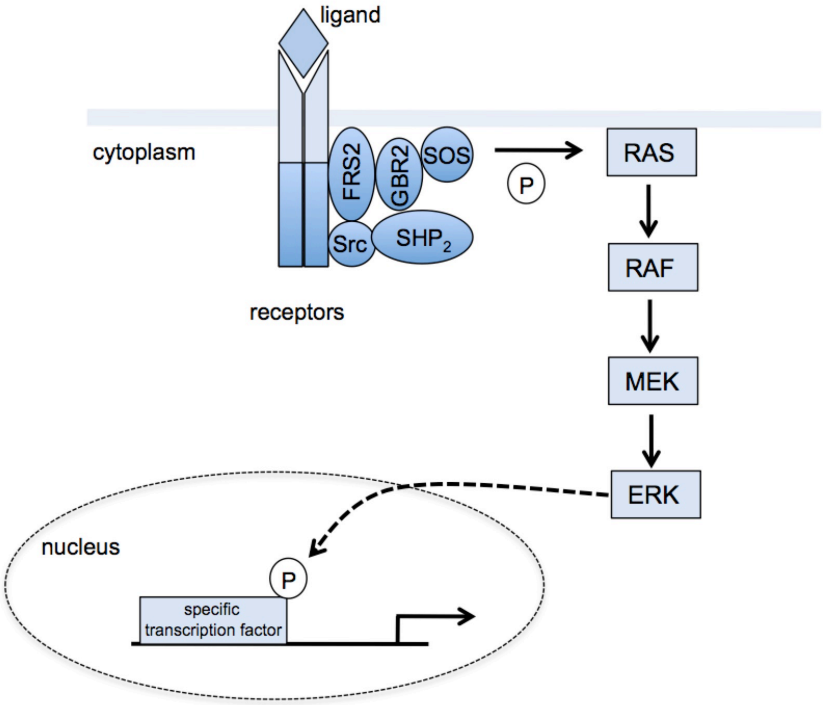

Figure 2: The FGF/MAPK signaling pathway. Binding of FGF ligands to a specific FGFR dimer results in conformational changes within the intracellular domains of the FGFR dimer. Tyrosine residues are phosphorylated and form a docking site for adaptor proteins namely FRS2, GBR2, SOS, Src and SHP_2. These adaptor proteins induce a phosphorylation (P) cascade of several kinases. The activation of ERK, a downstream kinase of the cascade, allows the entering of ERK into the nucleus and the activation of target genes by phosphorylating specific transcription factors (modificated from Dorey and Amaya, 2010).

During vertebrate eye development expression of several FGF ligands and their receptors are detected in both the neuroepithelium of the optic vesicle and the overlying surface ectoderm (Figure 3 A). For instance, in chick and rat FGF1, FGF2 and FGF19 (FGF15 in mice) proteins are present at high levels in the overlying surface ectoderm (de Longh and McAvoy, 1993; Pittack et al., 1997; Kurose et al., 2005). Furthermore, *Fgf8*, *Fgf9* and *Fgf19* (*Fgf15* in mice) transcripts are detected within the optic vesicle and are restricted to the NR domain (McWirther et al., 1997; Reifers et al., 1998; Vogel-Höpker et al., 2000; Kurose et al., 2005). Transcripts of the *Fgfr1*, which is known to bind FGF1 and FGF2 with high affinity, are detected throughout the optic vesicle (Wanaka et al., 1991). At early optic cup stages expression of *Fgfr1* is co-localised with the expression of *Fgfr2* in the NR and RPE (Tcheng et al., 1994a). These observations support the idea that FGF signaling is involved in initiating *Vsx2* expression, thereby inducing a NR cell fate (Wanaka et al., 1991; Tcheng et al., 1994b; Lunn et al., 2007; Furhmann, 2010). In fact, functional studies have shown that FGFs are the prime candidates to be involved in initiating NR development (Fuhrmann, 2010). The

exogenous application of FGF1 or FGF2 soaked beads following retinectomy in chicken optic cups can convert the RPE into NR. These effects are specific for FGFs, as exposure to other growth factors such as transforming growth factors-β (TGF-β) and insulin-like growth factor (IGF) had no effect (Park and Hollenberg, 1989, 1991). The application of FGF1 or FGF2 to chicken optic vesicle or RPE explant cultures have also been shown to induce the expression of neuronal markers (Pittack et al. 1991, 1997; Guillemont and Cepko, 1992; Opas and Dziak, 1994). Studies in both chick and mice suggest that surface ectoderm-derived FGF signaling has an inductive role in NR development. Here, *in vivo* and *in vitro* studies have shown that following ectoderm removal at optic vesicle stage, the application of FGF soaked beads is sufficient to rescue the expression of *Vsx2* and of neuronal markers (Hyer et al., 1998; Nguyen and Arnheiter, 2000). Furthermore, the implantation of FGF8 soaked beads temporal to the chicken optic vesicles or early optic cups induces ectopic NR development. The newly induced NR goes on to differentiate and expresses NR differentiation markers, such as ChAT or Islet-1 normally found in differentiating ganglion and amacrine cells (Vogel-Höpker et al., 2000). Overexpression of downstream effectors of the FGF signaling pathway are also able to induce a NR cell fate during early stages of vertebrate eye development (Fuhrmann, 2010). For example, ectopic overexpression of *Ras* in mice (see Fig. 2) prevents RPE development and instead induces the development of NR (Zhao et al., 2001). Moreover, overexpression of a constitutively active form of MEK (see Fig. 2), another downstream effector of the FGF signaling pathway, leads to a conversion of the RPE into a retina-like epithelium in the chick optic cups (Galy et al., 2002).

In agreement with the above-described observations, loss-of-function studies appear to show that FGF signaling is required for specifying a NR cell fate during early eye development (Fuhrmann, 2010). Addition of FGF2 neutralizing antibodies to chick optic vesicle explant cultures prevents NR development and differentiation (Pittack et al., 1997). Some studies reported, that disturbance of the downstream cascade of the FGF signaling in chicken and mice embryos support the idea of the involvement of the MAPK/ERK pathway in NR specification and differentiation. For instance, VSX2 protein is absent in *Frs2*α mutant mice carrying a point mutation in the binding sites of Shp2, suggesting that a recruitment of Shp2 is necessary to induce NR (Gotoh et al., 2004). Moreover, the conditional inactivation of *Shp2* at optic vesicle stage causes a downregulation of *Vsx2* in the ventral NR and an ectopic expression of *Mitf* within the retinal tissue (Cai et al., 2010). In contrast, overexpression of downstream effectors of FRS2 induces a conversion of the RPE into NR. Taken together, during vertebrate eye development FGFs released from the surface ectoderm appear to play an important role in inducing *Vsx2* expression and hence NR development in the distally located neuroepithelium of the optic vesicle (Figure 3).

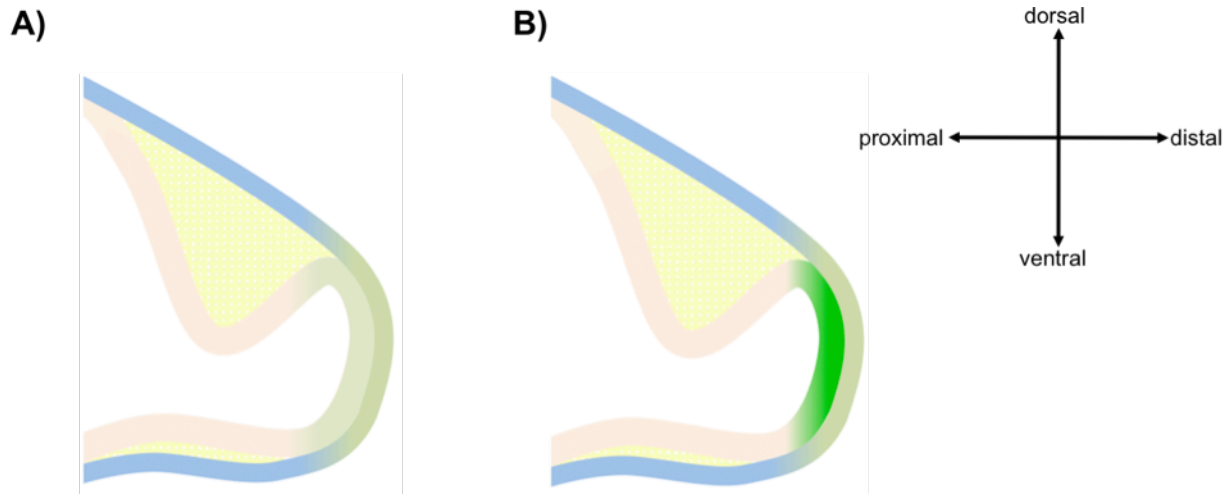

Figure 3: Surface ectoderm-derived FGF ligands are involved in NR specification. (A) FGF ligands and receptors are expressed in the surface ecotderm and in the neuroepithelium of the optic vesicle (light green) at the time when NR is induced. **(B)** The NR-specifying gene *Vsx2* (green) is expressed underneath the FGF expressing surface ectoderm, suggesting that FGF signaling is involved in NR specification. Surface ectoderm (light blue), mesenchymal cells (yellow), neuroepithelium (light orange).

1.4.3 Extraocular tissues appear to be involved in RPE specification

During vertebrate eye development, a signal released from the extraocular mesenchyme appears to be involved in inducing an RPE cell fate (Fuhrmann, 2010). Studies carried out in amphibians showed that RPE differentiation was always associated with the presence of mesenchyme (Lopashov and Stroeva, 1964). For example, in amphibians and sturgeons respecification of the NR into RPE was observed following transplantation of the presumptive retina into the surrounding mesenchyme. The same observation was made in the chick. When the surrounding tissues were removed from the chick optic vesicle and explants were placed in culture, these cells were induced to develop into RPE when co-cultured with mesenchyme (Fuhrmann et al., 2000). In several species, the neuroepithelium of the optic vesicle appears to be initially surrounded by mesenchyme (compare Figure 4 A and C with B and D; reviewed in Fuhrmann, 2010). Consistent with these observations, expression of *Mitf* is initially detected throughout the entire optic vesicle in mice, which is surrounded by mesenchyme (Figure 4 C; Fuhrmann, 2010; Nguyen and Arnheiter, 2000). In the chick, *Mitf* transcripts were first detected in the proximal region of the optic vesicle just adjacent to the extraocular mesenchyme at late optic vesicle stages (Figure 4 D; Mochii et al., 1998; Fuhrmann et al., 2000). Removal of the extraocular mesenchyme caused a downregulation of *Mitf*, whereas expression was still detectable in optic vesicles subjected only to the surface ectoderm ablation (Fuhrmann et al., 2000; Nguyen and Arnheiter, 2000). The observation that the surface ectoderm and the extraocular mesenchyme is involved in the specification of

the NR and RPE, respectively, led to the hypothesis that the vertebrate optic vesicle is patterned along the proximo-distal axis (Figure 4). Signals released from the extraocular mesenchyme are assumed to be responsible for allowing RPE development in the proximally located optic vesicle and optic cup, whereas signals released from the distally located surface ectoderm are thought to induce neural development in the underlying optic vesicle (reviewed in Fuhrmann, 2010).

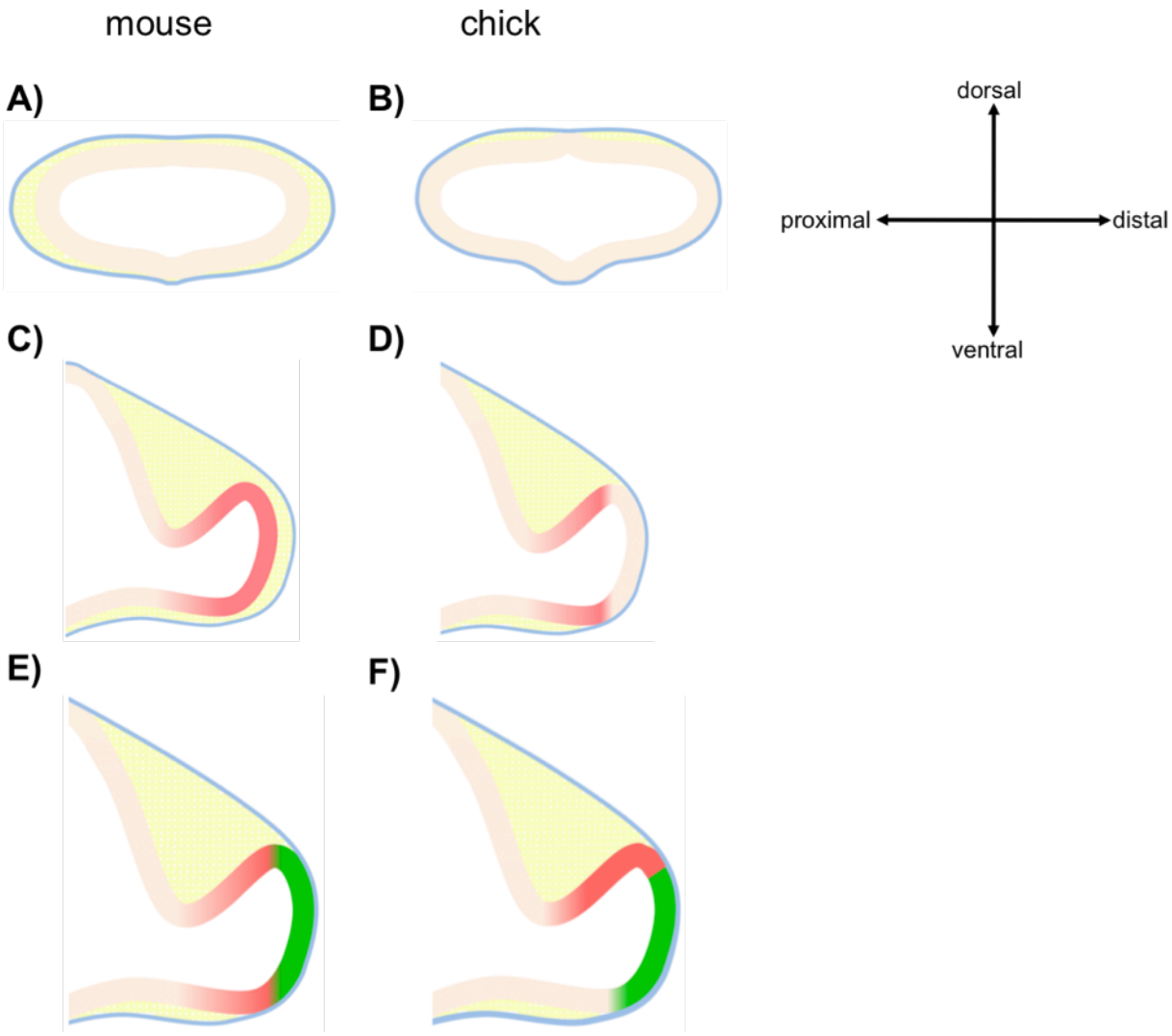

Figure 4: Specification of the RPE in mouse and chick. (A, B) During the outgrow of the optic vesicles, the neuroepithelium (light orange) of mouse embryos is surrounded by mesenchymal cells (yellow, **A**). In contrast to mice, the neuroepithelium of chicken embryos are adjacent to the overlying surface ectoderm (light blue, **B**). **(C, D)** The induction of the RPE-specific transcription factor *Mitf* (light red) occurs in mice throughout the optic vesicle (**C**). In chick, the *Mitf* expression was first detected in the proximal regions of the optic vesicle (**D**). **(E, F)** *Mitf* expression is downregulated following the induction of the NR-specific marker *Vsx2* (green) in the distal and disto-ventral region of the optic vesicle in mice and chick, respectively.

However, we have recently suggested, that the surface ectoderm rather than the extraocular mesenchyme is involved in initiating an RPE cell fate in the vertebrate optic vesicle (Steinfeld et al., 2013). In chick, *Mitf* transcripts and MITF protein are first detected in the distal optic

vesicle underneath the surface ectoderm (Müller et al., 2007; Steinfeld et al., 2013). Removal of the surface ectoderm, before *Mitf* expression and MITF is initiated in the underlying optic vesicle, prevents RPE development *in vivo* (Steinfeld et al., 2013). Furthermore, the lack of MITF is observed although mesenchymal cells are present (Steinfeld et al., 2013). Consistent with this, following *in vivo* transplantation of surface ectoderm-free optic vesicles, pigmentation was not observed in the transplanted optic vesicles (Steinfeld et al., 2013). Thus, the surface ectoderm appears to exert a dual function in initiating both RPE and NR development during optic vesicle patterning (see below).

Mitf expression in the neuroepithelium of the optic vesicle occurs prior to *Vsx2* expression and suggests that an RPE cell fate is first initiated in optic vesicle cells (Chow and Lang, 2001; Fuhrmann, 2010; Steinfeld et al., 2013). In both mice and chick, *Mitf* expression is downregulated in the distal and distoventral part of the optic vesicle (Figure 4 E and F), thereby becoming restricted proximally following the onset of *Vsx2* expression (Bora et al., 1998; Nguyen and Arnheiter, 2000; Müller et al., 2007). In *Vsx2* mutant mice the NR appears to acquire an RPE-like identity, as shown by the initiation of MITF expression in the NR domain (Horsford et al., 2005). Thus, it appears that during vertebrate eye development, initiation of *Mitf* and *Vsx2* expression is essential for establishing an RPE and NR domain in optic vesicle cells (Fuhrmann, 2010).

1.4.4 TGF-β signaling appears to be involved in RPE specification

As described above, initiation of *Mitf* expression in optic vesicle cells requires signals released from extraocular tissues in both chick and mouse (Nguyen and Arnheiter, 2000; Fuhrmann et al., 2000). Several extrinsic factors such as members of the transforming growth factors-β (TGF-β) superfamily, fibroblast growth factors (FGF) and WNTs are expressed in the extraocular tissues at the right time and place to be involved in patterning the optic vesicle into a NR and RPE domain (reviewed in Adler and Canto-Soler, 2007; Fuhrmann, 2010; Layer et al., 2010). The TGF-β superfamily consists of numerous growth factors, which share a highly common and conserved sequence. Based on sequence homology, members of this family have been divided into several subgroups. These subgroups are members of TGF-β family, the bone morphogenetic protein family (BMPs), activins and related proteins (Derynck and Zhang, 2003). TGF-β signaling is classified into two different groups, dependent on which SMAD is phosphorylated by the activated receptor type I (see below Table 1; Herpin and Cunningham, 2007).

Table 1: Combinatorial interaction of receptor type II and type I generate different responses. The combination of different type II and type I receptors causes two distinct responses involving different SMAD proteins. One response is the activation of the intracellular proteins SMAD1, SMAD5 or SMAD8, whereas the other response activates SMAD2 or SMAD3 (from Derynck and Zhang, 2003).

Type II	Type I	SMAD
BMPRII	ALK-2 (ActRI) ALK-3 (BMP-RIA) ALK-6 (BMP-RIB)	SMAD1, SMAD5, SMAD8
ActRII, ActRIIB	ALK-4 (ActRIB)	SMAD2
ActRIIB	ALK-7	SMAD2
TβRII	ALK-5 (TβRI)	SMAD2, SMAD3
TβRII	ALK-1 ALK-2	SMAD1, SMAD5
AMHR	ALK-2 ALK-3 ALK-6	SMAD1, SMAD5

The induction of TGF-β signaling occurs following the binding of homo- or heterodimers of BMP ligand to both type I and type II serine/threonine kinase receptors (Figure 5). In humans seven type I and five type II receptors (Table 1) have been identified. Binding of these ligands to the receptors induces the formation of a heterotetracomplex in which two type II receptors phosphorylate two type I receptors. The activated type I receptors phosphorylate intracellular proteins called SMADs. TGF-β, activins and related proteins activate SMAD2 and SMAD3. Following phosphorylation of SMAD2 or SMAD3 (pSMAD2 or pSMAD3) a complex is formed with SMAD4. This complex translocates into the nucleus to regulate specific gene transcription. In contrast to these proteins, signaling of BMPs induces the phosphorylation of SMAD1, 5 and/or 8 (pSMAD1, 5 and/or 8; Herpin and Cunningham, 2007).

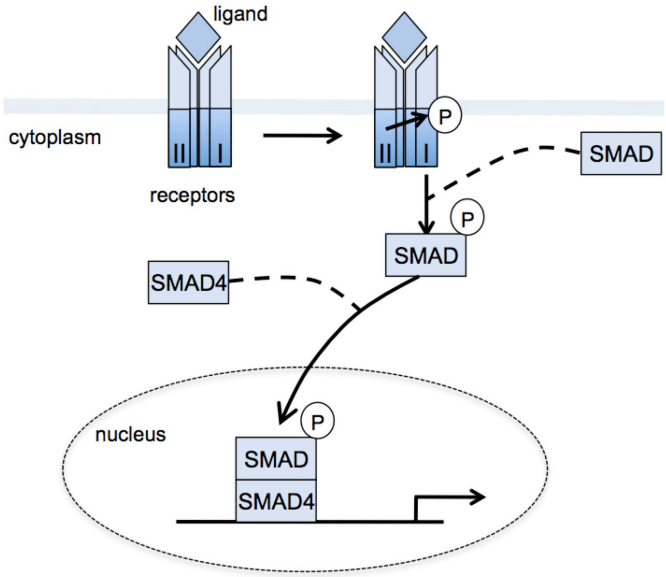

Figure 5: The TGF-β signaling pathway. Following ligand binding at the receptor heterotetracomplex, the receptor type II dimer phosphorylates (P) the receptor type I dimer. Receptor type I in turn phosphorylates the intracellular mediator SMAD. The phosphorylated SMAD forms a complex with SMAD4. The SMAD complex enters the nucleus and regulates the transcription of target genes.

TGF-β family members are good candidates to be involved in inducing an RPE cell fate. For example, activin βA and βB subunits are detected in the extraocular mesenchyme at optic vesicle and cup stages in frog and mouse (Dohrmann et al., 1993; Feijen et al., 1994) and activin receptors type IIA and IIB are expressed in the neuroepithelium of the chick optic vesicles (Stern et al., 1995; Fuhrmann et al., 2000; Hyer et al., 2003). However, although activin A can replace extraocular mesenchyme to induce *Mitf* in chicken optic vesicle explants, neither activin βA nor βB subunits are expressed in the extraocular mesenchyme in chicken (Fuhrmann et al., 2000; Connolly et al., 1995).

Taken together, RPE specification in vertebrates appears to be induced by signaling molecules belonging to the TGF-β superfamily. These signaling molecules may derive from the extraocular mesenchyme in the proximal region of the optic vesicle. The patterning of the optic vesicle in vertebrates into an RPE and a NR domain is summarized as classical or proximo-distal model of eye development (Figure 6).

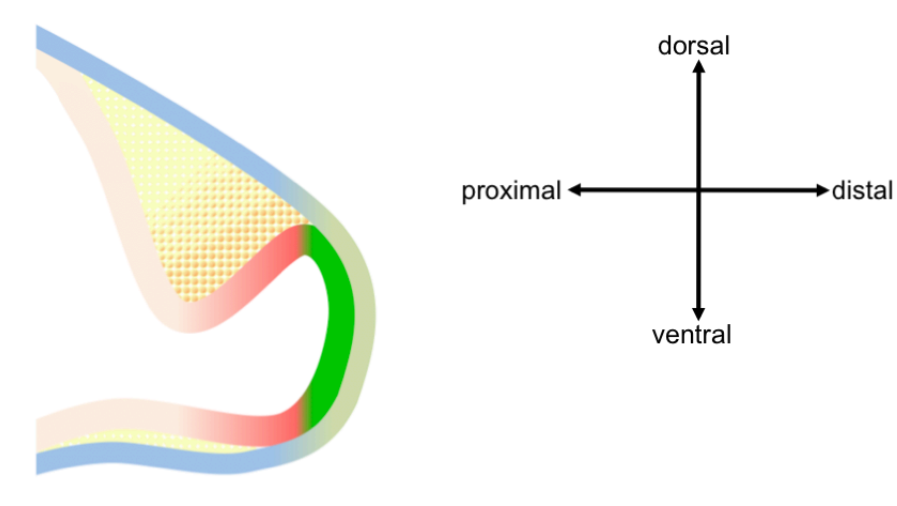

Figure 6: The proximo-distal model of early eye development. Different signaling molecules pattern the optic vesicle along the proximo-distal axis. The overlying surface ectoderm emanates FGF ligands (light green), which induce NR cell fate (green) in the distal portion of the optic vesicle. The mesenchymal cells (yellow dots) overlying the proximal part of the optic vesicle releases signaling molecules (orange dots), which belong to the TGF-β superfamily. These signaling molecules seem to induce RPE cell fate (red) during the evagination of the optic vesicle. Following NR specification, the RPE cell fate is stabilized in the proximal region.

1.5 The dorso-ventral model of the optic vesicle patterning

In contrast to the described proximo-distal model of optic vesicle patterning, transplantation experiments carried out in the chick suggest that the optic vesicle is patterned along the dorso-ventral axis (reviewed in Fuhrmann, 2010; Steinfeld et al., 2013). At Hamburger and Hamilton (HH) stage 10, the chick optic vesicle appears to be divided into a dorsal RPE and ventral NR domain (Uemonsa et al., 2002). When the dorsal optic vesicle is excised and cultured separately only RPE is generated, whereas culturing the ventral half of the optic vesicle gives rise to NR (Kagiyama et al., 2005; Hirashima et al., 2008; Fuhrmann, 2010; Kobayashi et al., 2010). It has been reported in the chick, that both *Mitf* transcripts and MITF protein are detected in the distal part of the optic vesicle at HH9 and HH10, respectively (Müller et al., 2007; Steinfeld et al., 2013). Thus, the detection occurs at the early optic vesicle stage and earlier as reported before (see above). Moreover, both *Mitf* transcripts and protein are initially restricted to the distal part of the chick optic vesicle just underneath the surface ectoderm (Müller et al., 2007; Steinfeld et al., 2013). Furthermore, the initiation of the expression of *Mitf* and the detection of MITF protein occurs at a time when mesenchymal cells are still absent (Müller et al., 2007; Steinfeld et al., 2013). Once *Vsx2* expression is initiated in the disto-ventral portion of the optic vesicle, localization of *Mitf* transcripts and MITF protein shifts to the dorsal part of the optic vesicle (Müller et al., 2007; Steinfeld et al., 2013). The removal of the surface ectoderm before the *Mitf* expression is initiated leads to

the absence of the MITF protein *in vivo*. Furthermore, the lack of MITF is observed despite the presence of mesenchymal cells (Steinfeld et al., 2013). This suggests that a signal released from the surface ectoderm is required for RPE specification in the chick. In both mouse and chick, *Bmp4* and *Bmp7* transcripts are expressed throughout the surface ectoderm at the time RPE cell fate specification occurs (Furuta et al., 1997; Furuta and Hogan, 1998; Croosley et al., 2001; Müller et al., 2007). Moreover, the intracellular proteins pSMAD1/5/8 are detected in the optic vesicle and co-localise with MITF protein (Steinfeld et al., 2013). Application of BMP5 soaked beads induces ectopic *Mitf* expression in the neural retina domain (Müller et al., 2007). Accordingly, inhibition of the BMP signaling pathway using either Noggin soaked beads, *noggin*-expressing Chinese hamster ovary (CHO) cells or viral overexpression of dominant-negative BMP receptor (BMPR) causes a downregulation of *Mitf* transcripts and loss of MITF protein and pigmentation (Müller et al., 2007; Steinfeld et al., 2013). Moreover, following removal of the surface ectoderm, application of BMP7 beads rescues RPE cell fate specification as shown by the presence of MITF protein in distal optic vesicle cells (Steinfeld et al., 2013). These results suggest that the BMP signaling appears to drive RPE cell fate decision.

Interestingly, although the localization of MITF protein shifts to the dorsal portion of the optic vesicle, *Bmp* transcripts are still detected throughout the surface ectoderm at this stage (Müller et al., 2007; Steinfeld et al., 2013). This suggests that an additional signal might be involved in restricting RPE development dorsally. Indeed, in the chick embryo, *Wnt2b* transcripts were detected in the dorsal surface ectoderm and in the dorsal portion of the optic vesicle during early stages of eye development (Jasoni et al., 1999; Fuhrmann et al. 2000; Müller et al., 2007; Steinfeld et al., 2013) and the combination of loss- and gain-of-function studies showed that surface ectoderm-derived BMP and WNT signaling act together to stabilize MITF at optic vesicle stages in the chick (Steinfeld et al., 2013). Taken together, surface ectoderm-derived signals appear to initiate both RPE and NR development during optic vesicle patterning in the chick (Figure 7; Layer et al., 2010).

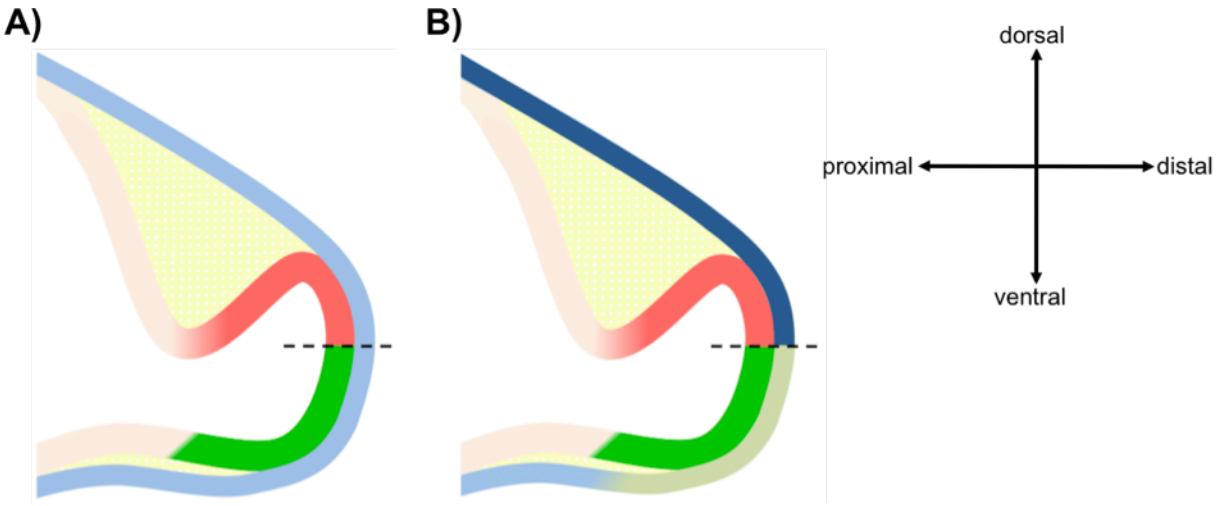

Figure 7: The dorso-ventral model of early eye development in vertebrates. (A) A dorso-ventral boundary within the optic vesicle is established by the expression of *Mitf* (red) and *Vsx2* (green) in the dorsal and ventral part, respectively (dashed line). **(B)** The induction of both transcription factors is surface ectoderm-dependent. BMP ligands are detected throughout the surface ectoderm (light blue, see **A**). The dorsal part of the surface ectoderm additionally releases WNT ligands (dark blue), which act together with the BMPs to restrict *Mitf* expression in the dorsal optic vesicle. The disto-ventral surface ectoderm releases FGF ligands (light green), which appear to be involved in specifying *Vsx2*-expressing retinal progenitor cells ventrally.

1.6 Controversies of NR specification

Although surface ectoderm-derived FGFs currently appear to be prime candidates to be involved in NR specification, there are several studies challenging this model. For instance, it has been shown that neither *Fgf1* and *Fgf2* knockout mice nor *Fgf1* and *Fgf2* double knockouts display evident eye defects (Dono et al., 1998; Ortega et al., 1998; Miller et al., 2000). Several observations suggest that BMP signaling pathway might also play a role in NR specification (reviewed by Fuhrmann, 2010; Layer et al., 2010). At the time of NR specification BMP family members and their receptors are expressed at the right time and place to initiate *Vsx2* expression. For example, in both chick and mouse, transcripts of the *BmpRIA* are detected throughout the surface ectoderm and in the presumptive NR (Zou et al., 1997; Furuta and Hogan, 1998; Hyer et al., 2003; Lim et al., 2005). Consistent with this, in *BmpRIA* and *IB* double knockout mice *Vsx2* expression is downregulated or lost, suggesting that BMPs indeed play a role in NR specification (Murali et al., 2005). Interestingly, rat optic vesicle explants cultured in the presence of a BMP7 blocking antibody seem to block NR development (Solursh et al., 1996). Moreover, *Bmp7* knockout mice exhibit severe eye malformations such as microphthalmia, including a fully pigmented optic vesicle (Morcillo et al., 2006). A more recent study suggests, that surface ectoderm-derived BMP4 is necessary to induce NR development in chicken optic vesicle explants (Pandit et al., 2015). According to this, conditional deletion of *Bmp4* in mice seems to have an effect on NR development (Huang et al., 2015b).

1.7 Aims

BMP signaling is emerging as a potential NR inducing pathway. However, the efforts made so far have not yet clarified the exact cellular and molecular mechanisms involved in NR specification. For this purpose, this thesis aims to identify the tissue and signals involved in NR specification. Here, expression studies in combination with gain- and loss-of-function studies in the chick embryos were carried out to elucidate:

a) the signaling molecule(s) and possible downstream target(s) involved in NR induction,
b) whether these signals are surface ectoderm-derived,
c) whether the identified signaling molecules act in concert to induce a NR cell fate. Combinatorial gain- and loss-of-function experiments may elucidate which downstream target(s) is/are involved in NR specification.

Possible findings may extend the current model of NR development. Furthermore, these findings could be extended on and be of major importance for stem cell-based and regenerative research.

2 Materials

2.1 Chemicals

Chemical	Supplier
2-(4-Amidinophenyl)-1*H*-indole-6-carboxamidine (DAPI)	PANA Tecs, Heilbronn, Germany
2-Amino-2-(hydroxymethyl)propane-1,3-diol (Tris)	Roth, Karlsruhe, Germany
5-Bromo-4-chloro-3-indolyl phosphate (BCIP)	Sigma-Aldrich, St. Louis, MO, USA
Agar	Roth, Karlsruhe, Germany
Agarose	PeqLab, Erlangen, Germany
Blocking reagent	Roche, Risch, CH
Bovine serum albumin (BSA)	Sigma-Aldrich, St. Louis, MO, USA
D (+) Sucrose	Merck, Darmstadt, Germany
Diethyl dicarbonate (DEPC)	Roth, Karlsruhe, Germany
Dimethyl sulfoxide (DMSO)	Roth, Karlsruhe, Germany
di-Sodium hydrogen phosphate dihydrate	Merck, Darmstadt, Germany
Dextran sulfate sodium salt	Roth, Karlsruhe, Germany
Ethanol	Merck, Darmstadt, Germany
Ethylenediaminetetraacetic acid (EDTA)	AppliChem, Darmstadt, Germany
Fastgreen FCF	Merck, Darmstadt, Germany
Ficoll 400	Roth, Karlsruhe, Germany
Formamide deionized	AppliChem, Darmstadt, Germany
Heat inactivated chicken serum	Gibco, Eggenstein, Germany
Hydrogen chloride	Merck, Darmstadt, Germany
Kaiser's glycerine gelatine	Merck, Darmstadt, Germany
Levamisole	Sigma-Aldrich, St. Louis, MO, USA
Lithium chloride	Roth, Karlsruhe, Germany
Loading buffer	New England BioLabs, Ipswich, MA, USA
Maleic acid	AppliChem, Darmstadt, Germany
Monosodium Phosphate (Monohydrate)	Merck, Darmstadt, Germany
Nile Blue Sulfate A (NBA)	Sigma-Aldrich, St. Louis, MO, USA
Nitro blue tetrazolium chloride (NBT)	Sigma-Aldrich, St. Louis, MO, USA
Paraformaldehyde (PFA)	Merck, Darmstadt, Germany
Potassium chloride	Merck, Darmstadt, Germany
Potassium phosphate	Merck, Darmstadt, Germany
Propan-2-ol	Merck, Darmstadt, Germany
Polyvinylpyrrolidone	Sigma-Aldrich, St. Louis, MO, USA
Roti-Phenol/Chloroform/Isoamyl alcohol	Roth, Karlsruhe, Germany
Roti-Safe GelStain	Roth, Karlsruhe, Germany
Sodium acetate	Merck, Darmstadt, Germany
Sodium chloride	Roth, Karlsruhe, Germany
Sodium hydrogen phosphate dihydrate	Merck, Darmstadt, Germany
Sodium hydroxide	Merck, Darmstadt, Germany
Trichloromethane	Roth, Karlsruhe, Germany

Trisodium citrate	AppliChem, Darmstadt, Germany
Triton X-100	Merck, Darmstadt, Germany
Tween-20	Roth, Karlsruhe, Germany
Tryptone	AppliChem, Darmstadt, Germany
Yeast extract	Roth, Karlsruhe, Germany

2.2 General solutions

Solution	Composition
DEPC-water	1 mL DEPC
	999 mL distilled water
Ink solution	10 drops of ink A17 into 10 mL 1x PBS
5x MABT (1000 mL)	58g Maleic acid
	43,75 g Sodium chloride
	Adjust pH to 7,5 with Sodium hydroxide
	Add DEPC-water
	1 mL Tween
10x PBS (1000 mL)	80g Sodium chloride
	2g Potassium chloride
	11,5g Sodium hydrogen phosphate dihydrate
	2g Potassium dihydrogen phosphate
	Adjust pH to 7,3 with Sodium hydroxide
TBSA (50 mL)	2,5g Bovine serum albumin
	500 µL Triton X-100
	Add with 1xPBS

2.3 Solutions for *in situ* hybridization

Solution	Composition
20x SCC (1000 mL; pH=7,0)	175,32g Sodium chloride
	88,23g Trisodium citrate
	Adjust pH to 7,0 with Sodium hydroxide
	Add DEPC-water
0,5M EDTA (1000 mL; pH=8,0)	186,12g
	23,37g Sodium hydroxide
	Add DEPC-water
10x Salt	15,3g Tris
	108,5g Sodium chloride
	13,8g Monosodium phosphate (monohydrate)
	10 mL 0,5M EDTA solution
50x Denhardt's (100 mL)	1g Bovine serum albumin
	1g Ficoll
	1g Polyvinylpyrrolidone
	Add DEPC-water
Dextran sulfate 50% (w/v)	5g in 5 mL DEPC-water

Hybridisation buffer (10 mL)	1 mL 10x Salt
	5 mL deionized Formamide
	2 mL 50% (w/v) Dextran sulfate
	1 mL yeast RNA (10 mg/mL)
	100 µL 50% Denhardt's
	900 µL DEPC-water
Washing solution (300 mL)	15 mL 20x SSC
	150 mL Formamide
	300 µL Tween-20
	135 mL DEPC-water
Alkaline phosphatase buffer (100 mL)	1,211g Tris
	1,016g Magnesium chloride
	0,5844g Sodium chloride
	100 µL Tween-20
	24mg Levamisole
	Add DEPC-water

2.4 Nutritional medium for bacteria

Medium	Composition
Luria-Bertani-medium	10g Tryptone
	5g yeast extract
	10g Sodium chloride
	Adjust pH to 7,5 with Sodium hydroxide
	Add distilled water

2.5 Enzymes, enzyme buffers and polymerase

Restriction enzyme and buffer	XbaI	Pharmacia, Uppsala, Sweden
	All-in-one buffer	Pharmacia, Uppsala, Sweden
	NcoI	New England BioLabs, Ipswich, MA, USA
	NEBuffer 3.1	New England BioLabs, Ipswich, MA, USA
***in vitro* transcription**	5x transcription buffer	Promega, Fitchburg, WI, USA
	DIG-RNA labelling mix	Promega, Fitchburg, WI, USA
	DNaseI, RNase-free (RQ1)	Promega, Fitchburg, WI, USA
	Dithiothreitol (DTT)	Promega, Fitchburg, WI, USA
	RNase inhibitor (RNasin)	Promega, Fitchburg, WI, USA
	RNA polymerase T3	Promega, Fitchburg, WI, USA

2.6 Primary antibodies

Antibody	Catalogue number	Host	Dilution	Supplier
anti-CHX10/VSX2	PA1-12566	Sheep	1:200	Thermo Fisher Scientific, Waltham, USA
Anti-DIG-AP-Fab fragment	11093274910	Sheep	1:3000	Roche, Risch, CH
anti-MITF	AV32329	Rabbit	1:1000	Sigma-Aldrich, St. Louis, MO, USA
anti-SMAD1/5/8	9511	Rabbit	1:500	Cell Signaling, Cambridge, UK

2.7 Secondary antibodies

Conjugation	Reactivity	Dilution	Supplier
Alexa488	Donkey anti rabbit	1:100	Dianova, Hamburg, Germany
Alexa488	Goat anti rabbit	1:100	Dianova, Hamburg, Germany
Cy3	Donkey anti sheep	1:100	Dianova, Hamburg, Germany

2.8 Plasmid DNA and Kit

Gene	Vector backbone and Properties	Supplier
Chx10/Vsx2	pBluescript KS Linearization NcoI or XbaI Antisense mRNA T3	Prof. Dr. Dorothea Schulte, Johann Wolfgang Goethe University, Frankfurt am Main, Germany
CA-hSMAD1-EVEMM	pCS2 Mutations resulting in a constitutive activated form (EVE term): S463E, S465E; mutations in the linker region avoid MAPK-mediated phosphorylation (MM term): S214A, S206A, S195A, S187A	Edward De Robertis (Addgene plasmid # 22994)
GFP	EGFP-N1	Clontech, Takara Bio Europe, Saint-Germain-en-Laye, France
Maxiprep	Qiagen Plasmid purification kit	Qiagen, Hilden, Germany

2.9 Instruments

Instrument	Type	Supplier
Binocular	Stemi 2000C	Carl Zeiss, Jena, Germany
Centrifuges	C-1200	Labnet, Edison, NJ, USA
	Z 233 MK-2	Hermle Labortechnik GmbH, Wehingen, Germany
	5810R	Eppendorf AG, Hamburg, Germany
Cameras	Nikon DS-Fi 1	Nikon, Tokyo; Japan
	Nikon SMZ 1500	Nikon, Tokyo, Japan
	Canon Powershot A640	Canon, Tokyo, Japan
Cryostat	Microm HM550	Microm, Walldorf, Germany
Egg incubator	BSS300	Ehret, Emmendingen, Germany
Electrophoresis	----	PeqLab, Erlangen, Germany
Electroporator and equipment	TSS20	Intracel, St Ives, UK
Freezers	ProfiLine	Liebherr, Ochsenhausen, Germany
Fume hood	2-453-DAHD	Köttermann, Uetze-Hänigsen
Gel documentation	Quantum ST4	PeqLab, Erlangen, Germany
Heat block	----	Bioblock Scientific Thernolyne corp., USA
Hot plate	Präzitherm 28-1	Störk-Tronic, Stuttgart, Germany
ISH incubator	Kelvitron T	Heraeus, Haunau, Germany
Magnetic stirring plate	IKA-Combimag RET	Janke &Kunkel, Staufen, Germany
Microscopes	Axiophot X10 Observer D1	Carl Zeiss, Jena, Germany
	Axiovert S100	Carl Zeiss, Jena, Germany
	Nikon H550L	Nikon, Tokyo, Japan
	Olympus SC35	Olympus, Hamburg, Germany
Microscope camera controller	Digital Sight DS-U2	Nikon, Tokyo, Germany
Microwave oven	MWG765	Clatronic, Kempen, Germany
Multizoom	AZ 100M	Nikon, Tokyo, Japan
NanoDrop	ND-1000	PeqLab, Erlangen, Germany
pH-meter	pH 523	WTW, Weilheim, Germany
Pipette	Pipetman	Gilson, Villiers le Bel, France
Refrigerator	ProfiLine	Liebherr, Ochsenhausen, Germany
Scales	MC1 Laboratory LC 620S	Sartorius, Göttingen, Germany
Thermocycler	PeqStar 2X Gradient	PeqLab, Erlangen, Germany
VisiLED controller	MC1500	Lighting and Imaging Schott, Mainz, Germany
Vortexer	Top-Mix 94323	Heidolph, Schwabach, Germany
QuantumCapt	Quantum ST4	PeqLab, Erlangen, Germany

2.10 Consumables

Consumables	Supplier
Affi-Gel agarose beads	BioRad, München, Germany
AG 1-X2 resin beads	BioRad, München, Germany
Cover glass 24x60 mm	Roth, Karlsruhe, Germany
CryoPure tube red	Sarstedt, Nümbrecht, Germany
Egg	LSL, Dieburg, Germany
Eppendorf tube 1,5 mL and 2,0 mL	Sarstedt, Nümbrecht, Germany
Falcon tubes 15 mL and 50 mL	Sarstedt, Nümbrecht, Germany
FSC 22 blue	Leica-Microsystems, Wetzlar, Germany
Injection needle Sterican 1,2x40 mm and 0,6x25 mm	Braun, Melsungen, Germany
Ink A17	Pelikan, Hannover, Germany
Liquid blocker Super PAP-Pen	Thermo Fisher Scientific, Waltham, MA, USA
Parafilm	NeoLab, Heidelberg, Germany
PCR tubes	Sarstedt, Nümbrecht, Germany
Petri dishes 35x10 mm and 60x15 mm	Sarstedt, Nümbrecht, Germany
Pipette tip	Greiner, Frickenhausen, Germany
Syringe 5 mL and 10 mL	Braun, Melsungen, Germany
Slide glass Superfrost Plus 25x75x1,0 mm	Menzel, Braunschweig, Germany
Scotch tape	Tesa, Hamburg, Germany

3 Methods

3.1 Developmental biology methods

3.1.1 Incubation and windowing of the chicken eggs

For all experiments, chicken embryos (*Gallus gallus*, Linnaeus, 1758) were used for experimental manipulations due to the rapid extracorporeal development and accessibility at specific developmental stages. Fertilized chicken eggs were purchased from the company LSL Rhein-Main (Dieburg, Germany). The eggs were stored at +14°C until their utilisation and for a maximum time of two weeks. The incubation occurred for all experiments at +38°C, 60% humidity and for two days (E2). At E2, the eggs were sterilized using 70% ethanol and finally windowed for the following stage determination according to Hamburger and Hamilton (Hamburger and Hamilton, 1951). To avoid to damage the embryo that is floating immediately under the shell, a 10 mL syringe equipped with a 1,2 x 40 mm needle was inserted at the blunt end of the egg and 3 mL of the watery albumen were removed. Hereby, the embryo was lowered and a little hole was made on the top of the egg to cut with a pair of scissors a window into the shell. To enhance the contrast between the white embryo and the underlying yolk, ink diluted 1:10 in 1xPBS/Diethylpyrocarbonat (DEPC)-water was injected with a 5 mL syringe equipped with a 0,6 x 25 mm needle under the embryo. Thus, the vitelline membrane was punctured at the margin of the area opaca and the needle was carefully moved underneath the embryo in order to inject a small quantity of diluted ink. The obtained contrast allows a precise stage determination according to Hamburger and Hamilton (1951).

3.2 Bead preparation

Two different types of beads were used for the experiments. The application of BMP7 protein occurred with agarose beads, whereas for chemicals resin beads were used. The agarose beads were placed in a petri dish and washed two times with 100 µL 1xPBS for 10 minutes (min). In a second petri dish 10 drops of each 10 µL 1xPBS were arranged in a circle, where afterwards a 2-3 µL protein drop was placed in the centre. After the second washing step, the beads were picked up with a pair of tweezers and transferred into the protein drop. It should be noted, that no 1xPBS was transferred into the protein drop to avoid a further dilution. The beads were soaked in protein solution for at least one hour at room temperature. The resin beads were stained before being used with 0,02% Fast Green FCF in

DEPC-water solution over night. At the next day, the beads were washed twice for 10 min at room temperature with 100 µL dimethyl sulfoxide (DMSO) and added in a second petri dish to 2-3 µL of the designated chemical. As with 1xPBS/DEPC-water, no DMSO was transferred into the chemical drop to avoid a further dilution. The beads were soaked in chemical solution for at least one hour at room temperature and, due to the light sensitivity, in a light-tight box. The chemicals used are listed in table 2:

Table 2: Solutions used for *in vivo* manipulations. The chemical or protein solution used for *in ovo* manipulation, were incubated at least for one hour with appropriate beads.

Chemicals	Bead	Used concentration	Supplier
Recombinant human BMP7	Affi-Gel agarose	1 µg/µL	Peprotech Germany, Hamburg
Cyclopamine	AG® 1-X2	1 µg/µL	Merck Millipore, Darmstadt
FR180204	AG® 1-X2	1 µg/µL	Tocris Germany, Wiesbaden-Nordenstadt
LDN-193189	AG® 1-X2	1 µg/µL	Stegment, Lexington, USA
SB505124	AG® 1-X2	1 µg/µL	Tocris Germany, Wiesbaden-Nordenstadt
U0126	AG® 1-X2	1 µg/µL	Promega, Fitchburg, WI, USA

3.3 Manipulation

3.3.1 Bead implantation

The embryonic (vitelline) membranes were removed after stage determination by a sharpened tungsten needle. A little incision was carefully made in the dorsal midline of the midbrain. A bead soaked in the desired solution was picked up with a pair of tweezers and put onto the incision made before. Through the incision the prepared bead was inserted and positioned either in the optic vesicle and/or in the ventral midline. The implantation occurred at HH10. The eggs were sealed and incubated again at +38°C, 60% humidity up to further three days. The manipulation occurred using a binocular and the resulting manipulations were documented photographically using Nikon DS-Fi-1 and processed with the software NIS-Elements D 3.1.

As control experiments beads soaked in DMSO and/or 1xPBS were implanted in the optic vesicles and analyzed at appropriate HH stadium (see Figure S1 Steinfeld et al., 2013 attached in appendix). No changes in gene expression pattern were observed (compare with Müller et al., 2007).

3.3.2 Ectoderm removal

Fine glass needles were prepared using a Bunsen burner to get a blunt end. Afterwards, Nile Blue sulfate A (NBA) was dissolved in 2% agarose/distilled water, to obtain a final NBA concentration of 2%. The needles were dipped into 2% NBA/agarose until the blunt edges of the needles were completely covered with it and left to dry at room temperature (Geetha-Loganathan et al., 2010). After the removal of the vitelline membranes, the prepared needles were put on the optic vesicle and wiped from the facing, dorsal part of the optic vesicle to the ventral part until the ectoderm was completely removed. Finally, all the ectodermal residues were rinsed using one drop of 1xPBS on the operated optic vesicle. As for the bead implantation, the removals of the ectoderm were photographically documented. The eggs were sealed and incubated again at +38°C, 60% humidity over night until HH15-16. The ectoderm removal occurred at HH10.

3.3.3 Removal of the ventral midline

The access to the ventral midline was obtained by a small incision in the dorsal midline of the midbrain. The divided parts were moved apart carefully. The facing ventral midline was removed using a sharpened tungsten needle. Thus, the tungsten needle was punctured close to the ventral midline, which appeared white, and moved slowly and several times from caudal to rostral and vice versa. The same was repeated on the opposite site of the ventral midline. Finally, the two incisions made vertically were connected by a most caudal and a most rostral horizontal incision, which allowed the removing of the midline tissue. After the removal of the ventral midline, the divided dorsal parts of the midbrain were reassembled. As for the bead implantation, the removals of the ventral midline were photographically documented. The eggs were sealed and incubated again at +38°C, 60% humidity over night until HH15-16. The removal of the ventral midline occurred at HH10.

3.3.4 *in ovo* electroporation

A gene misexpression was obtained through the incorporation of expression constructs into the optic vesicles by *in ovo* electroporation. For this, several glass needles were prepared. A glass needle was heated up using a Bunsen burner and pulled apart to get a fine capillary. The end was cut with a pair of scissors to ensure that the capillary was able to absorb the

electroporating solution. The solution consisted of the expression construct mixed with a GFP-expressing construct and, to enhance the visibility of the solution in the embryo, 1-2 µL of 0,02% Fastgreen. The capillary was attached to a hose, which was used to inject the solution through a little incision in the dorsal part of the forebrain. For each embryo, approximately 2 µL of the electroporating solution was injected into the lumen of the left optic vesicle. Afterwards, the anode (platinum) was positioned close to the manipulating optic vesicle, whereas the cathode was inserted carefully into the lumen of the midbrain. By means of the electroporator 2-4 pulses with 7V, a width of 30ms and a space of 970ms were applied. The negatively charged DNA moved towards the anode. Finally, a drop of 1xPBS was released on the treated optic vesicle. The electorporated optic vesicles were staged at HH10. After the electroporation, the eggs were sealed and incubated for 24 hours at +38°C and 60% humidity. The constructs used and the properties are listed and described in chapter 2.8.

3.4 Fixation and photographical documentation of the embryos

Manipulated and non-treated embryos, used as wild type, were fixed at the desired HH stages using 4-8% PFA/PBS. The embryos were cut out of the eggs using tungsten needles and transferred into a petri dish (35 mm) filled with 1xPBS/DEPC-water, to remove yolk and amniotic residues. Following this washing step, the embryos were incubated for two to 24 hours in 4-8%PFA/PBS at +4°C. At the next day, the embryos were cryoprotected by transferring them into 10% sucrose/DEPC-water solution over night at +4°C. The concentration of the solution was increased in the following two days up to 30%, by 10% each night. To document photographically the morphology in wild types and possible morphological alterations in the manipulated embryos, black 2% (w/v) agarose/DEPC-water petri dishes were prepared. To achieve this, agarose was solved and heated in DEPC-water in order to obtain a 2% final concentration. To enhance the contrast of the embryo, four drops of ink were added to the warm and liquid agarose solution and mixed until the solution turned completely black. The warm solution was poured into petri dishes, in which the agarose hardened. The photographical documentation occurred with Nikon DS-Fi-1 before and after the heads of the embryos were removed and prepared for sectioning.

3.5 Cryosectioning of treated and non-treated heads of chicken embryos

After the photographical documentation, the heads of the embryos were transferred from the 30% sucrose/DEPC-water solution into a silicon form filled with FSC22® blue. The heads were positioned to obtain coronal sections (from nasal to temporal). The heads were frozen up at -20°C for 30 min. By means of the cryostat, the head was consecutively sectioned in 10-14 µm thick sections. Following a predefined order, each section was in turn recorded on four different Superfrost Ultra Plus® glasses (Figure 8). The sections were used to assay *in situ* hybridisation and immunostaining and were stored until their utilisation at -20°C.

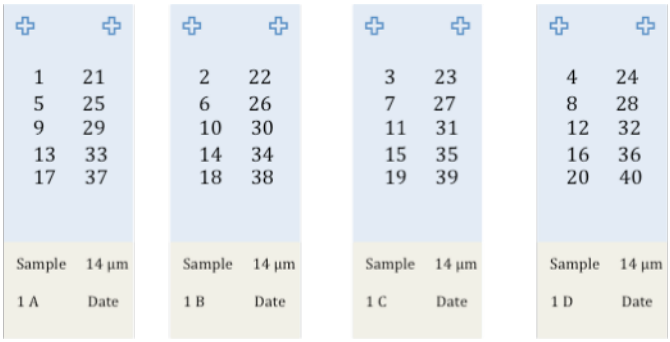

Figure 8: Recording of sections subjected to cryosectioning. Four different specimen glasses were used for each embryo. Recording the obtained parallel sections in a predefined order allows to analyze the embryos by comparative stainings.

3.6 Molecular biological methods

3.6.1 Elution of plasmid DNA

The used plasmid DNA and supplier are listed in chapter 2.8. A boarded area on a piece of paper containing the required plasmid DNA was cut out using an aseptic scalpel. The resulting pieces were transferred into a 2 mL tube and covered for 30 min at room temperature with 30 µL of TE-buffer (pH 8,0). The tube containing the resolved DNA and paper piece was stored at +4°C.

3.6.2 Transformation of E. coli DH5α

The transformation of competent bacterial cells occurred by the heat shock method. The used competent cells were the non-pathogenic E. coli strain K17 DH5α. After the competent cells were thawed on ice, the cells were gently mixed with the pipette tip and

100 µL were transferred into a pre-chilled 1,6 mL polypropylene CryoPure tube. Then, 5 µL of plasmid DNA containing the gene of interest were added. During the dispensing of the plasmid DNA into the tube containing the competent cells, the pipette was carefully moved to stir gently the content. The competent cells were incubated on ice for 10 min. The heat shock occurred by the incubation of the cells for 2 min at +42°C in water bath. To the heat shocked cells, 1 mL of Luria-Bertani-(LB)-Medium was added and gently stirred by tapping the tube. The cells were incubated and shaken for one hour at +37°C and 250 rpm. Due to the ampicillin resistance gene in the used plasmid DNA vectors, 100 µL of a 1:100 dilution of the transformed cells were spread onto LB agar plates containing 100 µg/mL ampicillin and incubated over night at +37°C. The next day, competent cells containing the transformed plasmid DNA were grown selectively on the plates. The plates were sealed with parafilm and stored at +4°C.

3.6.3 Spreading of bacterial cells on LB-medium

Cells containing the gene of interest were spread out onto LB agar plates containing 100 µg/mL ampicillin and incubated over night at +37°C. For this, the provided bacterial stab was opened close to a Bunsen burner. Using an aseptic toothpick, growing bacteria were transferred from the stab culture onto the surface of the LB plate and spread in order to obtain single colonies. The next day, cells containing the gene of interest were grown selectively on the plate. The plates were sealed and stored at +4°C.

3.6.4 Maxipreparation

The electroporation of foreign plasmid DNA and the utilisation of plasmid DNA for the generation of a RNA probe required a specific quantity (see section 3.3.4. and 3.6.9.). For this, transformed bacterial cells containing the gene of interest were used for maxipreparation. An isolated colony was picked using a pipette tip and released in 100 mL of LB-medium containing 10 mg/mL ampicillin. The used 500 mL flasks were incubated in an incubator shaker at 260 rpms over night at +37°C. The next day, the cells were harvested by centrifugation for 15 min at 18000 x *g* and +4°C. The isolation of plasmid DNA of the resulting pellet occurred with the Qiagen Plamid Maxi Kit100. The procedural steps were carried out as suggested by the supplier with the exception of the maximum of the

centrifugation speed, which was 18000 x *g*. After the plasmid DNA pellets were precipitated and air-dried, 100 µL of TE buffer (pH 8,0) containing RNase were applied on the pellet to redissolve the plasmid DNA. The concentration and purity were determined by UV/VIS spectrophotometry (see 3.6.5.) and controlled by a 1% (w/v) agarose/TAE gel (see 3.6.6.). The plasmid DNA was stored at -20 °C.

3.6.5 Determination of plasmid DNA concentration

The concentration of plasmid DNA was determined by the UV/VIS spectrophotometer NanoDrop2000c. To establish a blank, 1 µL of TE buffer (pH 8,0) was applied onto the pedestal of the NanoDrop and measured using the software provided (NanoDrop2000c). After the measurement, the pedestal was dried with a lint-free laboratory wipe and 1 µL of the DNA sample was applied onto the pedestal. The measurement determined the DNA concentration and its purity.

3.6.6 Electrophoresis with agarose gel

The DNA was subjected to the agarose gel electrophoresis to control its isolation and purification, the linearization and the generation of a gene specific probe. For this purpose, 1% (w/v) agarose/TAE gels were produced. The agarose was solved in 1xTAE buffer in a microwave for 5 min. Afterwards, 2 µL of Rotisafe® were added to the warm solved agarose and mixed. The liquid agarose was poured slowly in a gel tray, which was placed into a gel box. Then, the well combs were placed at the designated position. The gel solidified completely within 20 min at room temperature. Following solidification, the gel was covered completely with fresh 1xTAE buffer. The well combs were removed and the samples including the molecular weight ladder were loaded into the gel. Finally, the electrode holder was placed, such that the anode was on the bottom, and the gel was run for 45 min at 90V. The negative charged DNA/RNA moved towards the anode. The gels were photographically documented using QuantumCapt and analyzed with the provided software.

The linearization of the plasmid DNA containing the desired gene is the first step for the production of a specific RNA probe. To linearize the plasmid DNA, 25 µg of the purified plasmid DNA containing the gene of interest were mixed with 5 µL of the appropriated restriction enzyme and 5 µL of the proper buffer in a PCR tube. Due to the concentration of

the purified plasmid DNA, DEPC-water was added to get a final reaction mix volume of 50 µL. The reaction mix was incubated at +37°C for two hours. The digestion control was carried out with a 1% (w/v) agarose/TAE gel. The linearized plasmid DNA was compared to the circular, non-linearized DNA. For this, 2 µL of the DNA were mixed with 2 µL of DNA-loading buffer and left run at 90V for 45 min. The band of the linearized plasmid DNA did not move so far as that of the non-linearized DNA. Finally, the gel was documented photographically using the hardware Quantumcapt.

3.6.7 Linearization of plasmid DNA

The linearization of the plasmid DNA containing the desired gene is the first step for the production of a specific RNA probe. To linearize the plasmid DNA, 25 µg of the purified plasmid DNA containing the gene of interest were mixed with 5 µL of the appropriated restriction enzyme and 5 µL of the proper buffer in a PCR tube. Due to the concentration of the purified plasmid DNA, DEPC-water was added to get a final reaction mix volume of 50 µL. The reaction mix was incubated at +37°C for two hours. The digestion control was carried out with a 1% (w/v) agarose/TAE gel. The linearized plasmid DNA was compared to the circular, non-linearized DNA. For this, 2 µL of the DNA were mixed with 2 µL of DNA-loading buffer and left run at 90V for 45 min. The band of the linearized plasmid DNA did not move so far as that of the non-linearized DNA. Finally, the gel was documented photographically using the hardware Quantumcapt.

3.6.8 Purification of the linearized plasmid DNA

The purification of the linearized plasmid DNA with the containing gene of interest occurred by the phenol-chloroform extraction. For this, the reaction mix of the linearized plasmid DNA was filled up to 100 µL with DEPC-water. Then, 100 µL of phenol chloroform isoamyl alcohol were added to the linearized DNA. The sample was swirled up thoroughly and centrifuged for 5 min at +4°C and 14000 rpm. The resulting upper aqueous layer was removed and transferred into a new tube. Afterwards, 100 µL of chloroform were added to the sample. The sample was swirled up thoroughly and centrifuged for further 5 min at +4°C and 14000 rpm. At the end of the centrifugation, the upper aqueous layer was removed and transferred into a new tube, where 10 µL of 3M sodium acetate (pH 5,2) were added. The sample was swirled

up and 330 µL of 100% (cold) ethanol were added. Again, the sample was swirled up thoroughly and stored at -20°C to precipitate the DNA over night. The next day, the sample was centrifuged for 15 min at +4°C and 14000 rpm. The resulting supernatant was removed carefully without disturbing the DNA pellet. The pellet was washed with 900 µL of 75% (v/v) ethanol/distilled water for 5 min at room temperature. Then, the sample was centrifuged again for 15 min at +4°C and 14000 rpm. The supernatant was removed and the pellet air-dried for 5 min. The pellet was resuspended in 100 µL DEPC-water and the concentration measured using the NanoDrop 2000c as described above. The linearized and purified DNA was stored at -20°C.

3.6.9 *in vitro* transcription

For the detection of the endogenous transcripts through the *in situ* hybridization, a digoxgenin-labelled RNA probe was generated. For this purpose, 1 µg of the linearized, purified and gene of interest containing plasmid DNA, was added to the *in vitro* transcription mix (see chapter *Materials* section 2.5). Due to the concentration of linearized DNA, DEPC-water was added to get a final volume of 20 µL. The reaction mix was incubated for two hours and +37°C. Then, 1 µL of RNase-free DNaseI was added to the sample and incubated for 30 min at room temperature. For the precipitation over night, 3,5µL of 4M lithium chloride and 100 µL of 100% ethanol (cold) were added to the sample and incubated at -20°C. The next day, the sample was centrifuged for 30 min at +4°C and 13000 rpm. The supernatant was removed and the resulting pellet washed with 70% (v/v) ethanol/distilled water for 5 min at room temperature. Following this, the sample was centrifuged again for 30 min at +4°C and 13000 rpm. The supernatant was removed and the pellet air-dried for 5 min, before resuspended in 85 µL DEPC-water. To control if the transcription occurred, 2 µL of the generated RNA probe were mixed with RNA loading buffer and left run at 90V for 45 min on a 1% (w/v) agarose/TAE gel. A band on the gel confirmed the successful transcription. The probe was stored until its utilisation at -20°C.

3.7 Histological methods

3.7.1 *in situ* hybridization

The working protocol for the detection of endogenous transcripts in the eye tissues of frozen sections required three days. A light-tight box was covered with 100 mL of 50% (v/v) formamide/1x SSC. The selected specimen glasses with the frozen tissue were thawed and dried for 10 min at +37°C on a heating plate, bordered with a liquid blocker and afterwards placed onto glass holders into the light-tight box. The slides were incubated for 10 min at room temperature in the light-tight box containing the fomamide/1xSSC solution at the bottom, to adapt to the room temperature. In the meantime, the RNA probe was diluted 1:100 in hybridization buffer and incubated for a denaturation for 10 min at +70°C. Due to the section numbers on the specimen glass, 120 µL – 150 µL of the denatured probe were applied quickly on the sections and covered with coverslips (24 x 60 mm). The box containing the glasses was incubated in an incubator over night at +65°C. The next day, the slides were washed once and very shortly to remove the cover slips in cuvettes containing warm washing solution. Then, the slides were transferred into another cuvette containing fresh and warm washing buffer and incubated for one hour in the incubator at +65°C. After that, the slides were transferred into cuvettes containing 1xMABT/DEPC-water and rinsed once for 5 min, once for 10 min and twice for 15 min at room temperature. The sections were blocked with 20% (v/v) heat inactivated chicken serum in 1xMABT for one hour at room temperature. Meanwhile, the anti-DIG antibody was diluted 1:3000 in blocking reagent (diluted 1:5 in 1xMABT). The specimen glasses were placed onto glass holders inside the light-tight box, whose bottom part was covered with distilled water. Dependent on the section numbers on the specimen glass, 120 µL – 150 µL of the diluted anti-DIG antibody were applied to the sections. The specimen glasses were covered with coverslips and incubated over night at room temperature. The next day, the slides were transferred into cuvettes containing 1xMABT and rinsed once for 5 min, once for 10 min and twice for 15 min at room temperature. After that, the specimen glasses were placed again in the box and washed three times for each 10 min at room temperature with 300 µL of alkaline phosphatase buffer (pH 9,5). Dependently on the section number on the specimen glass, 120 µL – 150 µL of the substrate solution for the alkaline phosphatase were applied on the sections. These were covered with coverslips to avoid a precipitation due to the air oxygen. For several hours, they were incubated in a light-tight box, humidified with distilled water until the specific precipitation became robust. The specimen glasses were transferred into cuvettes containing 1xPBS and rinsed once for 5 min and once for 10 min to stop the precipitation. Finally, the slides were rinsed in distilled water, dried on the heating plate and covered with coverslips

using Kaiser's glycerol gelatine. The slides were stored in appropriate boxes at room temperature.

3.7.2 Protein detection by immunohistochemistry

Frozen head sections of manipulated and wild type embryos were subjected to immunohistochemistry to detect specific proteins for eye tissues. The used antibodies and their properties are listed in chapter *Materials* sections 2.6 and 2.7.

The selected specimen glasses with the frozen tissue were thawed and dried for 30 min at +37°C on a heating plate. The sections were covered and blocked with TBSA for 30 min at room temperature. Prior to this, to avoid that the blocking solution drained off, all sections on each specimen glass were bordered together with a liquid blocker. The dilution of the used antibodies occurred in TBSA. Dependent on the section numbers on the specimen glass, 120 µL – 150 µL of the diluted primary antibody were applied on the sections and incubated in a humid light-tight box over night at room temperature. Following the incubation, the slides were washed in cuvettes once shortly for 5 min and then again for 10 min with fresh 1xPBS. During the washing steps, dependently on the primary antibody and on a possible double staining, different with fluorochrome-conjugated secondary antibodies were diluted 1:100 in TBSA. For each slide, 100 µL of the secondary antibody were added and incubated in a humid light-tight box for one hour at room temperature. Following the incubation, the slides were washed again in cuvettes once shortly for 5 min and then again for 10 min with fresh 1xPBS. To obtain a DNA staining, the sections were treated for 1 min at room temperature with 100 µL of 1µg/mL DAPI. The slides were washed again in cuvettes once shortly for 5 min and then again for 10 min with fresh 1xPBS. Afterwards, the slides were rinsed twice each 5 min in distilled water and dried on the heating plate covered light-tight. Finally, the slides were covered with coverslips using Kaiser's glycerol gelatine. The covered slides were stored until their utilisation at +4°C.

4 Results

4.1 MEK1/2 seems to be involved in neural retina specification

Surface ectoderm-derived FGFs appear to be involved in inducing neural retina (NR) development (reviewed in Fuhrmann, 2010). In accordance with this, in chick embryos overexpression of constitutively activated MEK1, a downstream effector of the FGF signaling pathway, converts the RPE into a retina-like structure (Galy et al., 2002). To confirm this result, I examined the expression of *Vsx2* in optic vesicle cells following MEK1/2 inhibition, using the chemical U0126 which is known to specifically inhibit MEK1/2 (Favata et al., 1998; Davies et al., 2000). Therefore, I implanted U0126 soaked resin beads at optic vesicle stages (HH10; 10-11 somites; Figure 9A). One day following the manipulation (HH15/16), the formation of a fully developed optic cup was not observed (Figure 9B; n = 3/3). Moreover, these treated embryos developed rudiments of lens vesicles or lens placodes. In addition, inhibition of MEK1/2 resulted in a thinning of the distal neuroepithelium, with an RPE-like morphology. Immunohistochemical studies showed that in this region *Vsx2* expression was down-, and MITF expression upregulated when compared to the untreated, contralateral side (Figure 9C, D; n = 3/3; data not shown). Thus, consistent with the previous reported study, I confirm that MEK1/2 seems to be involved in initiating NR in multipotent optic vesicle cells.

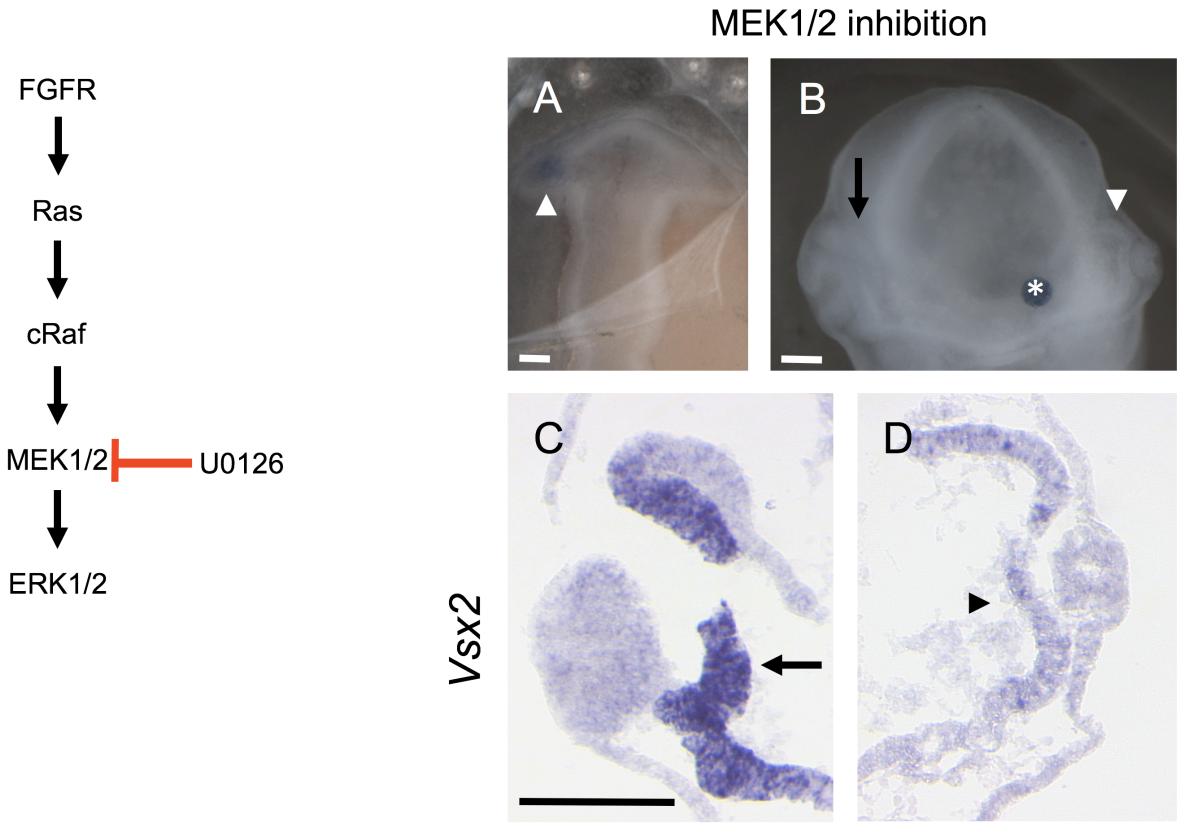

Figure 9: Inhibition of MEK1/2 has an effect on *Vsx2* expression. (**A**) Inhibition of MEK1/2 following implantation of U0126 soaked resin beads at HH10. The bead (arrowhead) was implanted into the left optic vesicle. (**B**) One day following bead implantation (asterisk) optic cup formation is disturbed and development of a proper lens vesicle did not occur (arrowhead) when compared with the untreated side (arrow). (**C**, **D**) Downregulation of *Vsx2* expression is observed in the treated eye (**D**, arrowhead), whereas a normal *Vsx2* expression is observed in the untreated eye (arrow). n = 3/3; scale bars 100 µm.

During FGF-mediated signaling, MEK1/2 phosphorylates the downstream effector ERK1/2, which in turn activates specific target genes (reviewed in Turner and Grose, 2010; Dorey and Amaya, 2010). Therefore, inhibition of MEK1/2 should prevent the phosphorylation of ERK1/2. To elucidate, if ERK1/2 inhibition results in the loss of *Vsx2* expression, I blocked specifically ERK1/2 by the implantation of FR180204 soaked resin beads at HH10 (Figure 10A; Ohori et al., 2005). One day following the manipulation at HH15/16, the treated optic vesicles developed an optic cup and a lens vesicle (Figure 10B; n = 4/4). In these treated eyes, the neuroepithelium appeared to be slightly thinner than the untreated, contralateral side, although *Vsx2* expression appeared not to be altered when compared to the untreated side (Figure 10C, D; compare with Figure 9D; n = 3/4). Taken together, the above-mentioned results suggest that MEK1/2 might induce a retinal cell fate in optic vesicle cells in an ERK1/2-independent way.

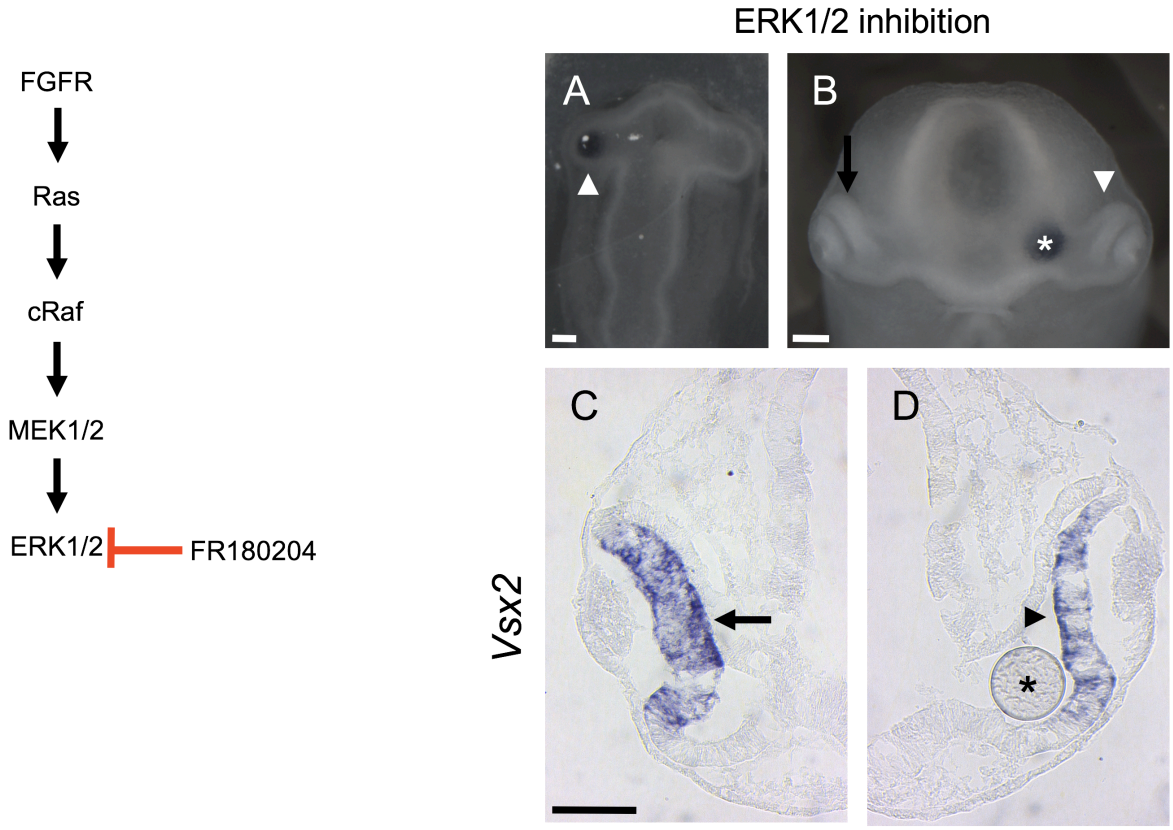

Figure 10. Inhibition of ERK1/2 does not appear to affect *Vsx2* expression. (**A**) Inhibition of the downstream effector ERK1/2 of the FGF signaling pathway by implantation of a FR180204 soaked bead into the left optic vesicle (arrowhead). (**B**) The embryos were fixed 24h later at HH15. The treated side (arrowhead) developed an optic cup similar to the untreated side (arrow). Surprisingly, in the treated optic vesicle (**D**, arrowhead) no downregulation of *Vsx2* transcripts was observed compared to the untreated side (**C**, arrow). The asterisks mark the implanted resin bead. n = 3/4; scale bars 100 µm.

4.2 pSMAD1/5/8 is co-localized with *Vsx2* expression

Fgf1 and *Fgf2* single- and *Fgf1* and *Fgf2* double-knockout mice have no evident eye defects (Dono et al., 1998; Ortega et al., 1998; Miller et al., 2000). This leads to the suggestion, that (an)other signal(s) might be involved in the induction of retinal identity during vertebrate eye development. Recent studies reported that surface ectoderm-derived BMP signaling mediates NR development in chick and mouse (Pandit et al., 2015; Huang et al., 2015b). The activation of BMP signaling is mediated by the phosphorylation of SMAD proteins (Herpin and Cuningham, 2007). During chick eye development, *Vsx2* expression is first detected in the distal part of the optic vesicle at HH10 (Figure 11A, D; Chen and Cepko, 2000; Müller et al., 2007). To test whether the BMP signaling pathway is active during NR specification, I compared the expression of *Vsx2* with phosphorylated SMAD1/5/8 (pSMAD1/5/8) localisation at optic vesicle stages (Figure 11). At the time NR is specified in

the chick (HH10/11), *Vsx2* expression co-localises with pSMAD1/5/8 in the distal and disto-ventral region of the optic vesicle (Figure 11B, C and Figure 11E, F; n = 3/3). Furthermore, at these stages pSMAD1/5/8 is also detected in the surface ectoderm overlying the neuroepithelium (Figure 11B, C and Figure 11E, F). Taken together, the BMP signaling pathway is active at the right time and place to be involved in specifying a NR cell fate in vertebrate optic vesicle cells.

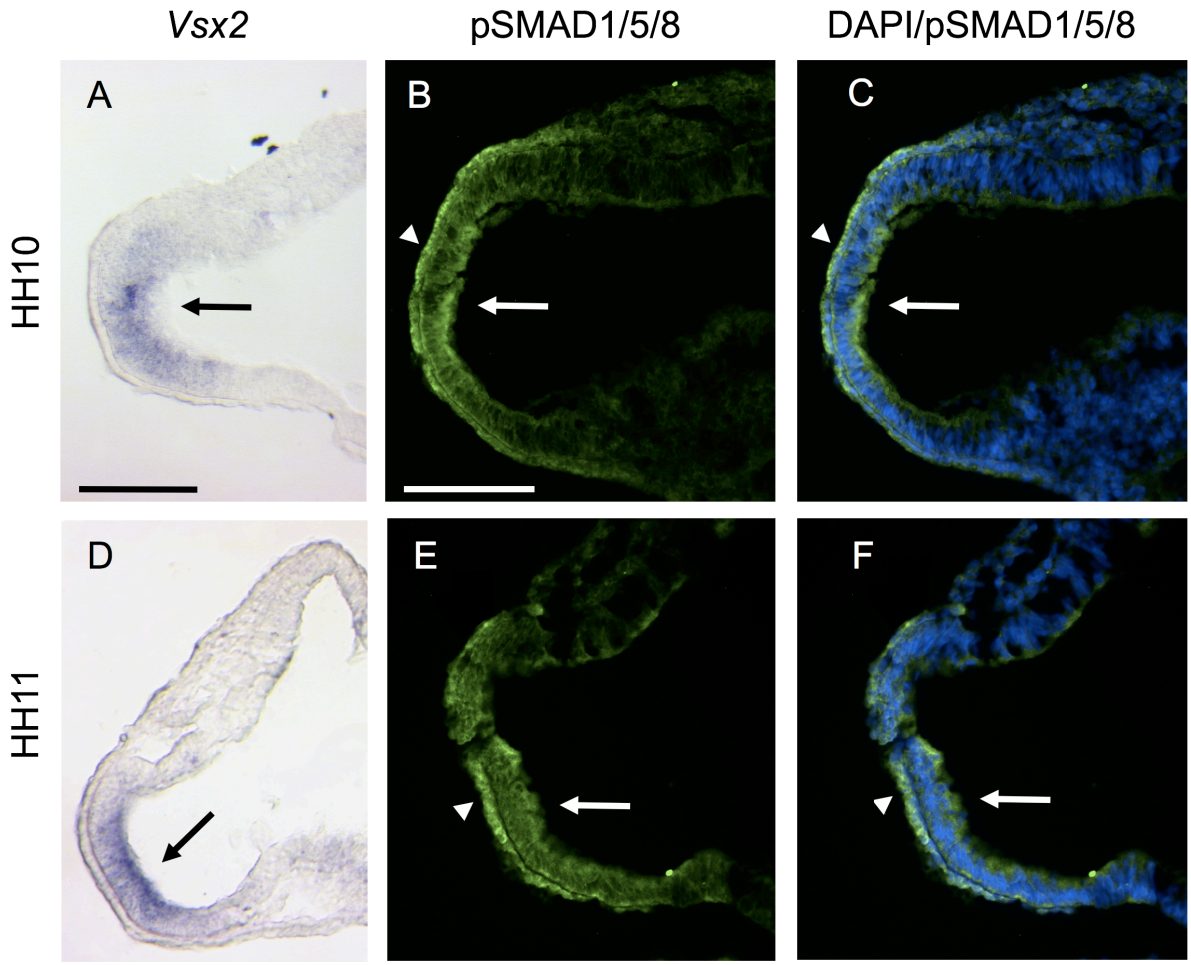

Figure 11: *Vsx2* expression co-localizes with pSMAD1/5/8 in the presumptive NR. (**A**) During late HH10 (12 somites), the expression of the neural retina marker *Vsx2* is detected in the distal neuroepithelium of the optic vesicle (arrow). (**B**, **C**) At the same time point, the detection of pSMAD1/5/8 is observed in the distal part of the optic vesicle (arrow) and the overlying surface ectoderm (arrowhead). (**D**) At HH11, strong *Vsx2* expression is observed in the disto-ventral part of the optic vesicle (arrow), consistent with the protein detection of pSMAD1/5/8 (**E**, **F**), which is detected in the neuroepithelium (arrow) and the adjacent surface ectoderm (arrowhead). n = 3/3; scale bars 100 µm.

4.3 Only inhibition of BMPR-mediated SMAD1/5/8 phosphorylation causes a downregulation of *Vsx2*

If it is correct that the BMP signaling is involved in NR induction, then preventing the BMPR-mediated SMAD phosphorylation should lead to a decrease or loss of *Vsx2* expression. To investigate this, I implanted LDN-193189 soaked resin beads at early HH10 (Figure 12A). LDN-193189 is known to inhibit the BMP signaling by the specific binding to the BMPR type I ALK-1, ALK-2, ALK-3 and ALK-6 (Horbelt et al., 2015). These receptor types mediate the phosphorylation of SMAD1/5/8 (Herpin and Cunningham, 2007). One day following the manipulation, formation of optic cups and lens vesicles were not observed (Figure 12B, n = 4/4). The treated side developed an optic vesicle-like morphology and *Vsx2* expression was not detected when compared to the untreated side (Figure 12C, D; n = 4/4). Moreover, pSMAD1/5/8 was not detected on the treated side, whereas pSMAD1/5/8 was localised in the dorsal retina, dorsal RPE and the lens (Figure 12E-H). These data strongly suggest, that BMPR-mediated SMAD1/5/8 phosphorylation is involved in inducing retinal progenitor cells in the neuroepithelium of the chick optic vesicle.

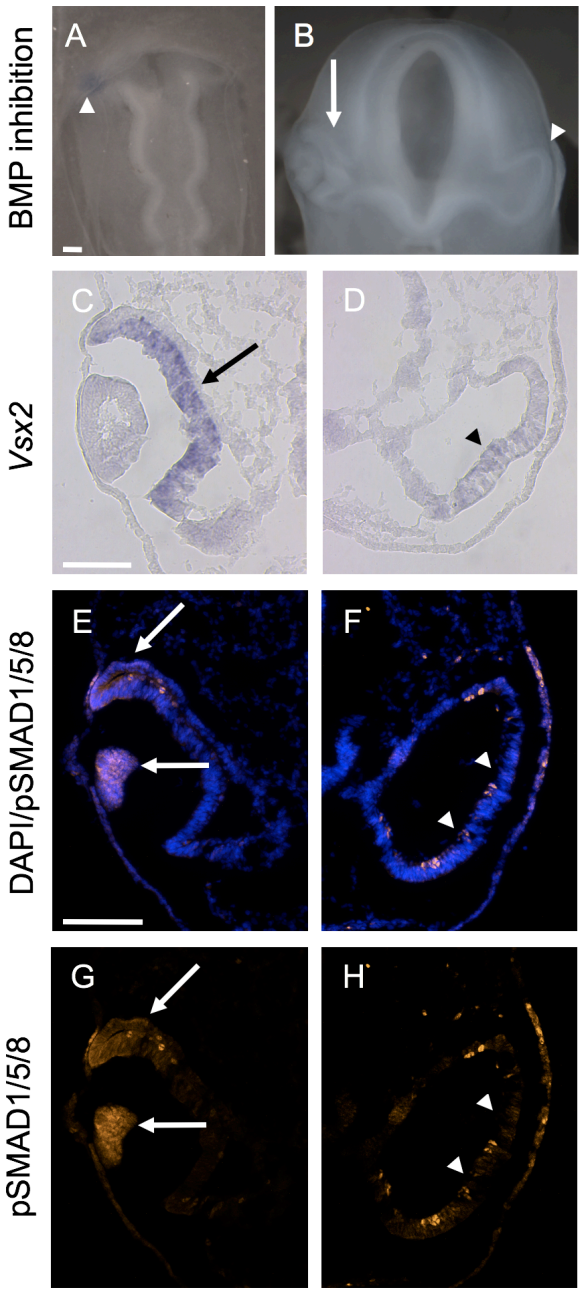

Figure 12: Inhibition of BMP signaling pathway leads to a downregulation of *Vsx2* and loss of pSMAD1/5/8. (**A**) Implantation of beads soaked in the BMP receptor inhibitor LDN-193189 at HH10 (arrowhead). (**B**) Embryo one day following the manipulation at HH15. The treated side arrested at optic vesicle stage (arrowhead), whereas on the contralateral side an optic cup developed (arrow). (**C, D**) BMP inhibition resulted in a downregulation of *Vsx2* on the treated side (arrowhead) when compared to the untreated side (arrow). The downregulation of *Vsx2* is consistent with the loss of pSMAD1/5/8 (**F, H**; arrowheads). At the contralateral side the localisation of pSMAD1/5/8 is restricted to the dorsal retina, dorsal RPE and the presumptive lens (**E, G**; arrows). n = 4/4; scale bars 100 µm.

BMPs belong to the TGF-β superfamily, a protein family consisting of numerous growth factors (Derynck and Zhang, 2003; Herpin and Cunningham, 2007). Whereas BMP signaling leads to the phosphorylation of SMAD1/5/8, other members of the TGF-β superfamily act by phosphorylating SMAD2/3. To exclude the possibility that this pathway is involved in inducing

a retinal cell fate, I blocked this pathway by implanting SB505124 at optic vesicle stages (Figure 13A). This compound is known to inhibit signaling through BMPR type I ALK-4, ALK-5 and ALK-7, thereby preventing the phosphorylation of SMAD2/3 (DaCosta Byfiled et al., 2004). One day following the implantation of a SB505124 soaked bead, the development of a complete optic cup was observed (Figure 13B; n = 6/8). In those cases, the expression of *Vsx2* was not affected, when compared to the untreated, contralateral side (Figure 13C, D; n = 6/8). Thus, it appears that retinal progenitor cells are specified via the BMP/SMAD1/5/8 and not by the TGF-β/SMAD2/3 signaling pathway.

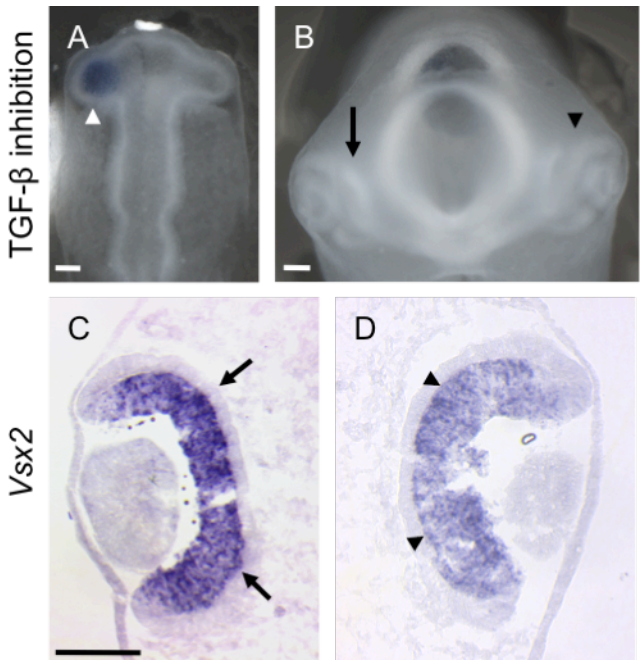

Figure 13: The selective inhibition of the TGF-β receptors ALK4, ALK5 and ALK7 with SB505124 suggests, that the SMAD2/3 pathway is not involved in retina specification. A resin bead soaked in SB505124 was implanted into the left optic vesicle at HH10 (**A**, arrowhead). (**B**) The embryos were fixed 24h following the manipulation. Both optic cups displayed normal phenotypes with normal formed lenses (arrowhead corresponds to the treated side; arrow shows untreated side). (**C; D**) The expression of *Vsx2* was not affected in the treated eye (**D**, arrowheads) when compared to the untreated eye (**C**, arrow). n = 6/8; scale bars 100 µm.

4.4 Constitutive active hSMAD1 is sufficient to restore and induce ectopic *Vsx2* expression following BMPR inhibition

To show that phosphorylation of SMAD1/5/8 leads to NR specification in optic vesicle cells, I implanted LDN-193189 soaked resin beads and simultaneously electroporated a constitutive active form of human SMAD1 (CA-hSMAD1-EVEMM see also chapter *Materials* page 19, section 2.8 for further properties; Fuentealba et al., 2007) at HH10 (Figure 14A, B). The manipulation caused an arrest of the development of the optic vesicle into an optic cup one

day following the operation (Figure 14C; n = 2/3). The untreated side developed an optic cup with a lens vesicle and the *Vsx2* expression pattern appeared to be unchanged (Figure 14C, D). In the treated eye, the electroporated CA-hSMAD1-EVEMM was sufficient to induce ectopically *Vsx2* expression (Figure 14E). The ectopic induction was confirmed by the detection of GFP, which was electroporated simultaneously with the CA-hSMAD1-EVEMM construct (Figure 14F, F'; see also chapter *Materials* and *Methods* page 19 and 24, section 2.8 and 3.3.4). These results demonstrate that the BMP signaling pathway via SMAD1(/5/8) is sufficient to induce NR identity by inducing *Vsx2* expression in multipotent optic vesicle cells *in vivo*.

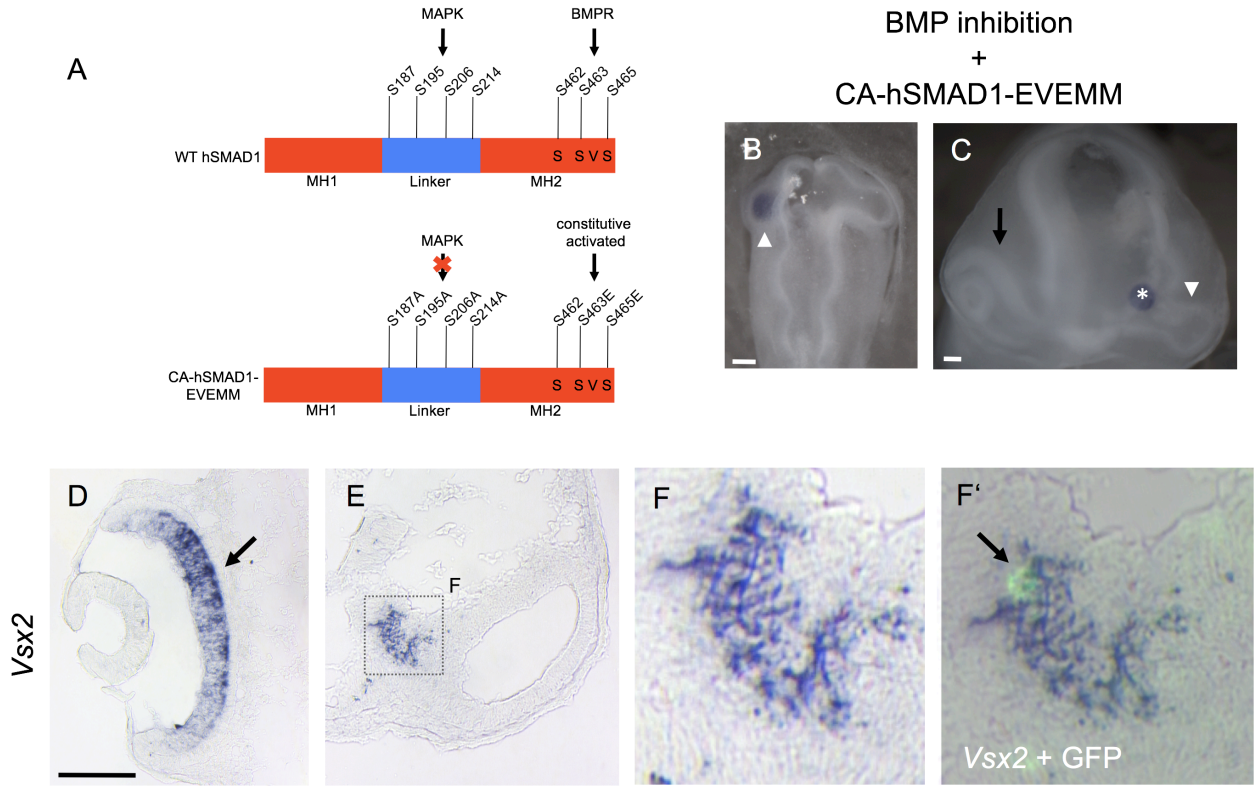

Figure 14: A constitutive active form of SMAD1 rescues *Vsx2* expression following LDN-193189 treatment. (**A**) The BMPR-mediated phosphorylation of wild-type SMAD1 occurs at a highly conserved sequence, namely SSVS, within the MH2 domain. It is also known that serine residues within the linker region are targets for MAPK-mediated phosphorylation. The used hSMAD1 construct had several mutations in the linker and MH2 region (see also *Materials*, section 2.8). (**B**) The constitutive active form of hSMAD1 was electroporated following BMPR inhibition by LDN-193189 (arrowhead). (**C**) One day following manipulation, the treated eye (arrowhead), was arrested in an optical vesicle stadium missing any lens structures. The untreated side developed an optic cup with a lens vesicle (arrow) and displayed a normal *Vsx2* expression pattern within the retina (**D**, arrow). The constitutive active form of hSMAD1 was able to induce an ectopic expression of *Vsx2* in the proximal region of the eye anlage on the treated side (**E**, dashed square). (**F**, **F'**) In a parallel section of (**E**), the co-electroporated GFP was detected in the ectopic *Vsx2* expressing cells (arrow). n = 2/3; scale bars 100 µm.

4.5 BMP7 and constitutive active hSMAD1 induce VSX2 independently from FGF signaling

My results have shown that interfering with MEK1/2, but not with ERK1/2, results in a downregulation of *Vsx2* expression (Figure 9 and 10). Like FGFs, BMPs are known to be able to signal via MEK1 (Derynck and Zhang, 2003; Bragdon et al., 2011). To see, if application of BMP7 is sufficient to rescue *Vsx2* following MEK1/2 inhibition at optic vesicle stages (HH10), I implanted an U0126 soaked resin bead followed by the implantation of a BMP7 soaked agarose bead. (Figure 15A). It is noteworthy, that due to the lack of space within the optic vesicle, the BMP7 bead was localized to a more proximal region (see arrowheads in Figure 15A). The embryos were analyzed one day following manipulation (Figure 15B). The treated side developed a normal optic cup with a lens vesicle (compare with Figure 15C and also Figure 9; n = 5/7). Interestingly, *Vsx2* expression was detected within the retinal tissue and ectopically in the ventral part of the optic cup, whereas the application of U0126 alone did not expressed *Vsx2* (Figure 15C, D; n = 3/3). In one case, the embryo was fixed three days following manipulation (Figure 15E, F). In this case the ventral regions of both eyes appeared to be affected (arrowheads). The ventral RPE lost its pigmentation, thickened and acquired NR identity as shown by the expression of VSX2 (Figure 15G-H').

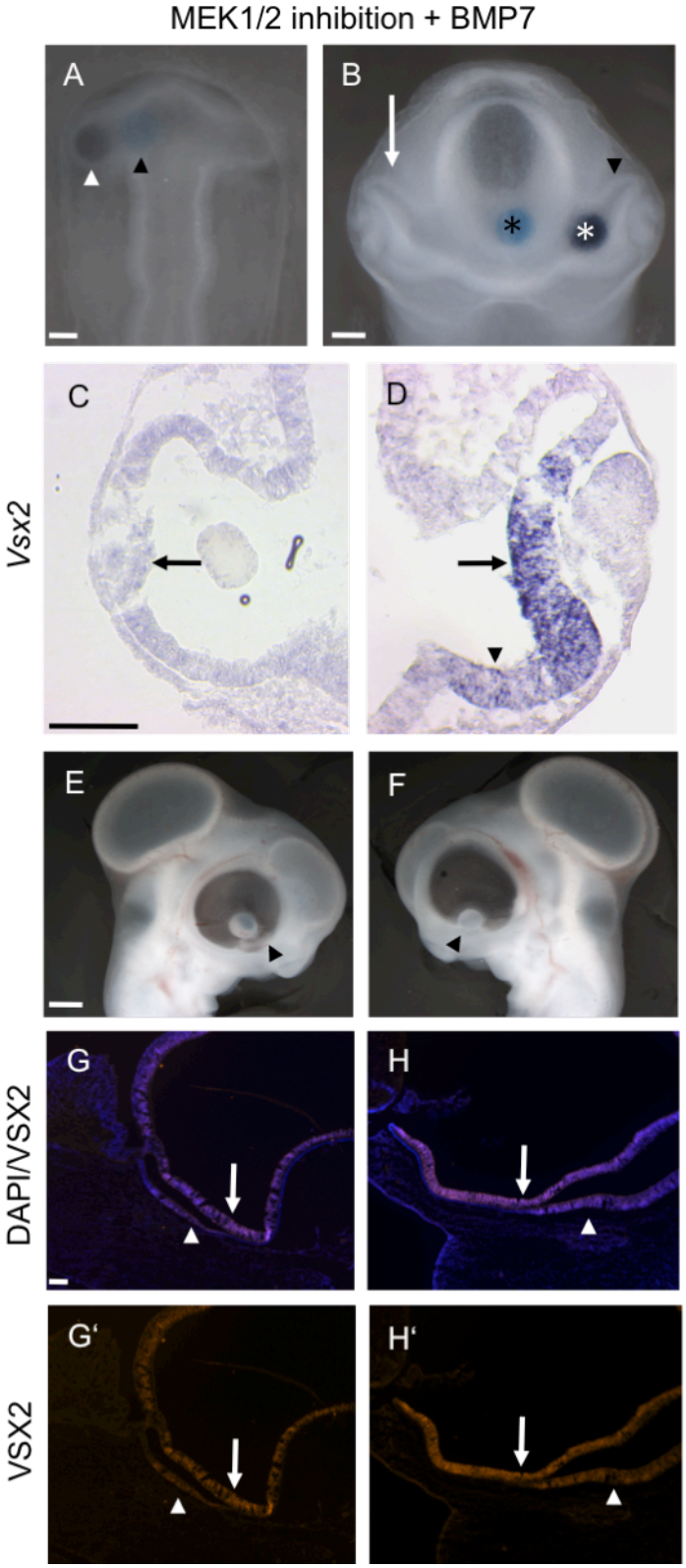

Figure 15: Following MEK1/2 inhibition BMP7 is sufficient to restore and induce ectopic *Vsx2* expression in the ventral presumptive RPE. (**A**) The manipulation occurred by the implantation of two beads simultaneously into the optic vesicle of a HH10 embryo. A U0126 soaked bead (white arrowhead) was followed by a BMP7 soaked bead (black arrowhead). (**B**) The treated side was not affected and a normal optic cup formation was observed (arrowhead), when compared to the untreated side (arrow). The asterisks mark the position of the beads. (**C**) Following MEK1/2 inhibition alone, no *Vsx2* expression was observed (arrow, compare also Figure 9). (**D**) The combination of MEK1/2 inhibition and endogenous application of BMP7 was sufficient to restore *Vsx2* within the NR tissue and to induce ventrally ectopic *Vsx2* expression (arrowhead). (**E**, **F**) Embryo which

was fixed three days following the manipulation. This embryo displayed malformations in the ventral part of the eyes on both sides (arrowheads). The treated eye (**F**) was most affected as shown by the loss of pigmentation in the ventral half of the eye (arrowhead). VSX2 protein distribution within the retina appeared to be unchanged on both eyes (arrows in **G-H'**). The ectopic detection of VSX2 was observed both distally in the ventral presumptive RPE (arrowheads in **H**, **H'**) and proximally in the presumptive RPE (arrowheads in **G**, **G'**). Scale bars in A-D and G-H' 100 µm; E-F 1000 µm.

In the next set of experiments, I tested if CA-hSMAD1-EVEMM is sufficient to rescue or induce ectopically VSX2 following MEK1/2 inhibition. To achieve this, I first electroporated CA-hSMAD1-EVEMM into the left optic vesicle cells at HH10 before implanting an U0126 soaked bead (Figure 16A). Similar to what I observed with BMP7, development of an optic cup and VSX2 expression was rescued one day following the operation (Figure 16B-D'; n = 3/4).

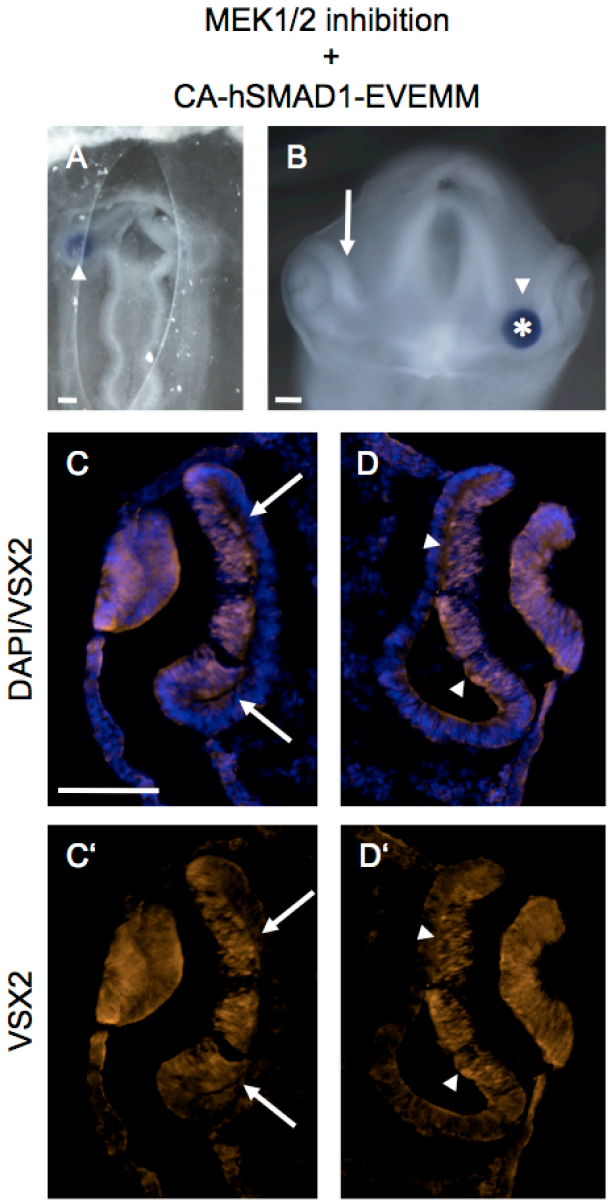

Figure 16: Constitutive active hSMAD1 rescues VSX2 expression following inhibition of MEK1/2. (**A**) Constitutive active hSMAD1-EVEMM was electroporated into the left optic vesicle simultaneously with the implantation of a bead soaked in the

MEK1/2 inhibitor U0126 (arrowhead). (**B**) Frontal view of the embryo one day following the manipulation. No morphological alterations were observed in the treated eye (arrowhead) when compared to the untreated eye (arrow). The asterisk marks the implanted bead. (**C**, **C'**) VSX2 is detected in the entire retina of the untreated, contralateral eye (arrows). (**D**, **D'**) Overexpression of CA-hSMAD1-EVEMM rescues VSX2 expression (arrowheads) following MEK1/2 inhibition. Note that there appear almost no morphological effects when compared to the contralateral side. n = 3/4; scale bars 100 µm.

Taken together, these results show that the BMP signaling pathway induces retinal progenitor cells during optic vesicle stages, independently from MEK1/2.

4.6 The surface ectoderm is not essential to induce retinal progenitor cells

Inductive signals released from the surface ectoderm appear to induce NR development in the distal portion of the optic vesicles (reviewed in Fuhrman, 2010; Venters et al., 2015; Müller et al., 2007; Pandit et al., 2015; Huang et al., 2015a; Huang et al., 2015b). If it is correct that surface ectoderm-derived BMP signals are necessary to induce NR development, then the removal of it should result in a loss or decrease of *Vsx2* expression. To examine this, I removed the surface ectoderm both dorsally and ventrally at early HH10 *in ovo* using Nile Blue sulfate A (Figure 17A). Following this manipulation, the surface ectoderm did not regrow one day following the operation at HH14/15 (Figure 17B; n = 7/9). The formation of an optic cup following surface ectoderm removal was not observed (n = 9/9). On the untreated side, the optic vesicle underwent an invagination to form an optic cup and the presumptive NR expressed *Vsx2* (Figure 17D). Surprisingly, removal of the surface ectoderm did not affect *Vsx2* expression within the optic vesicle (Figure 17C, n = 7/9). Taken together, it appears that signals released from the surface ectoderm are not required to induce *Vsx2*-expressing retinal progenitor cells in underlying neuroepithelium of the optic vesicle.

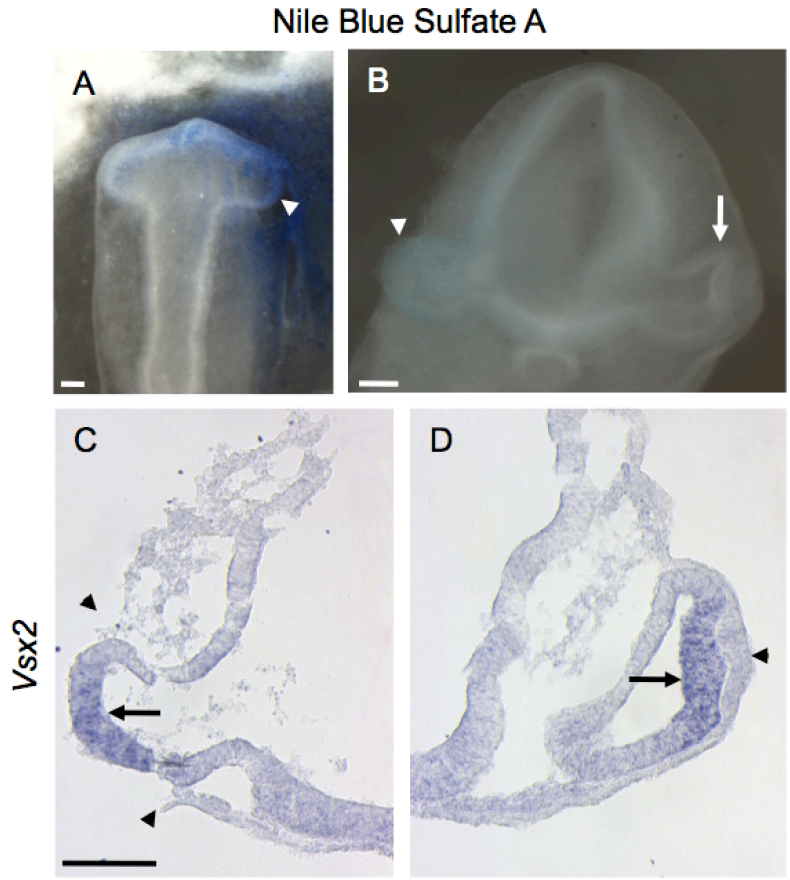

Figure 17: The surface ectoderm is not required for initiation of *Vsx2* expression. (**A**) Dorsal view of the manipulated embryo. The right optic vesicle of an early HH10 embryo was treated with Nile blue sulfate A to remove the surface ectoderm (arrowhead). (**B**) Frontal view of the treated embryo. The treated embryos were fixed 24h after manipulation at HH15. The removed surface ectoderm did not regrow on the manipulated side (arrowhead) and subsequently a lens placode did not form. Note that the optic vesicle did not invaginate to form an optic cup, whereas the contralateral side developed a proper optic cup (arrow). (**C**) In the absence of the surface ectoderm (arrowheads), *Vsx2* transcripts were still observed in the optic vesicle (arrow). The untreated side developed normally and *Vsx2* expression (**D,** arrow) was detected underneath the lens placode (arrowhead). n = 7/9; scale bars 100 µm.

4.7 The ventral midline is involved in NR specification in the chick

The fact, that the surface ectoderm is not involved in NR specification, leads to the hypothesis that an alternative signaling center might be involved in NR specification. Previous studies using explant cultures suggested that signals released from the ventral region might be involved in NR specification. When the ventral and dorsal optic vesicles in the chick embryo are excised and placed into culture only the cultured ventral halfs gave rise to NR (Kagiyama et al., 2005; Hirashima et al., 2008; Fuhrmann, 2010; Kobayashi et al., 2010). Moreover, *Bmp7* transcripts are expressed both in the surface ectoderm and in the ventral midline of chicken embryos (Figure 18B; Müller et al., 2007; Manning et al., 2006). Furthermore, at the time NR specification occurs in the chick, *Bmp7* expression co-localizes

with the expression of *Bmp2* in the ventral midline (Figure 18A; image courtesy of PD Dr. Astrid Vogel-Höpker; Manning et al., 2006).

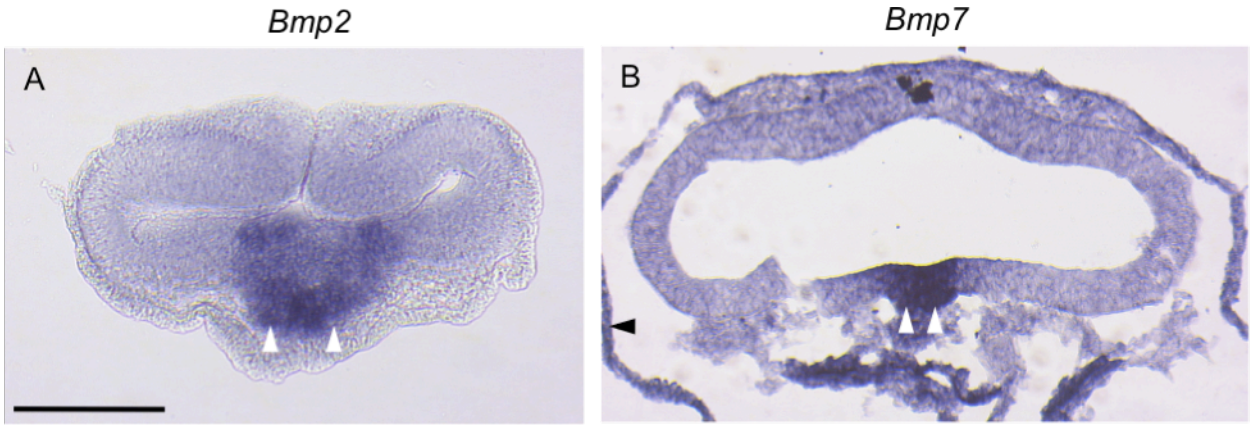

Figure 18: *Bmp* transcripts are expressed in the surface ectoderm and ventral midline prior to NR specification in the chick optic vesicle. (**A**) *Bmp2* expression is restricted to the ventral midline region at HH 10 (arrowheads). (**B**) *Bmp7* transcripts are found both in the ventral midline (white arrowheads) and the surface ectoderm (black arrowhead) at HH10. Scale bar 100 µm.

To test, if the *Bmp* expressing ventral midline is involved in NR specification, I carried out tissue ablation experiments in early HH10 staged embryos (Figure 19A). The ventral midline was removed using a sharpened tungsten needle. One day following manipulation the embryos were examined at HH15/16 (Figure 19B). Following removal of the ventral midline, the embryos appear to develop in the most cases optic cups on both sides without any phenotypic effects (n = 6/9). On the other hand, *Vsx2* expression was downregulated (n = 1/9) or lost (n = 2/9) on one or both sides of the embryo (Figure 19C-E). This suggests that the ventral midline might be involved in NR specification.

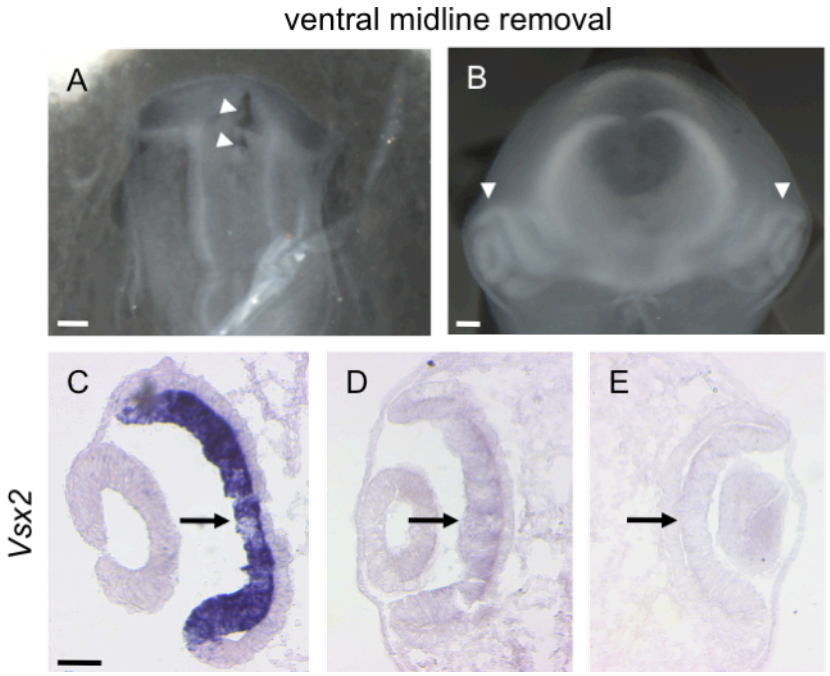

Figure 19: The ventral midline may have an effect on *Vsx2* expression. (**A**) The ventral midline (arrowheads) was removed using a sharpened tungsten needle at early HH10. (**B**) One day following manipulation the embryos were fixed at HH15/16. In the most cases (n = 6/9) the formation of an optic cup on both sides was observed (arrowheads). (**C**) Expression pattern of *Vsx2* in a wild-type HH16 embryo (arrow). (**D**, **E**) In some cases (n = 3/9), the treated embryos displayed at least a downregulation of *Vsx2* when compared with the wild-type (arrows). Scale bars 100 µm.

Like, *Bmp2* and *Bmp7*, transcripts of *Shh* are detected in the prechordal plate and notochord at the time the NR is specified (compare Figure 20 and Figure 18). *Shh* expression is also detected in the ventral forebrain region extending toward the optic vesicles (Figure 20). BMP7 and SHH act in a coordinative way to induce rostral diencephalic ventral midline cells (Dale et al., 1997). Here, BMP7 has a direct influence on neural cells, which modifies their response to SHH to differentiate into rostral diencephalic ventral midline cells. Furthermore, it has been shown that SHH regulates BMP7 expression and both act together to regulate *Pax2* expression in mouse retinal astrocyte precursors in mice (Sehgal et al., 2009).

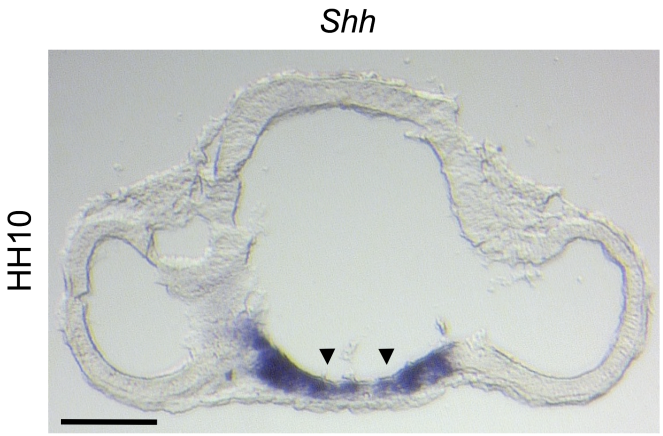

Figure 20: Expression pattern of *Shh* at the time the NR is specified in the chick optic vesicle at HH10. *Shh* transcripts are strongly expressed at the forebrain region (arrowheads). Scale bar 100 µm.

Due the co-localization of *Bmp* and *Shh* transcripts in the ventral midline region at optic vesicle stages, I hypothesized that a similar interplay between these two pathways might be involved in NR specification. To determine whether the SHH signaling might influence NR specification, I implanted cyclopamine soaked resin beads into the optic vesicles of HH10 staged embryos to inhibit the SHH signaling pathway (Figure 21A, Figure 22). The manipulated eyes developed an optic cup one day following manipulation at HH15/16 (Figure 21B, Figure 22; n = 10/11). Interestingly, the inhibition of the SHH pathway resulted in a downregulation or a complete loss of *Vsx2* expression in the treated optic vesicles (Figure 21D, Figure 22; n = 10/11). In some cases, the downregulation of *Vsx2* expression occurred in the dorsal part of the optic cup, while ventrally a faint *Vsx2* expression was observed (Figure 22D, n = 4/11). A normal pattern of *Vsx2* expression in the retinal tissue of the untreated eyes was observed (Figure 21C, Figure 22A). As expected VSX2 protein was co-localized with *Vsx2* expression in retinal progenitor cells (Figure 22A-C). In the treated eyes, VSX2 expression was not observed or limited to the ventral region of the optic cup (n = 1/2; Figure 22D-F). Furthermore, the downregulation or loss of *Vsx2* expression resulted in ectopic expression of MITF (n = 4/4; compare Figure 21E and E’ with F and F’). Taken together, SHH released from the ventral midline region might be involved in retinal cell fate specification at optic vesicle stages.

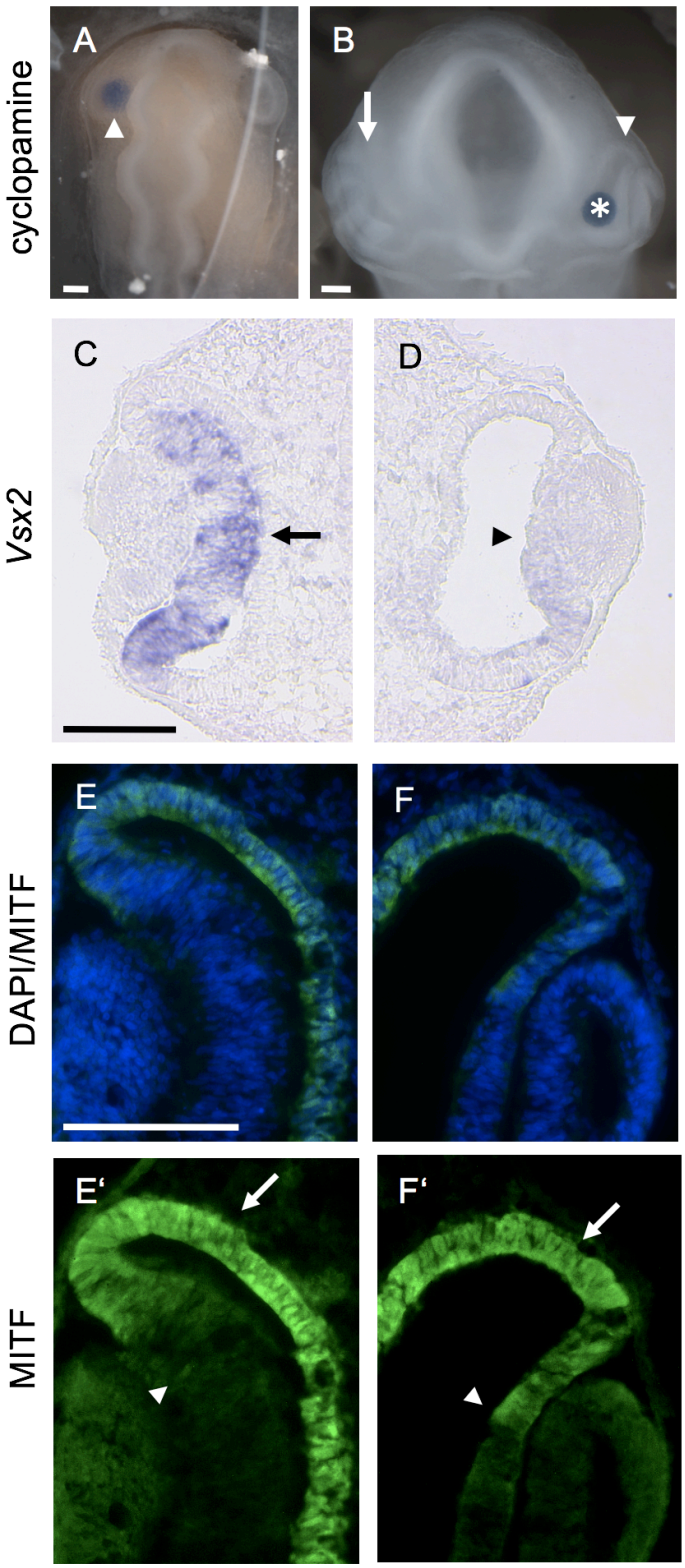

Figure 21: Inhibition of the SHH signaling pathway leads to a decrease or loss of *Vsx2* expression. (**A**) A cyclopamine soaked resin bead was implanted at early HH10 (arrowhead). (**B**) The treated embryos were fixed 24h after manipulation at HH15. The manipulated optic vesicles (arrowhead) formed an optic cup as the contralateral side (arrow). The asterisk marks the implanted bead. (**C**) *Vsx2* expression was not affected in the untreated eye (arrow). (**D**) Downregulation of *Vsx2* in the dorsal part of the forming optic cup (arrowhead) was observed. (**E-F'**) The RPE-specific marker MITF was observed in the presumptive RPE of both treated and untreated optic cups (arrows). A few MITF positive cells are detected in the *Vsx2*-negative NR (arrowhead in **F',** compare with **E'**). Scale bars 100 µm.

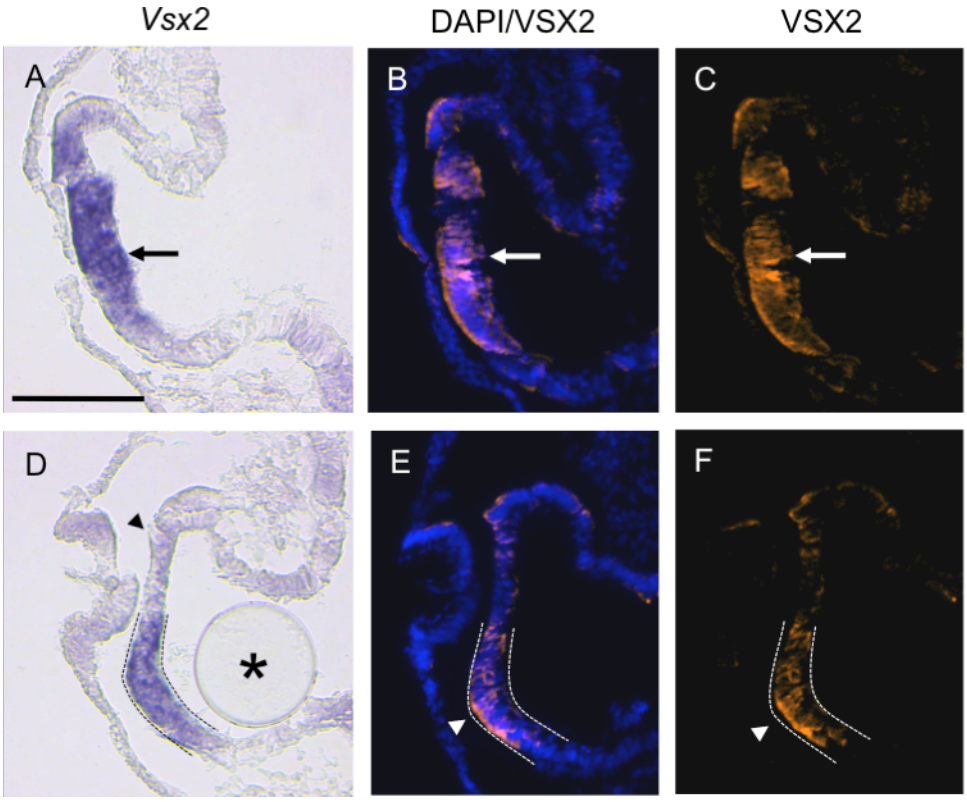

Figure 22: Following cyclopamine implantation some *Vsx2*-positive cells are present in the ventral part of the optic cup. (**A**) Contralateral side of a cyclopamine treated embryo. A robust *Vsx2* expression (arrow) is detected in the presumptive retina. (**B**, **C**) As assumed, VSX2 is co-localized with the detection of the transcripts shown in (**A**) (arrows). (**D**) In some cyclopamine treated embryos (n = 4/11), *Vsx2* expression was restricted to the ventral part of the optic cup (dashed lines), whereas no transcripts were found in the dorsal part (arrowhead). (**E**-**F**) VSX2 protein detection is congruent with *Vsx2* expression and limited to the ventral part of the presumptive retina (arrowheads and dashed lines). The asterisk marks the position of the implanted bead. Scale bar 100 µm.

4.8 BMP7 and constitutive active hSMAD1 are able to rescue VSX2 following the inhibition of SHH signaling

Together with previous studies my results suggest that the SHH and BMP signaling pathways act in concert or by regulating themselves to induce a NR cell fate in optic vesicle cells (Dale et al, 1997; Sehgal et al., 2009). Moreover, inhibition of the SHH signaling pathway using cyclopamine caused a decrease of BMP7 protein level in retinal astrocytes of rats (Sehgal et al., 2009). If SHH acts upstream of BMPs, then downregulation of *Vsx2* expression following SHH inhibition might be a consequence of the lack of BMP signaling. In order to determine whether BMP7 and/or SMAD1 are able to restore VSX2 following SHH inhibition, I carried out two rescue experiments. First, I inhibited the SHH signaling pathway using cyclopamine and simultaneously activated the BMP signaling pathway by implanting a BMP7 soaked bead at HH10 (Figure 23A). One day following manipulation, formation of an optic cup was observed (Figure 23B, n = 6/6). Despite the inhibition of the SHH signaling

pathway, application of BMP7 was sufficient to rescue VSX2 expression in the retinal tissue (Figure 23C-D'; n = 3/3).

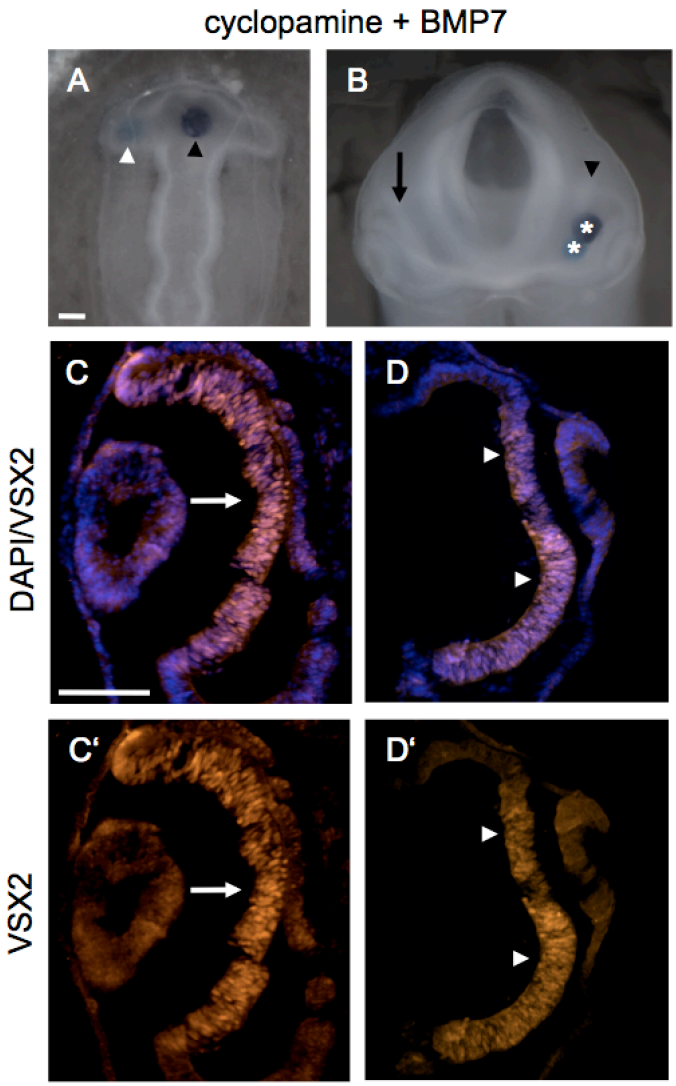

Figure 23: BMP7 rescues VSX2 following SHH inhibition. (**A**) The manipulation occurred by the implantation of two beads simultaneously into the optic vesicle of a HH10 embryo. A BMP7 soaked agarose bead (white arrowhead) was implanted into the left optic vesicle of a HH10 embryo and followed by a cyclopamine soaked resin bead (black arrowhead). (**B**) One day following manipulation the embryos were fixed at HH15/16. The treated side developed a proper optic cup (arrowhead), when compared with the untreated side (arrow). The asterisks mark the implanted beads. (**C**, **C'**) The implantation of a DMSO and a PBS soaked bead, as control experiment, had no influence on the formation of a proper optic cup and detection of VSX2 (arrows, images courtesy of Tina Uhlmer). (**D**, **D'**) Following SHH inhibition, BMP7 was sufficient to rescue VSX2 within the presumptive retina (arrowheads). n = 3/3, scale bars 100 µm.

In the second set of the rescue experiments, I implanted cyclopamine beads and simultaneously electroporated CA-hSMAD1-EVEMM and a GFP construct at HH10 (Figure 24A). The embryos were analyzed two days following the manipulation at HH24/25 and the formation of an optic cup with a lens vesicle was observed (Figure 24B, n = 5/5). On the contralateral side VSX2 expression was restricted to the dorsal and central retina,

whereas in the ventral part expression was affected presumably due to the influence of the implanted cyclopamine beads (Figure 24C). As seen with BMP7 application, CA-hSMAD1-EVEMM was able to restore VSX2 expression within the dorsal retinal tissue (Figure 24D; n = 3/3; compare also with Figure 21 and 22). Ectopic VSX2 expression was also detected in the ventral GFP-positive region of the optic cup (Figure 24D-F''). In summary, the results suggest that SHH might act upstream of the BMP signaling pathway to initiate NR development via SMAD1 in multipotent optic vesicle cells.

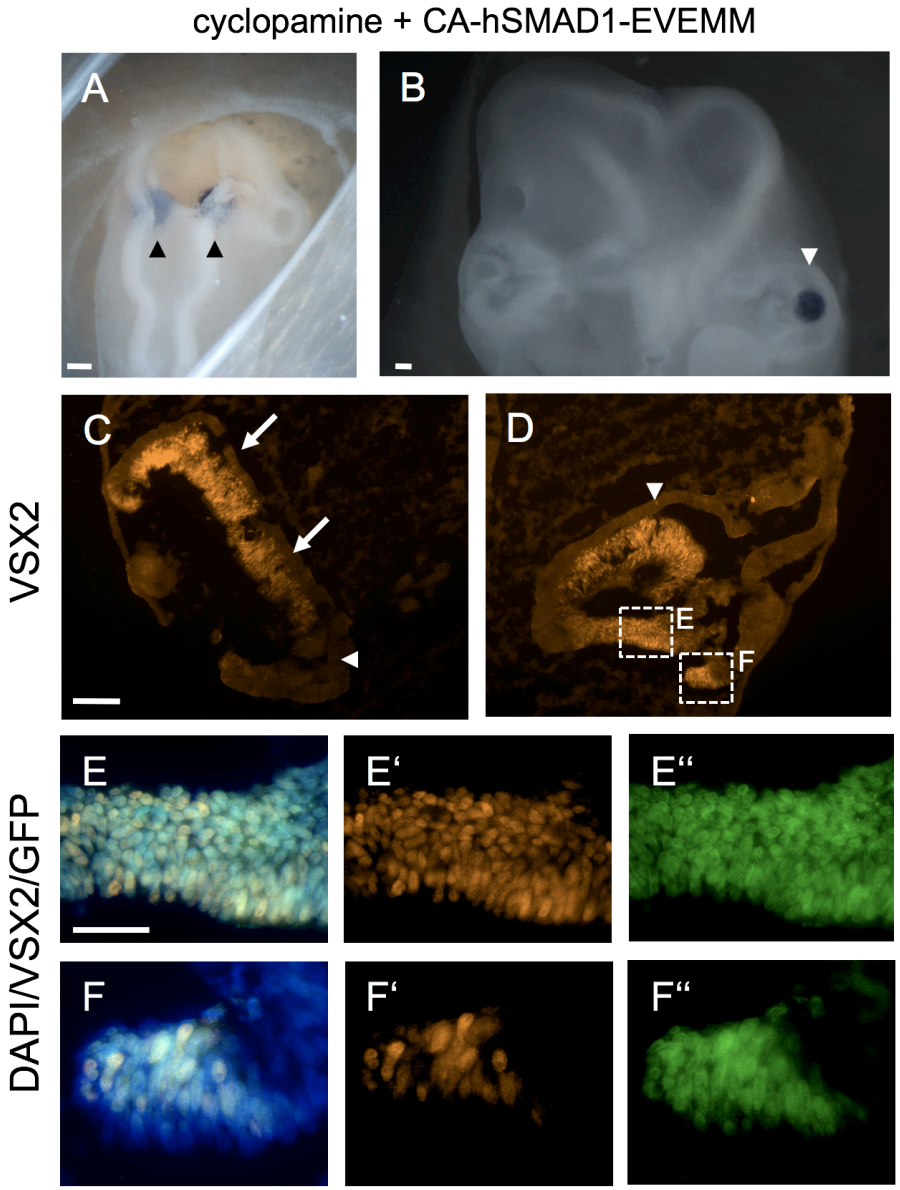

Figure 24: Constitutive active hSMAD1 rescues VSX2 following inhibition of the SHH signaling pathway. (**A**) Two resin beads soaked in cyclopamine were implanted in the left optic vesicle and ventral midline of a HH10 staged embryo (arrowheads), after a constitutive active form of hSMAD1 was electroporated into the left optic vesicle. (**B**) Two days following the manipulation, the optic cup of the treated eyes was malformed (arrowhead). (**C**) VSX2 was detectable in the dorsal and central part of the untreated contralateral eye (arrows). The detection of VSX2 was lost in the ventral part of the untreated eye (arrowhead). (**D**) VSX2 detection was rescued in the dorsal part of the eye (arrowhead) and ectopically induced in the ventral part of the treated eye (two white dashed rectangles). (**E-E''**) Detailed section of the ectopic induced NR (E in D). (**F-F''**) Detailed section of the ectopic induced NR (F in D). Ectopic VSX2 protein was detected in the GFP-positive ventral region of the optic cup. Scale bars in A-D 100 µm; E-F'' 25 µm.

5 Discussion

The proximo-distal model of vertebrate eye development assumes, that surface ectoderm-derived signals induce retinal progenitor cells in distally located optic vesicle cells. The present thesis shows for the first time in the developing chick embryo, that signals released from the surface ectoderm are not involved in NR specification. Furthermore, I demonstrate that ventral midline-derived SHH and BMP signals are involved in NR specification. These results suggest that the optic vesicle is initially patterned into a dorsal RPE and ventral NR domain.

5.1 Signals released from the ventral midline are required for NR induction in the developing chick embryo

The formation of a proper vertebrate eye requires the interaction of the neuroepithelium of the optic vesicle with the surface ectoderm (see introduction). Following removal of the surface ectoderm a pigmented vesicle develops and NR development is not observed (Hyer et al., 1998). Recently, it has been proposed that surface ectoderm-derived BMP4 induces NR development and regulates *Fgf8* expression within the presumptive chick NR (Pandit et al., 2015). Similarly, in conditional *Bmp4* knockout mice *Fgf15* expression is downregulated and proliferation of retinal progenitor cells within the presumptive NR is reduced (Huang et al., 2015b). These studies suggested that the surface ectoderm is not only necessary to induce NR identity but also appears to regulate proliferation of the underlying neuroepithelial cells. However, my results show that at the time of NR specification removal of the surface ectoderm and thereby the removal of the physiological source of BMPs and FGFs does not affect *Vsx2* expression in the underlying optic vesicle cells (Figure 17). This finding is in contradiction to the proximo-distal model, which attributes the surface ectoderm a fundamental role in NR induction (reviewed in Fuhrmann, 2010). It seems that the signal which induces *Vsx2*-expressing retinal progenitor cells during the initial stages of eye development derives from a different source. The optic vesicles at HH10 are symmetrical and have a dorso-ventral polarity (Uemonsa et al. 2002; Kagiyama et al., 2005; Hirashima et al., 2008; Kobayashi et al., 2010). When the dorsal or ventral forebrain region including the optic vesicles is separately placed in culture only the ventral part is able to give rise to NR. Here the authors proposed that the ventral midline might establish the ventral identity of the optic vesicle. My results show that the excision of the ventral midline at HH10 leads in a few cases to a downregulation of *Vsx2* expression (Figure 19). That a signal released from the

midline region of the forebrain region and not from the surface ectoderm induces *Vsx2* expression in the optic vesicle is further supported by *in vitro* studies carried out in our laboratory (Ichie Steinfeld, unpublished data). Here, the optic vesicles were isolated before NR specification had occurred (HH9-10 staged embryos) and the surface ectoderm removed. The treated optic vesicles were then implanted back to a host embryo. In the absence of the surface ectoderm the transplanted optic vesicle started to express *Vsx2* one day following the manipulation.

5.2 FGF signaling does not appear to be involved in inducing NR development

FGF signaling via MAPK/ERK pathway appears to be involved in NR induction in vertebrates (Figure 9; de Longh and McAvoy, 1993; Pittack et al., 1997; McWirther et al. 1997; Reifers et al., 1998; Vogel-Höpker et al., 2000; Kurose et al., 2005). Several FGF ligands and their receptors are expressed in optic vesicle cells and surrounding tissues at the time of NR induction. In fact, numerous studies have shown that FGFs are able to convert embryonic RPE into NR (Pittack et al., 1991, 1997; Guillemont and Cepko, 1992; Opas and Dziak, 1994; Hyer et al., 1998; Nguyen and Arnheiter, 2000; Vogel-Höpker et al., 2000). Following the inhibition of MEK1/2, *Vsx2* expression was downregulated suggesting its involvement in NR specification (see Figure 9). Vice versa, the ectopic overexpression of MEK1 in chicken embryo caused a depigmentation of the RPE and a conversion into a NR-like structure (Galy et al., 2002). It should be taken into consideration that this experiment was carried out at stage HH15 (see material and methods in Galy et al., 2002), when retinal progenitor cells have already been specified (Chen and Cepko, 2000). In order to explore, whether another downstream target of the FGF signaling pathway is necessary to induce NR cell fate, I inhibited ERK1/2, which is known to be the direct target of MEK1/2 (Figure 10). Surprisingly, *Vsx2* expression appeared not to be altered in optic vesicle cells, suggesting that the FGF/MAPK pathway is not involved in NR induction. Indeed, *Fgf1* and *Fgf2* single and *Fgf1* and *Fgf2* double knockout mice do not display evident eye defects (Dono et al., 1998; Ortega et al., 1998; Miller et al., 2000). This suggests that an alternative signaling pathway is involved in NR specification in vertebrates.

5.3 The BMP signaling pathway is active during NR specification in the chick

Recent studies suggested that BMP signaling derived from the surface ectoderm is involved in NR specification (Pandit et al., 2015; Huang et al., 2015a; Huang et al., 2015b). Retinal progenitor cells are first detected in the distal optic vesicle at HH10 in the developing chick embryo as visualised by the expression of *Vsx2* (Figure 11; Chen and Cepko, 2000). *Bmp4* and *Bmp7* transcripts are detected in the overlying surface ectoderm, while *Bmp2* and *Bmp7* transcripts are detected in the ventral midline region at the time point of NR induction (Figure 18; Furuta et al., 1997; Furuta and Hogan, 1998; Crossley et al, 2001; Manning et al., 2006; Müller et al., 2007). At the same time, transcripts of *BmpR* IA and IB are found both in the surface ectoderm, midline region and presumptive NR (Zou et al., 1997; Furuta and Hogan, 1998; Hyer et al., 2003; Lim et al., 2005). The spatio-temporal expression pattern of BMP ligands and their receptors support a possible involvement of BMP signaling pathway during NR specification in the chick. My results show that the BMP signaling pathway is active at the time of NR cell fate induction; this applies for both the *Bmp*-expressing surface ectoderm and the presumptive NR (Figure 11).

5.4 BMP signaling is involved in NR specification in the chick

Functional studies that indicate an involvement of the BMP signaling pathway in NR specification are provided by studies of *Bmp* gene knockout mice. Here, especially *Bmp7* knockout mice display a fully pigmented eye without any retinal morphology and *Vsx2* expression is not observed (Morcillo et al., 2006). *BmpR* IA and IB mediate the phosphorylation of SMAD1/5/8 (Derynck and Zhang, 2003) and conditional *BmpR* IA and IB double knockout mice lacks *Vsx2* expression in retinal cells (Murali et al., 2005). In this thesis, I confirm these results and show that following inhibition of the BMP signaling pathway eye development is severely affected and *Vsx2* expression is not observed (Figure 12). In contrast, inhibition of the TGF-β signaling pathway did not appear to affect *Vsx2* expression (Figure 13). Remarkably, following BMPR inhibition and simultaneous overexpression of constitutive activated SMAD1, *Vsx2* expression is ectopically induced in the developing chick embryo (Figure 14). These findings show that BMPR-mediated SMAD1(/5/8) phosphorylation is sufficient to induce *Vsx2*-expressing retinal progenitor cells in the chick.

As described above, MEK1/2 inhibition results in the downregulation of *Vsx2* expression in optic vesicle cells (Figure 9). Similar to FGFs, BMP signaling can activate the MAPK

signaling pathway and hence MEK1/2 (Derynck and Zhang, 2003; Bragdon et al., 2011). Therefore, it is possible that initiation of *Vsx2* expression in optic vesicle cells is mediated by the activation of MEK1/2 in an ERK1/2-independent way (see above). To test this hypothesis, I carried out rescue experiments following MEK1/2 inhibition (Figure 15 and Figure 16). Inhibition of MEK1/2 using U0126 soaked beads and the simultaneous activation of the BMP signaling pathway resulted in a conversion of the ventral RPE into *Vsx2*-expressing NR. Moreover, inhibition of MEK1/2 and the simultaneous overexpression of constitutive activated SMAD1 also rescued VSX2 expression in chick optic vesicle cells. Thus, MEK1/2 does not appear to be a downstream target during BMP-induced NR specification in the chick. Further work is required to clarify whether MEK1/2 is involved in NR specification in vertebrates.

5.5 SHH appears to act upstream of the BMP signaling pathway

At the time of NR specification, the ventral midline region in the chick expresses both *Bmps* and *Shh* (Figure 18 and 20). My results show that SHH signaling is involved in initiating NR development in the chick (Figure 21 and 22). Inhibition of SHH signaling caused a dramatic downregulation or loss of *Vsx2* expression, whereas the RPE-specific marker MITF was distally induced. In a few cases *Vsx2* expression was still detected in the ventral optic vesicle/cup (Figure 22). A possible reason for this might be the provenance of the cells and the exposure to position-dependent signals. Fate mapping studies using DiI-crystals indicate that cells of the ventral optic vesicle (HH10) move dorsally and end up in the dorsal optic cup (diploma thesis Meggi-Lee Hampel and Tamara Migge; Manning et al., 2006; Venters et al., 2015). Thus, it might be possible that short-term exposure to cyclopamine following bead implantation only affected dorsal NR cells.

The finding that the inhibition of both BMP and SHH signaling results in a downregulation of *Vsx2* suggests that both pathways are essential to specify NR cell fate. Interestingly, following SHH inhibition both exogenous BMP7 application and constitutive activated hSMAD1 were able to restore VSX2 expression in the NR. Moreover, the ventral RPE transformed into VSX2-positive NR-like tissue (Figure 23 and Figure 24). These findings suggest that the SHH signaling pathway acts upstream of the BMP signaling pathway to induce *Vsx2*-expressing retinal progenitor cells in multipotent optic vesicle cells. However, the exact molecular mechanism remains to be clarified.

5.6 BMPs are involved in optic cup formation

Signals released from the surface ectoderm are required for optic cup formation (Hyer et al., 2003). Here, I confirm that the surface ectoderm is required to form a proper optic cup (Figure 17; Hyer et al., 1998; Hyer et al., 2003; Nguyen and Arnheiter, 2000; Steinfeld et al., 2013). In contrast, removal of the midline region had no effect on optic cup formation (Figure 19). BMPs released from the surface ectoderm appear to be involved in optic cup formation. Following the inhibition of the BMP/SMAD1/5/8 signaling pathway, formation of the optic cup is not observed (Figure 12). This is consistent with our previously published observation, which shows that BMPs are able to rescue optic cup formation following surface ectoderm removal in the chick embryo (Steinfeld et al., 2013). Moreover, following inhibition of the BMP signaling pathway, eye development regresses and/or invagination of the distal region of the optic vesicle is not observed (Figure 12; Steinfeld et al., 2013; Huang et al., 2015a). It has been proposed that in *Bmp4* knockout mice this phenomenon might be due to the reduced proliferation rate of optic vesicle cells (Huang et al., 2015a; Huang et al., 2015b). Considering previous studies and my observations, the surface ectoderm appears to be necessary (i) to induce an RPE cell fate in optic vesicle cells (Steinfeld et al., 2013), (ii) for proper formation of the optic cup (Hyer et al., 1998; Hyer et al., 2003; Nguyen and Arnheiter, 2000; Steinfeld et al., 2013 and this study) and (iii) by expressing signals such as BMP and FGF to promote a proper proliferation of the presumptive NR tissue (Huang et al., 2015a; Huang et al., 2015b; Pandit et al., 2015).

5.7 Dorso-ventral model of optic vesicle patterning in the chicken embryo

The findings obtained in this thesis leads to a dorso-ventral model of optic vesicle patterning in vertebrates. While in the dorsal part of the optic vesicle surface ectoderm-derived BMP and WNT signaling induce and stabilize an RPE cell fate (Steinfeld et al., 2013), the NR is specified in optic vesicle cells by SHH and BMP signals derived from the ventral midline. Once the NR cells have been specified, FGF and BMP signaling derived from the surface ectoderm may maintain the acquired identity of NR cells and ensure optic cup formation during vertebrate eye development (Figure 25).

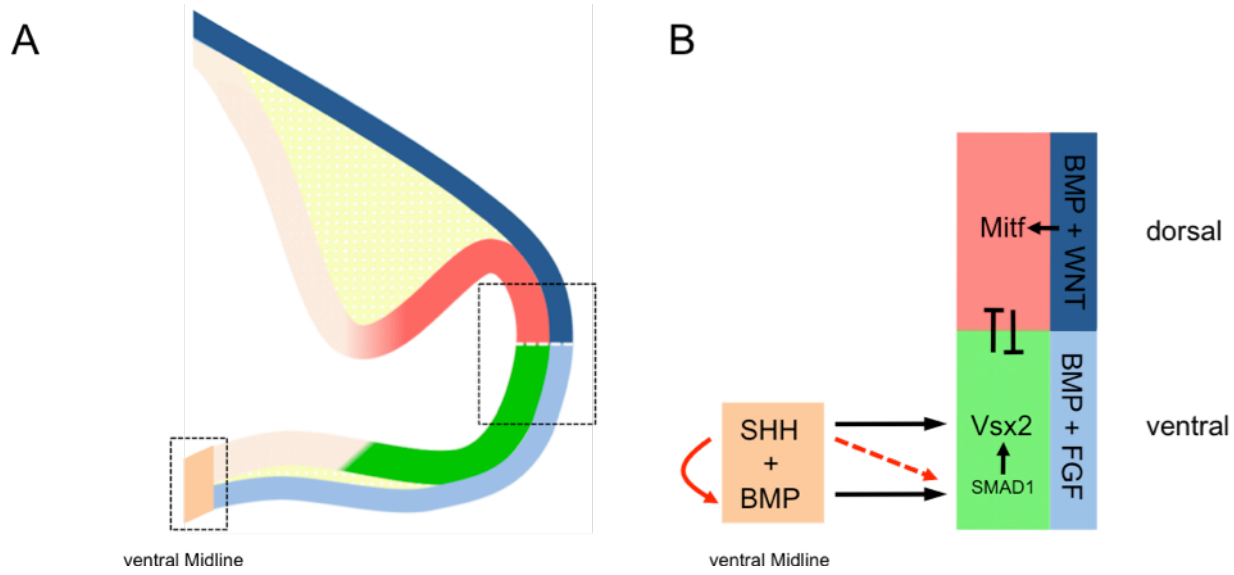

Figure 25: Proposed dorso-ventral model of optic vesicle patterning in the developing chick embryo. (**A**) The optic vesicle is patterned into a dorsal RPE (red) and ventral NR (green) domain in the chick embryo. The dorsal surface ectoderm is indicated in dark blue and the ventral surface ectoderm in light blue. (**B**) BMPs and WNTs released from the dorsal surface ectoderm (dark blue) specify the RPE by inducing *Mitf* expression in the underlying optic vesicle (Steinfeld et al., 2013). SHH and BMP derived from the ventral midline (orange) are both involved in inducing a NR cell fate in the ventral region of the optic vesicle. SHH acts upstream of BMP signaling (red arrows) to specify the NR. BMP-induced phosphorylation of SMAD1/5/8 induces *Vsx2*-expressing retinal progenitor cells. Surface ectoderm-derived FGF and BMP signaling (light blue) then maintain NR identity and proliferation to ensure proper development of the optic cup.

5.8 Conclusion and further direction

During embryonic development, the highly coordinated spatio-temporal gene expression results in proper formation of organs and whole organisms. The findings presented in this thesis give insight, on how uncommitted neuroepithelial cells of the optic vesicle are instructed to develop into retinal progenitor cells. These new findings could be of interest for regenerative ophthalmologists and help to improve current *in vitro* protocols, which are aimed to generate sufficient NR tissue required for successful transplantations.

6 Literature

Adler, R., and Canto-Soler, M.V. (2007). Molecular mechanisms of optic vesicle development: complexities, ambiguities and controversies. *Developmental biology* **305**, 1-13.

Belloni, E., Muenke, M., Roessler, E., Traverso, G., Siegel-Bartelt, J., Frumkin, A., Mitchell, H.F., Donis-Keller, H., Helms, C., Hing, A.V., et al. (1996). Identification of Sonic hedgehog as a candidate gene responsible for holoprosencephaly. *Nature genetics* **14**, 353-356.

Bora, N., Conway, S.J., Liang, H., and Smith, S.B. (1998). Transient overexpression of the Microphthalmia gene in the eyes of Microphthalmia vitiligo mutant mice. *Developmental dynamics: an official publication of the American Association of Anatomists* **213**, 283-292.

Bragdon, B., Moseychuk, O., Saldanha, S., King, D., Julian, J., and Nohe, A. (2011). Bone Morphogenetic Proteins: A critical review. *Cellular signalling* **23**, 609-620.

Burmeister, M., Novak, J., Liang, M.Y., Basu, S., Ploder, L., Hawes, N.L., Vidgen, D., Hoover, F., Goldman, D., Kalnins, V.I., et al. (1996). Ocular retardation mouse caused by Chx10 homeobox null allele: impaired retinal progenitor proliferation and bipolar cell differentiation. *Nature genetics* **12**, 376-384.

Cai, Z., Feng, G.S., and Zhang, X. (2010). Temporal requirement of the protein tyrosine phosphatase Shp2 in establishing the neuronal fate in early retinal development. *The Journal of neuroscience: the official journal of the Society for Neuroscience* **30**, 4110-4119.

Chen, C.M., and Cepko, C.L. (2000). Expression of Chx10 and Chx10-1 in the developing chicken retina. *Mechanisms of development* **90**, 293-297.

Chiang, C., Litingtung, Y., Lee, E., Young, K.E., Corden, J.L., Westphal, H., and Beachy, P.A. (1996). Cyclopia and defective axial patterning in mice lacking Sonic hedgehog gene function. *Nature* **383**, 407-413.

Chow, R.L., and Lang, R.A. (2001). Early eye development in vertebrates. *Annual review of cell and developmental biology* **17**, 255-296.

Connolly, D.J., Patel, K., Seleiro, E.A., Wilkinson, D.G., and Cooke, J. (1995). Cloning, sequencing, and expressional analysis of the chick homologue of follistatin. *Developmental genetics* **17**, 65-77.

Crossley, P.H., Martinez, S., Ohkubo, Y., and Rubenstein, J.L. (2001). Coordinate expression of Fgf8, Otx2, Bmp4, and Shh in the rostral prosencephalon during development of the telencephalic and optic vesicles. *Neuroscience* **108**, 183-206.

DaCosta Byfield, S., Major, C., Laping, N.J., and Roberts, A.B. (2004). SB-505124 is a selective inhibitor of transforming growth factor-beta type I receptors ALK4, ALK5, and ALK7. *Molecular pharmacology* **65**, 744-752.

Dale, J.K., Vesque, C., Lints, T.J., Sampath, T.K., Furley, A., Dodd, J., and Placzek, M. (1997). Cooperation of BMP7 and SHH in the induction of forebrain ventral midline cells by prechordal mesoderm. *Cell* **90**, 257-269.

Davies, S.P., Reddy, H., Caivano, M., and Cohen, P. (2000). Specificity and mechanism of action of some commonly used protein kinase inhibitors. *The Biochemical journal* **351**, 95-105.

de longh, R., and McAvoy, J.W. (1993). Spatio-temporal distribution of acidic and basic FGF indicates a role for FGF in rat lens morphogenesis. *Developmental dynamics: an official publication of the American Association of Anatomists* **198**, 190-202.

Derynck, R., and Zhang, Y.E. (2003). Smad-dependent and Smad-independent pathways in TGF-beta family signalling. *Nature* **425**, 577-584.

Dragomirov N. 1937. The influence of neighboring ectoderm on the organization of eye rudiment. *Doklady Akademii Nauk SSSR* **15**, 61–64.

Dohrmann, C.E., Hemmati-Brivanlou, A., Thomsen, G.H., Fields, A., Woolf, T.M., and Melton, D.A. (1993). Expression of activin mRNA during early development in Xenopus laevis. *Developmental biology* **157**, 474-483.

Dono, R., Texido, G., Dussel, R., Ehmke, H., and Zeller, R. (1998). Impaired cerebral cortex development and blood pressure regulation in FGF-2-deficient mice. *The EMBO journal* **17**, 4213-4225.

Dorey, K., and Amaya, E. (2010). FGF signalling: diverse roles during early vertebrate embryogenesis. *Development* **137**, 3731-3742.

Echelard, Y., Epstein, D.J., St-Jacques, B., Shen, L., Mohler, J., McMahon, J.A., and McMahon, A.P. (1993). Sonic hedgehog, a member of a family of putative signaling molecules, is implicated in the regulation of CNS polarity. *Cell* **75**, 1417-1430.

Ekker, S.C., Ungar, A.R., Greenstein, P., von Kessler, D.P., Porter, J.A., Moon, R.T., and Beachy, P.A. (1995). Patterning activities of vertebrate hedgehog proteins in the developing eye and brain. *Current biology* **5**, 944-955.

Esteve, P., and Bovolenta, P. (2006). Secreted inducers in vertebrate eye development: more functions for old morphogens. *Current opinion in neurobiology* **16**, 13-19.

Favata, M.F., Horiuchi, K.Y., Manos, E.J., Daulerio, A.J., Stradley, D.A., Feeser, W.S., Van Dyk, D.E., Pitts, W.J., Earl, R.A., Hobbs, F., et al. (1998). Identification of a novel inhibitor of mitogen-activated protein kinase kinase. *The Journal of biological chemistry* **273**, 18623-18632.

Feijen, A., Goumans, M.J., and van den Eijnden-van Raaij, A.J. (1994). Expression of activin subunits, activin receptors and follistatin in postimplantation mouse embryos suggests specific developmental functions for different activins. *Development* **120**, 3621-3637.

Fuentealba, L.C., Eivers, E., Ikeda, A., Hurtado, C., Kuroda, H., Pera, E.M., and De Robertis, E.M. (2007). Integrating Patterning Signals: Wnt/GSK3 Regulates the Duration of the BMP/Smad1 Signal. *Cell* **131**, 980-993.

Fuhrmann, S. (2010). Eye morphogenesis and patterning of the optic vesicle. *Current topics in developmental biology* **93**, 61-84.

Fuhrmann, S., Levine, E.M., and Reh, T.A. (2000). Extraocular mesenchyme patterns the optic vesicle during early eye development in the embryonic chick. *Development* **127**, 4599-4609.

Furuta, Y., and Hogan, B.L. (1998). BMP4 is essential for lens induction in the mouse embryo. *Genes & development* **12**, 3764-3775.

Furuta, Y., Piston, D.W., and Hogan, B.L. (1997). Bone morphogenetic proteins (BMPs) as regulators of dorsal forebrain development. *Development* **124**, 2203-2212.

Galy, A., Neron, B., Planque, N., Saule, S., and Eychene, A. (2002). Activated MAPK/ERK kinase (MEK-1) induces transdifferentiation of pigmented epithelium into neural retina. *Developmental biology* **248**, 251-264.

Geetha-Loganathan, P., Nimmagadda, S., Christ, B., Huang, R., and Scaal, M. (2010). Ectodermal Wnt6 is an early negative regulator of limb chondrogenesis in the chicken embryo. *BMC developmental biology* **10**, 32.

Gotoh, N., Ito, M., Yamamoto, S., Yoshino, I., Song, N., Wang, Y., Lax, I., Schlessinger, J., Shibuya, M., and Lang, R.A. (2004). Tyrosine phosphorylation sites on FRS2alpha responsible for Shp2 recruitment are critical for induction of lens and retina. *Proceedings of the National Academy of Sciences of the United States of America* **101**, 17144-17149.

Green, E.S., Stubbs, J.L., and Levine, E.M. (2003). Genetic rescue of cell number in a mouse model of microphthalmia: interactions between Chx10 and G1-phase cell cycle regulators. *Development* **130**, 539-552.

Guillemot, F., and Cepko, C.L. (1992). Retinal fate and ganglion cell differentiation are potentiated by acidic FGF in an in vitro assay of early retinal development. *Development* **114**, 743-754.

Hamburger, V., and Hamilton, H.L. (1951). A series of normal stages in the development of the chick embryo. *Journal of morphology* **88**, 49-92.

Herpin, A., and Cunningham, C. (2007). Cross-talk between the bone morphogenetic protein pathway and other major signaling pathways results in tightly regulated cell-specific outcomes. *The FEBS journal* **274**, 2977-2985.

Hirashima, M., Kobayashi, T., Uchikawa, M., Kondoh, H., and Araki, M. (2008). Anteroventrally localized activity in the optic vesicle plays a crucial role in the optic development. *Developmental biology* **317**, 620-631.

Holtfreter J. (1939). Gewebeaffinität, ein Mittel der embryonalen Formbildung. *Archiv für experimentelle Zellforschung, besonders Gewebezüchtung* **23**, 169–209.

Horbelt, D., Boergermann, J.H., Chaikuad, A., Alfano, I., Williams, E., Lukonin, I., Timmel, T., Bullock, A.N., and Knaus, P. (2015). Small molecules dorsomorphin and LDN-193189 inhibit myostatin/GDF8 signaling and promote functional myoblast differentiation. *The Journal of biological chemistry* **290**, 3390-3404.

Horsford, D.J., Nguyen, M.T., Sellar, G.C., Kothary, R., Arnheiter, H., and McInnes, R.R. (2005). Chx10 repression of Mitf is required for the maintenance of mammalian neuroretinal identity. *Development* **132**, 177-187.

Huang, J., Liu, Y., Filas, B., Gunhaga, L., and Beebe, D.C. (2015a). Negative and positive auto-regulation of BMP expression in early eye development. *Developmental biology* **407**, 256-264.

Huang, J., Liu, Y., Oltean, A., and Beebe, D.C. (2015b). Bmp4 from the optic vesicle specifies murine retina formation. *Developmental biology* **402**, 119-126.

Hyer, J., Kuhlman, J., Afif, E., and Mikawa, T. (2003). Optic cup morphogenesis requires pre-lens ectoderm but not lens differentiation. *Developmental biology* **259**, 351-363.

Hyer, J., Mima, T., and Mikawa, T. (1998). FGF1 patterns the optic vesicle by directing the placement of the neural retina domain. *Development* **125**, 869-877.

Jasoni, C., Hendrickson, A., and Roelink, H. (1999). Analysis of chicken Wnt-13 expression demonstrates coincidence with cell division in the developing eye and is consistent with a role in induction. *Developmental dynamics: an official publication of the American Association of Anatomists* **215**, 215-224.

Kagiyama, Y., Gotouda, N., Sakagami, K., Yasuda, K., Mochii, M., and Araki, M. (2005). Extraocular dorsal signal affects the developmental fate of the optic vesicle and patterns the optic neuroepithelium. *Development, growth & differentiation* **47**, 523-536.

Kobayashi, T., Yasuda, K., and Araki, M. (2010). Coordinated regulation of dorsal bone morphogenetic protein 4 and ventral Sonic hedgehog signaling specifies the dorso-ventral polarity in the optic vesicle and governs ocular morphogenesis through fibroblast growth factor 8 upregulation. *Development, growth & differentiation* **52**, 351-363.

Kurose, H., Okamoto, M., Shimizu, M., Bito, T., Marcelle, C., Noji, S., and Ohuchi, H. (2005). FGF19-FGFR4 signaling elaborates lens induction with the FGF8-L-Maf cascade in the chick embryo. *Development, growth & differentiation* **47**, 213-223.

Layer, P.G., Araki, M. and Vogel-Höpker, A. (2010). New concepts for reconstruction of retinal and pigment epithelial tissues. *Expert Review of Ophthalmology* ***5*****(4)**, 523-543.

Li, H., Tierney, C., Wen, L., Wu, J.Y., and Rao, Y. (1997). A single morphogenetic field gives rise to two retina primordia under the influence of the prechordal plate. *Development* **124**, 603-615.

Lim, Y., Cho, G., Minarcik, J., and Golden, J. (2005). Altered BMP signaling disrupts chick diencephalic development. *Mechanisms of development* **122**, 603-620.

Liu, I.S., Chen, J.D., Ploder, L., Vidgen, D., van der Kooy, D., Kalnins, V.I., and McInnes, R.R. (1994). Developmental expression of a novel murine homeobox gene (Chx10): evidence for roles in determination of the neuroretina and inner nuclear layer. *Neuron* **13**, 377-393.

Lopashov G.V., Stroeva O.G. (1964). Development of the Eye. *New York: Davey & Co*.

Lunn, J.S., Fishwick, K.J., Halley, P.A., and Storey, K.G. (2007). A spatial and temporal map of FGF/Erk1/2 activity and response repertoires in the early chick embryo. *Developmental biology* **302**, 536-552.

Mangold, O. (1931). Das Determinationsproblem. III. Das Wirbeltierauge in der Entwicklung und Regeneration. *Ergebnisse der Biologie* **7**, 193-403.

Manning, L., Ohyama, K., Saeger, B., Hatano, O., Wilson, S.A., Logan, M., and Placzek, M. (2006). Regional morphogenesis in the hypothalamus: a BMP-Tbx2 pathway coordinates fate and proliferation through Shh downregulation. *Developmental cell* **11**, 873-885.

McWhirter, J.R., Goulding, M., Weiner, J.A., Chun, J., and Murre, C. (1997). A novel fibroblast growth factor gene expressed in the developing nervous system is a downstream target of the chimeric homeodomain oncoprotein E2A-Pbx1. *Development* **124**, 3221-3232.

Mikami Y. (1939). Reciprocal transformation of the parts in the developing eye-vesicle, with special reference to the inductive influence of the lens-ectoderm on the retinal determination. *Zoological Magazine* **51**, 253–56.

Miller, D.L., Ortega, S., Bashayan, O., Basch, R., and Basilico, C. (2000). Compensation by fibroblast growth factor 1 (FGF1) does not account for the mild phenotypic defects observed in FGF2 null mice. *Molecular and cellular biology* **20**, 2260-2268.

Mochii, M., Mazaki, Y., Mizuno, N., Hayashi, H., and Eguchi, G. (1998). Role of Mitf in differentiation and transdifferentiation of chicken pigmented epithelial cell. *Developmental biology* **193**, 47-62.

Morcillo, J., Martinez-Morales, J.R., Trousse, F., Fermin, Y., Sowden, J.C., and Bovolenta, P. (2006). Proper patterning of the optic fissure requires the sequential activity of BMP7 and SHH. *Development* **133**, 3179-3190.

Müller, F., Rohrer, H., and Vogel-Höpker, A. (2007). Bone morphogenetic proteins specify the retinal pigment epithelium in the chick embryo. *Development* **134**, 3483-3493.

Murali, D., Yoshikawa, S., Corrigan, R.R., Plas, D.J., Crair, M.C., Oliver, G., Lyons, K.M., Mishina, Y., and Furuta, Y. (2005). Distinct developmental programs require different levels of Bmp signaling during mouse retinal development. *Development* **132**, 913-923.

Nakamura, H., Katahira, T., Sato, T., Watanabe, Y., and Funahashi, J. (2004). Gain- and loss-of-function in chick embryos by electroporation. *Mechanisms of development* **121**, 1137-1143.

Nguyen, M., and Arnheiter, H. (2000). Signaling and transcriptional regulation in early mammalian eye development: a link between FGF and MITF. *Development* **127**, 3581-3591.

Opas, M., and Dziak, E. (1994). bFGF-induced transdifferentiation of RPE to neuronal progenitors is regulated by the mechanical properties of the substratum. *Developmental biology* **161**, 440-454.

Ohori, M., Kinoshita, T., Okubo, M., Sato, K., Yamazaki, A., Arakawa, H., Nishimura, S., Inamura, N., Nakajima, H., Neya, M., et al. (2005). Identification of a selective ERK inhibitor and structural determination of the inhibitor-ERK2 complex. *Biochemical and biophysical research communications* **336**, 357-363.

Ortega, S., Ittmann, M., Tsang, S.H., Ehrlich, M., and Basilico, C. (1998). Neuronal defects and delayed wound healing in mice lacking fibroblast growth factor 2. *Proceedings of the National Academy of Sciences of the United States of America* **95**, 5672-5677.

Pandit, T., Jidigam, V.K., Patthey, C., and Gunhaga, L. (2015). Neural retina identity is specified by lens-derived BMP signals. *Development* **142**, 1850-1859.

Park, C.M., and Hollenberg, M.J. (1989). Basic fibroblast growth factor induces retinal regeneration in vivo. *Developmental biology* **134**, 201-205.

Park, C.M., and Hollenberg, M.J. (1991). Induction of retinal regeneration in vivo by growth factors. *Developmental biology* **148**, 322-333.

Pera, E.M., and Kessel, M. (1997). Patterning of the chick forebrain anlage by the prechordal plate. *Development* **124**, 4153-4162.

Pittack, C., Grunwald, G.B., and Reh, T.A. (1997). Fibroblast growth factors are necessary for neural retina but not pigmented epithelium differentiation in chick embryos. *Development* **124**, 805-816.

Pittack, C., Jones, M., and Reh, T.A. (1991). Basic fibroblast growth factor induces retinal pigment epithelium to generate neural retina in vitro. *Development* **113**, 577-588.

Reifers, F., Bohli, H., Walsh, E.C., Crossley, P.H., Stainier, D.Y., and Brand, M. (1998). Fgf8 is mutated in zebrafish acerebellar (ace) mutants and is required for maintenance of midbrain-hindbrain boundary development and somitogenesis. *Development* **125**, 2381-2395.

Sehgal, R., Sheibani, N., Rhodes, S.J., and Belecky Adams, T.L. (2009). BMP7 and SHH regulate Pax2 in mouse retinal astrocytes by relieving TLX repression. *Developmental biology* **332**, 429-443.

Solursh, M., Langille, R.M., Wood, J., and Sampath, T.K. (1996). Osteogenic protein-1 is required for mammalian eye development. *Biochemical and biophysical research communications* **218**, 438-443.

Stavridis, M.P., Lunn, J.S., Collins, B.J., and Storey, K.G. (2007). A discrete period of FGF-induced Erk1/2 signalling is required for vertebrate neural specification. *Development* **134**, 2889-2894.

Steinfeld, J., Steinfeld, I., Coronato, N., Hampel, M.L., Layer, P.G., Araki, M., and Vogel-Höpker, A. (2013). RPE specification in the chick is mediated by surface ectoderm-derived BMP and Wnt signalling. *Development* **140**, 4959-4969.

Stern, C.D., Yu, R.T., Kakizuka, A., Kintner, C.R., Mathews, L.S., Vale, W.W., Evans, R.M., and Umesono, K. (1995). Activin and its receptors during gastrulation and the later phases of mesoderm development in the chick embryo. *Developmental biology* **172**, 192-205.

Tcheng, M., Fuhrmann, G., Hartmann, M.P., Courtois, Y., and Jeanny, J.C. (1994a). Spatial and temporal expression patterns of FGF receptor genes type 1 and type 2 in the developing chick retina. *Experimental eye research* **58**, 351-358.

Tcheng, M., Oliver, L., Courtois, Y., and Jeanny, J.C. (1994b). Effects of exogenous FGFs on growth, differentiation, and survival of chick neural retina cells. *Experimental cell research* **212**, 30-35.

Turner, N., and Grose, R. (2010). Fibroblast growth factor signalling: from development to cancer. *Nature reviews Cancer* **10**, 116-129.

Uemonsa, T., Sakagami, K., Yasuda, K., and Araki, M. (2002). Development of dorsal-ventral polarity in the optic vesicle and its presumptive role in eye morphogenesis as shown by embryonic transplantation and in ovo explant culturing. *Developmental biology* **248**, 319-330.

Venters, S.J., Mikawa, T., and Hyer, J. (2015). Early divergence of central and peripheral neural retina precursors during vertebrate eye development. *Developmental dynamics: an official publication of the American Association of Anatomists* **244**, 266-276.

Vogel-Höpker, A., Momose, T., Rohrer, H., Yasuda, K., Ishihara, L., and Rapaport, D.H. (2000). Multiple functions of fibroblast growth factor-8 (FGF-8) in chick eye development. *Mechanisms of development* **94**, 25-36.

Wanaka, A., Milbrandt, J., and Johnson, E.M., Jr. (1991). Expression of FGF receptor gene in rat development. *Development* **111**, 455-468.

Zhang, X.M., and Yang, X.J. (2001). Temporal and spatial effects of Sonic hedgehog signaling in chick eye morphogenesis. *Developmental biology* **233**, 271-290.

Zhao, S., Hung, F.C., Colvin, J.S., White, A., Dai, W., Lovicu, F.J., Ornitz, D.M., and Overbeek, P.A. (2001). Patterning the optic neuroepithelium by FGF signaling and Ras activation. *Development* **128**, 5051-5060.

Zou, H., Wieser, R., Massague, J., and Niswander, L. (1997). Distinct roles of type I bone morphogenetic protein receptors in the formation and differentiation of cartilage. *Genes & development* **11**, 2191-2203.

Appendix

A1 Declaration / Ehrenwörtliche Erklärung

Ich erkläre hiermit ehrenwörtlich, dass ich die vorliegende Arbeit entsprechend den Regeln guter wissenschaftlicher Praxis selbstständig und ohne unzulässige Hilfe Dritter angefertigt habe.

Sämtliche aus fremden Quellen direkt oder indirekt übernommenen Gedanken sowie sämtliche von Anderen direkt oder indirekt übernommenen Daten, Techniken und Materialien sind als solche kenntlich gemacht. Die Arbeit wurde bisher bei keiner anderen Hochschule zu Prüfungszwecken eingereicht.

Darmstadt, den 09. November 2016

.....
(Nicola Coronato)

A2 Figures contribution

All figures shown in this thesis are results obtained during my experimental work, with the exception of:

Figure 14 and 15: Mrs Meggi-Lee Hampel assisted me during the manipulation

Figure 18: images courtesy of PD Dr. Astrid Vogel-Höpker

Figure 23 C and C': images courtesy of Mrs Tina Uhlmer

A3 Curriculum vitae

Name:	Nicola Coronato
Date of birth:	26th of August 1982
Place of birth:	Darmstadt, Germany
Gender:	Male
Marital status:	Married

Education

Since December 2011	Doctorate, Technische Universität Darmstadt, Germany Institute of Developmental Biology and Neurogenetics (Prof. Layer) Supervisor: PD Dr. Astrid Vogel-Höpker
January – October 2011	Diploma thesis Institute of Developmental Biology and Neurogenetics (Prof. Layer) Supervisor: PD Dr. Astrid Vogel-Höpker Role of retinoic acid during dorso-ventral patterning of the chicken eye
2006 – 2011	Diplom Biologie Technische Universität Darmstadt, Germany
2002 – 2006	Diplom Chemie Technische Universität Darmstadt, Germany Studies without graduation
2002	Abitur / A-levels Bertolt-Brecht-Schule, Darmstadt, Germany

List of publications

Steinfeld, J., Steinfeld, I., Coronato, N., Hampel, M.L., Layer, P.G., Araki, M. and Vogel-Höpker, A. (2013). RPE specification in the chick is mediated by surface ectoderm-derived BMP and Wnt signalling. *Development* **140**, 4959-4969

Steinfeld, J., Steinfeld, I., Bausch, A., Coronato, N., Hampel, M.L., Depner, H., Layer, P.G. and Vogel-Höpker, A. (2016). BMP-induced reprogramming of the retina into RPE requires WNT signalling in the developing chick optic cup. *Biology open*, **Manuscript in revision.**

Coronato, N., Hampel, M.L., Steinfeld, J., Steinfeld, I., Layer, P.G. and Vogel-Höpker, A. Midline-derived BMP signalling is involved in specification of Vsx2-positive retinal progenitor cells during chick eye development. **Manuscript in preparation.**

Conference contribution

International Joint Meeting of the German Society for Cell Biology (DGZ) and the German Society of Developmental Biology (GfE); Heidelberg, Germany, March 20-23, 2013

Poster: The role of BMPs in chick Neural Retina development

17th International Congress of Developmental Biology; Cancun, Mexico, June 16-20, 2013

Poster: The role of BMPs in chick Neural Retina development

21th Biennial Meeting of the International Society for Eye Research; San Francisco, CA, USA, July 20-24, 2014

Poster: BMP signalling induces transdifferentiation of NR cells into RPE in chick

Joint Meeting of the German and French Societies of Developmental Biology; Nürnberg, Germany, March 11-14, 2015

Poster: BMP-mediated midline signaling is involved in retinal cell fate specification in chick

Talks

NeoStem Oncology; Irvine, CA, USA, July 29, 2014

Title: BMP induces transdifferentiation in neural retina

Sue and Bill Gross Stem Cell Research Center, University of Irvine; Irvine, CA, USA, July 31, 2014

Title: Surface ectoderm-derived signals involved in RPE specification and transdifferentiation

Grants and Honors

2015	Travel Grant Gesellschaft für Entwicklungsbiologie (GfE)
2014	Development publication was selected and published in Global Medical Discovery Series

Membership

Since 2011	Gesellschaft für Entwicklungsbiologie e.V. (GfE)

A4 Publication

During the initial phase of my doctorate, I have worked with my colleagues to identify the cellular and molecular signals involved in RPE specification in the chicken embryo (Steinfeld et al., 2013). Here, I contributed to the results shown in Figures 1, 4, 6, 7 and S3 of the attached publication.

© 2013. Published by The Company of Biologists Ltd | Development (2013) 140, 4959-4969 doi:10.1242/dev.096990

RESEARCH ARTICLE

RPE specification in the chick is mediated by surface ectoderm-derived BMP and Wnt signalling

Jörg Steinfeld[1,*], Ichie Steinfeld[1,2,*], Nicola Coronato[1], Meggi-Lee Hampel[1], Paul G. Layer[1], Masasuke Araki[2] and Astrid Vogel-Höpker[1,‡]

ABSTRACT

The retinal pigment epithelium (RPE) is indispensable for vertebrate eye development and vision. In the classical model of optic vesicle patterning, the surface ectoderm produces fibroblast growth factors (FGFs) that specify the neural retina (NR) distally, whereas TGFβ family members released from the proximal mesenchyme are involved in RPE specification. However, we previously proposed that bone morphogenetic proteins (BMPs) released from the surface ectoderm are essential for RPE specification in chick. We now show that the BMP- and Wnt-expressing surface ectoderm is required for RPE specification. We reveal that Wnt signalling from the overlying surface ectoderm is involved in restricting BMP-mediated RPE specification to the dorsal optic vesicle. *Wnt2b* is expressed in the dorsal surface ectoderm and subsequently in dorsal optic vesicle cells. Activation of Wnt signalling by implanting Wnt3a-soaked beads or inhibiting GSK3β at optic vesicle stages inhibits NR development and converts the entire optic vesicle into RPE. Surface ectoderm removal at early optic vesicle stages or inhibition of Wnt, but not Wnt/β-catenin, signalling prevents pigmentation and downregulates the RPE regulatory gene *Mitf*. Activation of BMP or Wnt signalling can replace the surface ectoderm to rescue MITF expression and optic cup formation. We provide evidence that BMPs and Wnts cooperate via a GSK3β-dependent but β-catenin-independent pathway at the level of pSmad to ensure RPE specification in dorsal optic vesicle cells. We propose a new dorsoventral model of optic vesicle patterning, whereby initially surface ectoderm-derived Wnt signalling directs dorsal optic vesicle cells to develop into RPE through a stabilising effect of BMP signalling.

KEY WORDS: Cell fate, Eye, Gsk3β, Mitf, Optic vesicle patterning, Optic cup, Retinal development, Smad, Vsx2

INTRODUCTION

During vertebrate eye development, the optic neuroepithelium is specified into three domains: retinal pigment epithelium (RPE), neural retina (NR) and optic stalk. Once these domain specifications have occurred, the surface ectoderm overlying the presumptive NR thickens to form the lens placode. Subsequently, the distal portion of the optic vesicle (ov) invaginates and a double-layered optic cup develops, connected to the brain by the optic stalk. The external layer of the optic cup forms the single-layered, pigmented RPE and the inner layer develops into the multilayered NR (reviewed by Fuhrmann, 2010).

[1]Fachgebiet Entwicklungsbiologie und Neurogenetik, Technische Universität Darmstadt, Schnittspahnstrasse 13, D-64287 Darmstadt, Germany. [2]Developmental Neurobiology Laboratory, Faculty of Science, Nara Women's University, Nara 630-8506, Japan.
*These authors contributed equally to this work

‡Author for correspondence (vogel@bio.tu-darmstadt.de)

Received 18 April 2013; Accepted 26 September 2013

Little is known about the cellular and molecular mechanisms that lead to the subdivision of the ov into an RPE and NR domain (reviewed by Adler and Canto-Soler, 2007; Fuhrmann, 2010). Members of the transforming growth factor β (TGFβ) superfamily, the hedgehog (HH) and fibroblast growth factor (FGF) families appear to be involved in domain specification by modulating the expression of transcription factors (reviewed by Clegg et al., 2008; Fuhrmann, 2010). The boundaries between the RPE and NR domains are established by the *Microphthalmia-associated transcription factor* (*Mitf*) and the paired-like homeodomain transcription factor *Vsx2*, also known as *Chx10* (Rowan et al., 2004; Horsford et al., 2005). Disruption of the *Mitf* gene in mice leads to a hyperproliferating, unpigmented RPE (reviewed by Bharti et al., 2006). Besides MITF, members of the *orthodenticle-related family of transcription factors*, *Otx1/Otx2*, the paired domain protein *Pax6* and the homeodomain proteins *Vax1/Vax2* and *Lhx2* are involved in RPE development (reviewed by Bharti et al., 2006; Bharti et al., 2011; Bharti et al., 2012; Fuhrmann, 2010; Nishihara et al., 2012; Ou et al., 2013). In both mouse and chick, *Mitf* expression is observed in ov cells before NR commitment. In the mouse, the entire ov initially expresses *Mitf*, whereas in the chick *Mitf* expression is initially restricted to distal ov cells (Nguyen and Arnheiter, 2000; Müller et al., 2007; Ishii et al., 2009). FGFs released from the overlying surface ectoderm appear to repress RPE specification by inducing *Vsx2* expression (Horsford et al., 2005; Nguyen and Arnheiter, 2000). Once NR specification has occurred in the distal ov, *Mitf* expression becomes restricted to the dorsal ov (Nguyen and Arnheiter, 2000; Nakayama et al., 1998; Müller et al., 2007; Ishii et al., 2009). At this stage, the chick ov is divided into a dorsal RPE and ventral NR domain (Kagiyama et al., 2005; Hirashima et al., 2008; Kobayashi et al., 2010).

Activins and BMPs belong to the TGFβ superfamily and appear to be involved in RPE specification (reviewed by Fuhrmann, 2010; Layer et al., 2010). Activin can substitute for the mesenchyme to induce/maintain RPE-specific gene expression in ov explants (Fuhrmann et al., 2000). During early eye development BMP application inhibits NR and optic stalk development, and instead induces RPE (Ohkubo et al., 2002; Hyer et al., 2003; Müller et al., 2007; Kobayashi et al., 2010). By contrast, inhibition of BMP signalling downregulates RPE-specific genes and results in loss of pigmentation (Adler and Belecky-Adams, 2002; Müller et al., 2007).

In several vertebrates, including humans, Wnt family members and their receptors are expressed during the initial stages of eye development, suggesting that Wnt signalling is involved in ov patterning. Overexpression of *Wnt2b* induces *Bmp7* expression and results in thinning of the NR (Ohta et al., 2011), whereas BMP application at ov stages induces *Wnt2b* and *Wnt8b* expression (Müller et al., 2007; Teraoka et al., 2009). By contrast, NR specification requires suppression of *Wnt8b* in the mouse (Liu et al., 2010). However, at the time the RPE and NR are specified, the

Development (2013) doi:10.1242/dev.096990

Wnt/β-catenin signalling pathway is not active in ov cells (reviewed by Fuhrmann, 2010).

Although several growth factors and transcriptional regulators have been identified, we still do not know which tissues are involved in RPE specification and how the different signalling pathways integrate to regulate cell fate decisions within the ov. We previously proposed that the BMP-expressing surface ectoderm rather than the mesenchyme is involved in RPE specification (reviewed by Clegg et al., 2008; Layer et al., 2010). *Mitf* expression is induced in the distal ov just underneath the BMP-expressing surface ectoderm at a time when mesenchymal cells are absent (Müller et al., 2007). Here, we show that BMPs and Wnts are released from the surface ectoderm to specify the RPE. *Wnt2b* is expressed at the right time and place to be involved in directing dorsal ov cells towards an epithelial cell fate. We provide gain-of-function evidence that Wnt-mediated GSK3β inhibition elicits RPE development *in vivo*. Accordingly, interfering with Wnt signalling prevents MITF expression and hence RPE development. Finally, we show that BMPs and Wnts cooperate at the level of pSmad to induce MITF expression in ov cells. We present a new model in which Wnts, via a GSK3β-dependent but β-catenin-independent pathway, stabilise BMP signalling to specify the RPE in dorsal ov cells.

RESULTS

Molecular signals involved in optic vesicle patterning

In the chick, *Mitf* transcripts were first detected in the distal ov underneath the BMP-expressing surface ectoderm at stage 9 (Müller et al., 2007), whereas MITF protein expression was not yet observed (Fig. 1A). At stage 10, MITF protein expression was restricted to the distal ov adjacent to the overlying surface ectoderm (Fig. 1B).

Activation of the BMP signalling pathway results in receptor-mediated phosphorylation (p) of Smad1, 5 and/or 8 (pSmad), an indicator for BMP signalling. We compared the distribution of pSmad and MITF. At stage 10, pSmad was strongly detected in the surface ectoderm and in the nuclei of the entire distal ov (Fig. 1C-D′). At stage 10/11, pSmad labelling appeared to be stronger in the dorsal ov (Fig. 1E,E′). Thus, at ov stages the pattern of pSmad correlates well with the Mitf/MITF expression pattern.

At stage 10/11, when the distal ov is divided into a dorsal *Mitf*- and ventral *Vsx2*-expressing domain, *Bmp4* and *Bmp7* transcripts are still detected throughout the surface ectoderm (Crossley et al., 2001; Müller et al., 2007). This suggests that another signal is involved in progressively restricting *Mitf* expression to the dorsal ov. The Wnt signalling pathway directs dorsal cell fate decisions during embryonic development (reviewed by Klaus and Birchmeier, 2008). Therefore, we next studied the expression patterns of various Wnt family members, such as *Wnt2b*, *Wnt3a* and *Wnt8b* (see also Garcia-Lopez et al., 2004; Rossi et al., 2007; Quinlan et al., 2009; Van Raay and Vetter, 2004). Of the analysed Wnt ligands, only *Wnt2b* transcripts were restricted to the dorsal surface ectoderm and dorsal ov at the time the RPE is specified (Fig. 1G-K). At this time the Wnt/β-catenin signalling is not active in ov cells (Fig. 1F,F′). Co-localisation of MITF and nuclear β-catenin was detected only in a few cells beginning at the late optic vesicle stage (stage 12/13; supplementary material Fig. S1A-D). Taken together, the spatial and temporal expression pattern of *Wnt2b* and β-catenin suggests that perhaps Wnt signalling, via a β-catenin-independent signalling pathway, is involved in RPE specification.

The surface ectoderm is required for RPE specification

It has been supposed that the surface ectoderm does not play a role in RPE specification (Fuhrmann et al., 2000; Nguyen and Arnheiter, 2000). Because surface ectoderm removal in these studies was carried out after *Mitf* expression had been initiated, we removed the surface ectoderm before or at the time *Mitf* expression is initiated. One day following surface ectoderm removal at stages 7 to 9 (Fig. 2A,B), optic cup and lens formation was not observed (Fig. 2C-H′, Fig. 3C,C′). Despite the presence of Pax7-positive neural-crest-derived mesenchymal cells, MITF protein expression and pSmad labelling was only weak or not detected (12/13 cases; Fig. 2E-H′; supplementary material Fig. S1F-J,Q-R″).

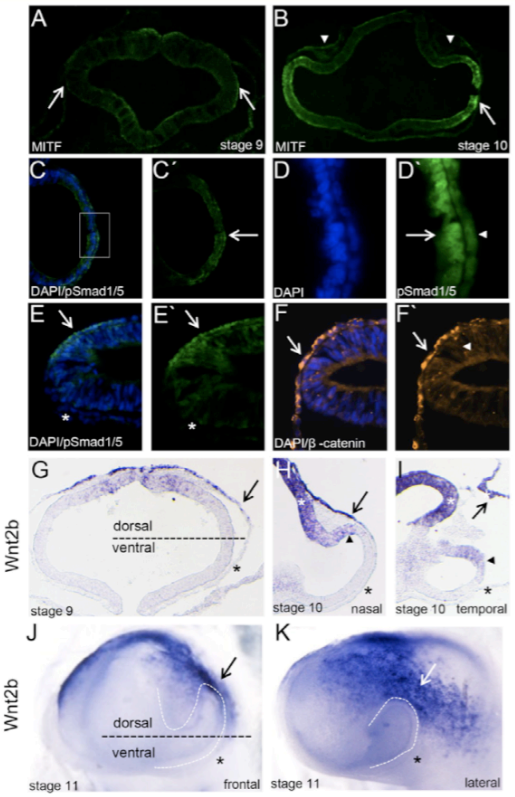

Fig. 1. Signals involved in early optic vesicle patterning in the chick. (A) At stage HH 9, MITF protein is not detected in the ov (arrows). (B) At stage 10, MITF protein is present throughout the distal ov (arrow). Mesenchymal cells (arrowheads) are located dorsally. (C,C′) At stage 10, pSmad1/5 is detected in the entire distal ov (arrow). (D,D′) Higher magnification of C, showing pSmad1/5 labelling in neuroepithelial cells (arrow) and in the surface ectoderm (arrowhead). (E,E′) Stronger accumulation of pSmad1/5 is observed in the dorsal ov (arrows) compared with the ventral region (asterisks). (F,F′) Parallel section of E. Strong β-catenin labelling in the entire surface ectoderm/prospective lens ectoderm (arrow). Nuclear β-catenin is not observed in the ov (arrowhead). (G-I) *Wnt2b* expression during the initial stages of eye development. *Wnt2b* expression is restricted to the dorsal surface ectoderm (arrow), dorsal ov (arrowhead) and dorsal prosencephalon (white asterisks). *Wnt2b* transcripts are not detected in the ventral surface ectoderm and ov (asterisks). (J,K) Frontal and lateral view of a stage 10/11 chick head. *Wnt2b* transcripts in the ectoderm (arrows) covering the dorsal ov (white dashed line). Expression is not detected ventrally (asterisks). In all panels, dorsal is up.

Development (2013) doi:10.1242/dev.096990

Additional experiments confirmed that the surface ectoderm is required for RPE specification. Optic vesicles from stage 9 and 10 chick embryos were isolated, the surface ectoderm removed and transplanted back to the chicken embryo (Fig. 2I,J). Optic vesicles, where the surface ectoderm had been removed at stages 9 and 10 (ten somites), completely lacked pigmentation 3 days after the operation (3/4 cases, compare Fig. 2K-M). Some pigmentation was observed when the surface ectoderm was removed at late stage 10 (11 and 12 somites; 17/26 cases; data not shown). Reduced pigmentation was also observed in cultured ov explants when surface ectoderm removal was carried out up to the ten-somite stage (36/37 cases; data not shown). Our data demonstrate that the surface ectoderm is required for RPE specification during the initial stages of ov patterning.

BMPs and Wnts can replace the function of the surface ectoderm to initiate MITF expression

If it is correct that BMPs and/or Wnts from the surface ectoderm are responsible for RPE specification, then replacing the removed surface ectoderm with BMP- or Wnt3a-soaked beads should at least in part restore MITF expression. Following surface ectoderm removal at stage 8 to 10, a BMP7-soaked bead was placed either into the lumen of the ov or temporal to it and the embryos were allowed to develop until the late ov or early optic cup stage (stages 13 to 15; Fig. 3D,E,H,I). One day following the operation, we observed strong MITF and pSmad labelling in the distal ov or outer optic cup (Fig. 3F-G,J-K′). Remarkably, in the absence of the surface ectoderm, BMP7 application rescued optic cup and lens formation in 47% (9/19 cases; Fig. 3I-K′).

Next, we removed the surface ectoderm at ov stages and activated the Wnt signalling pathway by implanting Wnt3a-soaked beads (Fig. 3L,O). Like Wnt2b, Wnt3a is a known agonist of both the canonical and noncanonical Wnt signalling pathways (Abdul-Ghani et al., 2011; Gessert and Kühl, 2010; Qiu et al., 2011; Qu et al., 2013), and in contrast to Wnt2b, functional Wnt3a protein is commercially available. In the absence of the surface ectoderm, Wnt3a was sufficient to rescue optic cup and lens formation (8/16 cases) and MITF expression one day after the operation (4/8 cases; Fig. 3N,N′,Q-R′). Alsterpaullone (AP) is a chemical compound that specifically inhibits GSK3β (Broun et al., 2005), thereby mimicking Wnt signalling. When the surface ectoderm was removed and AP-soaked beads implanted at ov stages, only faint MITF expression was observed (3/3 cases; Fig. 3S-U′). In control experiments, where the surface ectoderm was removed and beads soaked in either phosphate-buffered saline (PBS) or dimethyl sulfoxide (DMSO) were implanted, MITF expression and pSmad labelling was not, or only weakly, detected (Fig. 3A-C; supplementary material Fig. S1). Taken together, these results show that BMP or Wnt signalling can replace the surface ectoderm to direct neuroepithelial cells towards an RPE cell fate and to allow optic cup and lens development.

Wnt signalling is essential for RPE specification

To investigate whether Wnt signalling is required for RPE specification, we interfered with the Wnt signalling pathways at ov stages. Soluble-frizzled-related proteins (sFRP-1) and the Wnt-inhibiting factor-1 (WIF-1) bind to all Wnt ligands, thereby blocking both the canonical and noncanonical Wnt signalling pathways (Kawano and Kypta, 2003). Following treatment with sFRP-1 or WIF-1, some of the embryos were analysed 3 days after the operation to monitor the appearance of pigment granules. The eyes that developed were reduced in size and only faint pigmentation was observed (Fig. 4A,D). A dramatic downregulation or loss of MITF expression in the ov/cup was already observed 1 day after the operation (9/14 cases; Fig. 4B-C′,E-F′). The NR-specific marker *Vsx2* was weakly induced in the RPE, which still had RPE-like morphology (supplementary material Fig. S3D,E).

We next carried out experiments that interfered with the Wnt/β-catenin signalling pathway at ov stages. Dickkopf-1 (Dkk1) specifically inhibits the Wnt/β-catenin signalling pathway by binding to low density lipoprotein receptor-related protein 5 or 6 (reviewed by MacDonald et al., 2009). Following implantation of

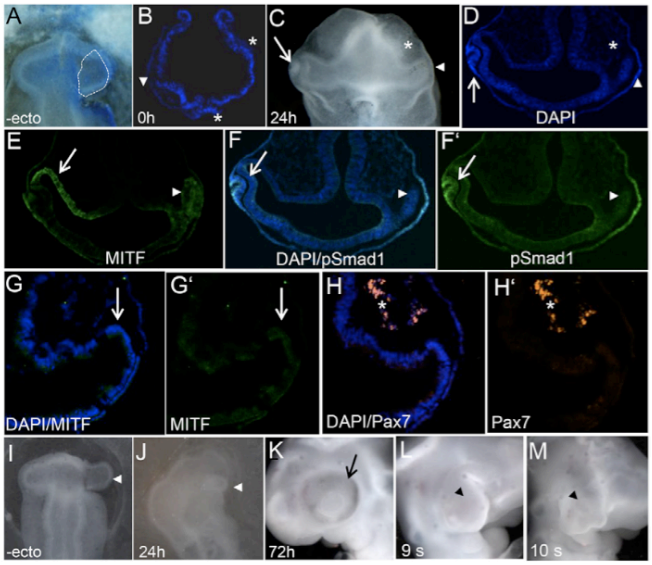

Fig. 2. The surface ectoderm is required for RPE specification in the chick. (A) The surface ectoderm of the right ov of a stage-9 chick embryo was removed (white dashed line). (B) Section stained with DAPI to show the extent of surface ectoderm removal (asterisks) at stage 8/9. The surface ectoderm of the untreated side is indicated by an arrowhead. (C,D) One day later, mesenchymal cells are located dorsally (asterisks) and optic cup and lens development is not observed (arrowheads). The arrows indicate the contralateral lens. (E-F′) Surface ectoderm removal results in decreased MITF and pSmad labelling (arrowheads). On the untreated side, MITF and pSmad protein is detected in the presumptive lens (arrows). (G-H′) Following surface ectoderm removal, MITF expression (arrows) is dramatically downregulated although Pax7-positive mesenchymal cells are present (asterisks). (I) Following surface ectoderm removal, the ov is transplanted back to the chick embryo (arrowhead). (J) Transplanted ov (arrowhead) one day following the operation. (K) Contralateral side of the operated embryo showing pigmentation at stage 24 (arrow). (L,M) Transplanted ov isolated from a stage 9 (nine somites) and stage 10 (ten somites) embryo completely lack pigmentation (arrowheads) three days following the operation. Note that optic cup formation failed to occur.

Development (2013) doi:10.1242/dev.096990

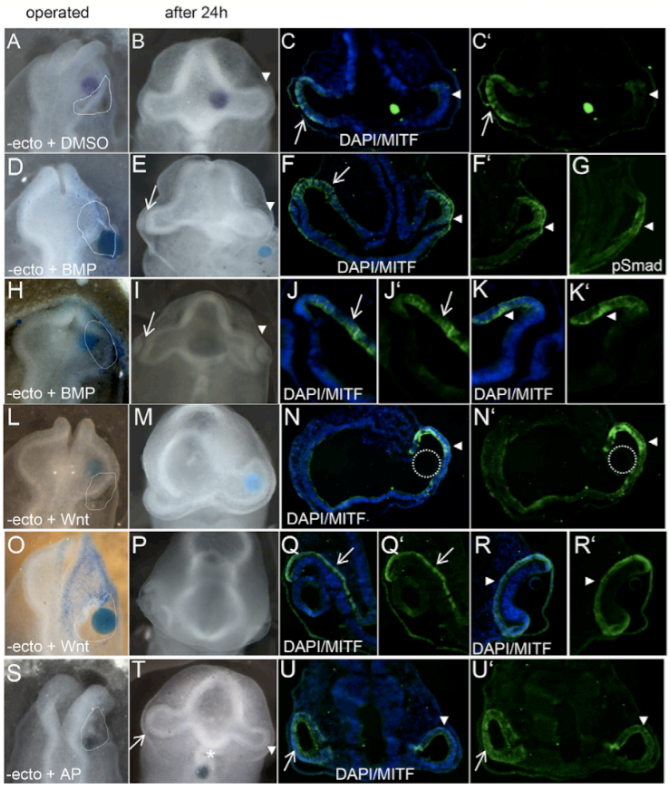

Fig. 3. BMPs or Wnts can replace the function of the surface ectoderm to induce MITF expression in chick optic vesicle cells. (A) DMSO-soaked bead (blue) in the right ov following surface ectoderm removal (white dashed line) at stage 8. (B) One day later, optic cup and lens development is not observed (arrowhead). The bead is located in a more proximal position. (C,C') MITF expression is downregulated following surface ectoderm removal (arrowheads). The untreated side (arrows) still expresses MITF. (D,H) Surface ectoderm removal (white dashed line) and BMP7 application at stage 8. (E,I) The lens placode developed (arrow) on the unoperated side and on the treated side (arrowhead in I). The bead is attached to the surface ectoderm. (F-G) MITF expression in the presumptive RPE (F, arrow) of the untreated side. Following surface ectoderm removal, BMP application rescued MITF expression and pSmad distally (arrowheads). (J-K') MITF expression in the presumptive RPE of the untreated (J,J' , arrows) and BMP-treated side (K,K'). Note that BMP application rescued optic cup and lens formation. (L,O) Surface ectoderm removal and Wnt3a application at stage 9. (M,P) Operated embryos one day after the operation. (N,N') Wnt3a application (white dashed lines) rescued MITF expression (arrowheads) in the absence of the surface ectoderm. (Q-R') MITF expression in the presumptive RPE of the untreated (Q,Q'; arrows) and Wnt3a-treated side (R,R'; arrowheads). Note that Wnt3a treatment following surface ectoderm removal rescued optic cup formation (arrowheads). (S) Surface ectoderm removal at stage 8, and application of the GSK3β inhibitor Alsterpaullone (AP). (T) One day later, the treated vesicle is smaller (arrowhead) compared with the contralateral side (arrow). The bead is located in the ventral forebrain (asterisk). (U,U') Only faint MITF expression is observed (arrowheads) on the treated side. In the presence of the surface ectoderm, exposure to AP induced MITF expression in the entire ov (arrows).

Dkk1-soaked beads at stages 8 to 10, eye development appeared to be normal (Fig. 4G). Pigmentation and MITF expression was not affected compared with the contralateral eye (6/7 cases; Fig. 4G-I′). Thus, we extended previous findings in the mouse (Fujimura et al., 2009; Westenskow et al., 2009) to the ov stage, showing that the Wnt/β-catenin signalling pathway is not required for RPE specification.

To see whether Wnt2b is required for RPE specification, we targeted *Wnt2b* by electroporating Wnt2b siRNA at ov stages. One day later, MITF expression was not affected in the operated eye compared with the contralateral eye (6/6 cases; supplementary material Fig. S2A-D′). This is in agreement with the observation that Wnt2b mutant mice do not exhibit any eye phenotypes (Tsukiyama and Yamaguchi, 2012). However, these data suggest that Wnt signalling, possibly via a Wnt/β-catenin-independent signalling pathway, is required for RPE specification.

Wnt-mediated GSK3β inhibition induces an RPE cell fate in the entire optic vesicle

To test the potential role of Wnt signalling in RPE specification, we carried out gain-of-function experiments and implanted Wnt3a beads at ov stages. Compared with controls (Fig. 5A-E), the Wnt3a-treated embryos developed a small pigmented eye with a rudimentary lens 3 days after the operation (Fig. 5F,G). Histological examination showed that Wnt3a treatment prevented optic cup formation (Fig. 5G) and that the entire vesicle had RPE-like morphology, being strongly pigmented (11/15 cases; Fig. 5H,I). Moreover, NR development was completely inhibited and the entire ov, including the optic stalk region, expressed MITF (Fig. 5J; data not shown).

In the chick and frog, both BMP and Wnt signalling cooperate to induce an epidermal cell fate (Wilson et al., 2001; Fuentealba et al., 2007; Patthey et al., 2009). Wnt-mediated GSK3β inhibition stabilises BMP signalling by preventing the degradation of pSmad1, thereby inducing an epidermal cell fate (Fuentealba et al., 2007). To test whether a similar mechanism exists during ov patterning, we inhibited GSK3β at these stages (9-14 somites). Following AP treatment, a small, strongly pigmented, MITF-expressing vesicle developed, phenocopying Wnt3a treatment (34/41 cases; compare Fig. 5F-J with 5K-Y). In those vesicles, pSmad labelling (Fig. 5R,W) was observed, colocalised with the RPE-specific marker RPE65 (Fig. 5X,Y). By contrast, the expression of NR markers, such as *Vsx2*, was downregulated or lost (supplementary material Fig. S3A,C). We did not detect any nuclear β-catenin staining in the neuroepithelium of AP-treated vesicles 1-3 days after the operation (6/6 cases; Fig. 5S,T). No changes were observed in control experiments (10/10 cases; supplementary material Fig. S1). Thus, our data suggest that Wnt-mediated GSK3β inhibition can, independently of β-catenin nuclear transfer, induce MITF expression in chick ov cells.

Development (2013) doi:10.1242/dev.096990

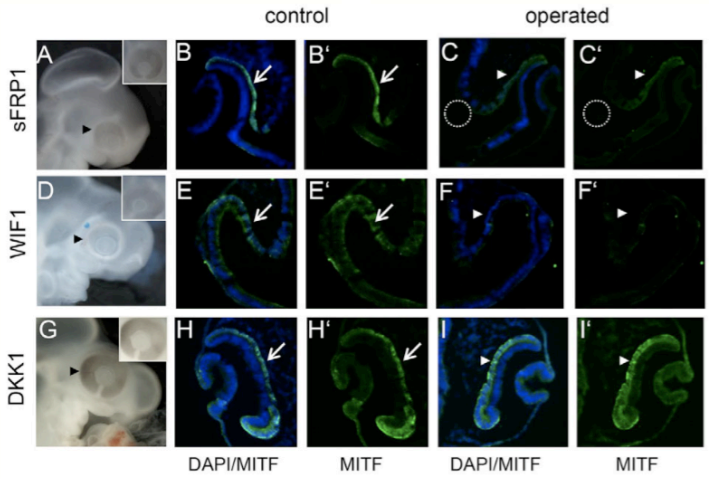

Fig. 4. Wnt signalling, but not Wnt/β-catenin signalling, is required for RPE specification. (A-I′) Loss-of-function experiments. Following inhibition of Wnt signalling, pigmentation was assayed 3 days after (A,D,G), and MITF expression 1 day after the operation. (A,D) Implantation of a bead soaked in sFrp1 (A) or WIF-1 (D) at ov stages results in optic cup and lens formation, but reduced pigmentation (arrowheads) of the treated eye compared with the contralateral eye (insets) is observed. (B-F′) MITF expression with and without DAPI staining. (C,C′) Implantation of a bead soaked in sFrp1 (white dashed line) downregulates MITF expression (arrowheads) compared with the contralateral side (B,B′, arrows). (F,F′) Application of a WIF-1-soaked bead downregulates MITF expression (arrowheads) compared with the contralateral side (E,E′, arrows). (G) Following implantation of a Dkk1-soaked bead eye, morphology and pigmentation appears normal (arrowhead) compared with the contralateral eye (inset). (H-I′) Dkk1 treatment does not affect MITF expression in the presumptive RPE of both the contralateral (H,H′, arrows) and operated eye (I,I′, arrowheads). Note that the insets in A, D and G show the contralateral eyes in the same magnification.

Wnt-mediated GSK3β inhibition supports BMP/pSmad signalling to initiate MITF expression in optic vesicle cells

BMP application at ov stages induces both ectopic *Wnt2b* and *Mitf* expression in the presumptive NR (Müller et al., 2007). Thus, it is possible that BMP-induced Wnt signalling maintains MITF expression and hence RPE development. Alternatively, Wnt-mediated GSK3β inhibition could stabilise BMP signalling to induce an epithelial phenotype in ov cells (see above). Therefore, we next inhibited BMP signalling by implanting Noggin-soaked beads, simultaneously activating the Wnt signalling pathway.

Exposure to Wnt3a or GSK3β inhibition converts the entire ov into a strongly pigmented and MITF-expressing vesicle (Fig. 5). By contrast, in the absence of BMP signalling, activation of Wnt signalling was no longer able to induce MITF expression (4/5 cases; Fig. 6A-E′). In those embryos, we observed only faint, or no, pSmad labelling in the distal ov and surface ectoderm (Fig. 6F,F′).

To investigate whether Wnt signalling is required for BMP-induced MITF expression, we inhibited Wnt signalling by simultaneously activating the BMP signalling pathway. Exposure to BMP alone induces strong MITF/*Mitf* expression in the ov (Fig. 3) (Müller et al., 2007). Following implantation of two beads, soaked in BMP7 and WIF-1 into the ov (Fig. 6G), activation of the BMP signalling pathway was no longer able to induce or maintain MITF expression and only faint or no pSmad staining was observed (6/6 cases; Fig. 6H-L′). In control experiments, pSmad and MITF expression was observed only in the dorsal ov or optic cup and in the dorsal surface ectoderm (5/5 cases; supplementary material Fig. S1K-P).

Wnts can signal through Smad1 (Fuentealba et al., 2007). Here, GSK3β inhibition prevents degradation of pSmad1, thereby stabilising BMP signalling (reviewed by Eivers et al., 2008). To see whether a similar mechanism exists during ov patterning, we implanted WIF1-soaked beads in the presence of the GSK3β-inhibitor AP (Fig. 6M). One day after the operation, eye development arrested at the ov stage and nuclear β-catenin labelling was not observed (3/4 cases; Fig. 6N-R′). Strikingly, in the absence of Wnt signalling, GSK3β inhibition was sufficient to stabilise pSmad and rescue MITF expression in both the dorsal and ventral ov (3/4 cases; Fig. 6Q-R′), suggesting that pSmad is sufficient to induce MITF expression in the absence of the surface ectoderm.

pSmad mediates RPE specification

To confirm that pSmad mediates RPE specification, we removed the surface ectoderm and electroporated a constitutively active form of human Smad1 (CA-Smad1) (Fuentealba et al., 2007) into ov cells (Fig. 7A). In the absence of the surface ectoderm CA-Smad1 was sufficient to rescue MITF expression (6/6 cases; Fig. 7B-C′). In a control experiment, wild-type Smad1 (Fuentealba et al., 2007) did not lead to MITF expression in ov cells in the absence of the surface ectoderm (5/5 cases; Fig. 7D,D′).

In *Xenopus*, it has been shown that in the absence of Wnt signalling pSmad is degraded, thereby inducing a neuronal cell fate (Fuentealba et al., 2007). *Wnt2b* expression is restricted to the dorsal surface ectoderm (Fig. 1), so that a similar mechanism could exist in the ov to allow NR development ventrally. To test this, we tried to inhibit pSmad degradation thereby directing presumptive NR cells towards an RPE cell fate. Application of the proteasomal inhibitor MG132 (Lee and Goldberg, 1998) at ov stages (7-10 somites) induced ectopic MITF expression in the ov/cup (4/7 cases; Fig. 7E-G′,J-L′). One to three days following the operation pSmad labelling was increased in the inner optic cup, and downregulation of the NR-specific marker *Vsx2* was observed (Fig. 7H,I,M). Taken

Development (2013) doi:10.1242/dev.096990

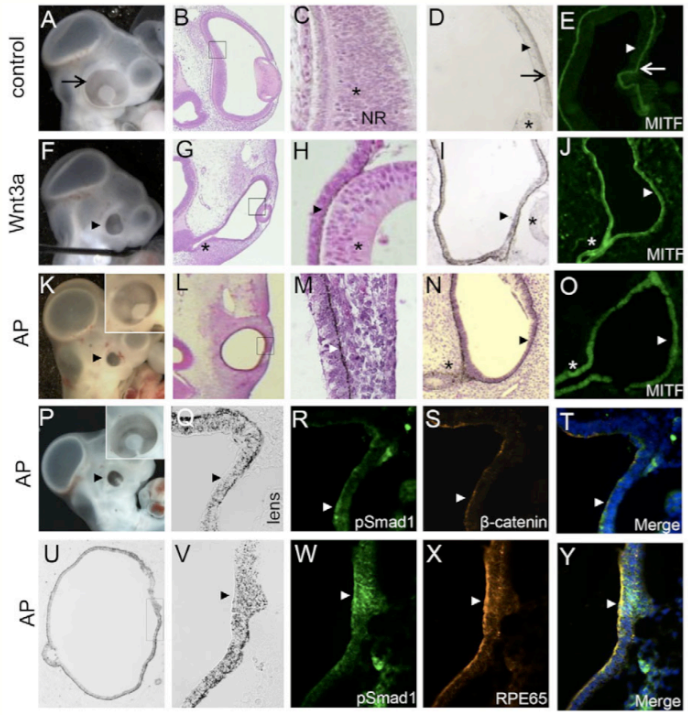

Fig. 5. Wnt/GSK3β-mediated signalling induces RPE development *in vivo*. (A) Untreated pigmented eye of a stage-24 chick embryo (arrow). (B) Section of the eye stained with haematoxylin/eosin. (C) Higher magnification of B showing the pseudostratified NR (asterisk) and single-layered RPE. (D) Peripheral region of a stage-24 chick eye with the pigmented RPE (arrow), NR (arrowhead) and lens (asterisk). (E) Dorsal eye cup. MITF is restricted to the RPE (arrow) and is not detected in the NR (arrowhead). (F-O) Wnt gain-of-function experiments. (F) Wnt3a-treated side of the embryo shown in A. The eye is microphthalmic and strongly pigmented (arrowhead, compare with A). (G) Eye morphology following Wnt3a treatment. The optic stalk is indicated by an asterisk. Optic cup formation is prevented and the entire vesicle has RPE-like morphology compared with the untreated side (shown in B). (H) Higher magnification of G. The presumptive NR is respecified and develops into a pigmented layer (arrowhead; asterisk marks the lens vesicle). (I,J) Following Wnt3a treatment, the entire eye vesicle is strongly pigmented (arrowhead; asterisk marks the lens), and the presumptive NR (white arrowhead) and optic stalk region (white asterisk) express MITF. (K) Following treatment with the GSK3β inhibitor AP, a small pigmented eye developed (arrowhead). The inset shows the contralateral eye. (L) The vesicle that developed has RPE-like morphology. (M) Higher magnification of the boxed region in L. The arrowhead indicates basally located pigment granules in the respecified NR. (N,O) Following GSK3β inhibition, the eye vesicle, including the presumptive NR (arrowhead) and optic stalk (asterisk) is pigmented and expresses MITF (white arrowhead and asterisk). (P,Q,U,V) Three days following AP treatment, a strongly pigmented eye vesicle developed (arrowheads). The inset shows the contralateral eye. (R-T) The induced RPE shows pSmad- and β-catenin labelling (arrowheads). The overlay in T shows that β-catenin labelling is restricted to the apical side (arrowhead), whereas pSmad labelling is observed apically and in the nuclei of the induced RPE. (U-Y) Section of the embryo shown in P-T. Following GSK3β inhibition, the neuroepithelium is pSmad-positive and expresses the RPE-specific differentiation marker RPE65 (arrowheads).

together, our data are consistent with a model, according to which Wnt-mediated GSK3β inhibition stabilises BMP signalling, thereby restricting RPE development to the dorsal ov.

DISCUSSION

The classical model of ov patterning holds that the distally located surface ectoderm induces NR development, whereas proximally signals released from the mesenchyme elicit RPE development. In this study, we show that signals released from the surface ectoderm, and not from the mesenchyme, promote RPE specification.

BMP and Wnt ligands expressed in the surface ectoderm specify the RPE

Fate-mapping studies in the chick showed that the distalmost part of the ov at stages 9 and 10 contributes to the eye, whereas the dorsalmost region of the ov consists of telencephalic precursors (Garcia-Lopez et al., 2009; Pombero and Martinez, 2009). Consistent with this, RPE specification initiates distally underneath the surface ectoderm, but soon the MITF domain becomes restricted to the dorsal ov and optic cup (Fig. 1) (Müller et al., 2007; Ishii et al., 2009). Similarly, polarisation of active BMP signalling to dorsal ov cells is observed in both the chick and mouse (this study; Monteiro et al., 2004). However, at this time point BMPs are still expressed in the entire surface ectoderm (Furuta et al., 1997; Müller et al., 2007), suggesting that another signal(s) is involved in restricting MITF expression to the dorsal ov/cup. BMP and Wnt family members are often co-expressed in dorsal tissues and co-regulate vertebrate pattern formation (e.g. Abu-Khalil et al., 2004; Szeto and Kimelman, 2004; Ramel et al., 2005; Zechner et al., 2007; Ohta et al., 2011). Here, we identified Wnt2b as a candidate gene involved in RPE specification.

Development (2013) doi:10.1242/dev.096990

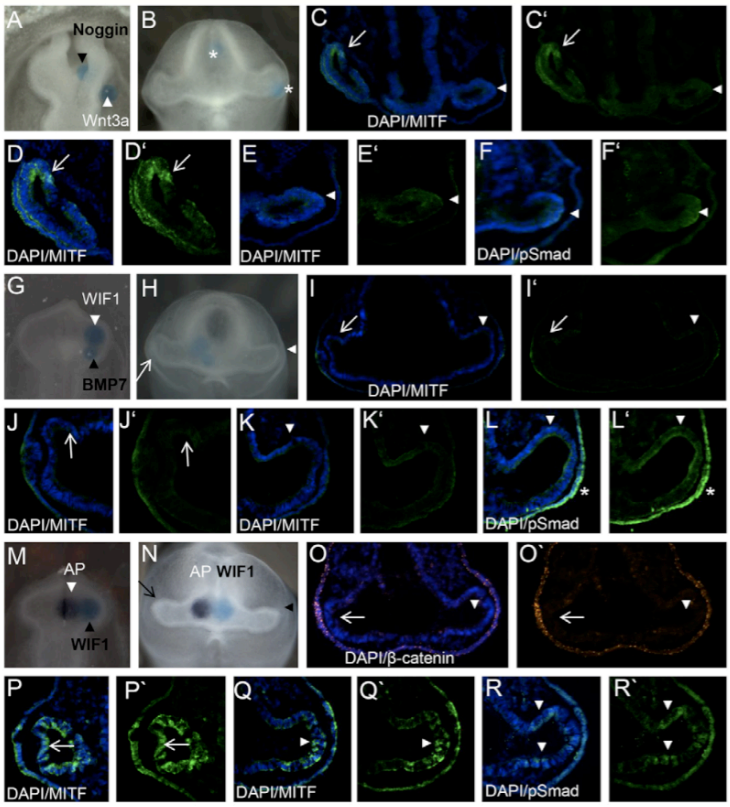

Fig. 6. Initiation of MITF expression requires the activation of both the BMP and Wnt/GSK3β signalling pathways. (A-F′) Activation of the Wnt signalling pathway in the absence of BMP signalling at ov stage. (A) Two beads, one soaked in the BMP inhibitor Noggin (black arrowhead) and one soaked in Wnt3a (white arrowhead), were implanted. (B) One day following the operation, optic cup formation is not observed (asterisks indicate the localisation of beads). (C,C′) In the absence of BMP signalling, activation of the Wnt signalling pathway is no longer capable of inducing MITF expression (arrowheads). The contralateral side still expresses MITF (arrows). (D-E′) Higher magnification of the untreated (D,D′) and treated side (E,E′) shown in C. MITF expression is downregulated (arrowheads) compared with the untreated side (arrows) and to Wnt activation alone (Fig. 5J). (F,F′) Following activation of the Wnt signalling pathway and Noggin treatment, pSmad is only weakly detected (arrowheads; parallel section of E. (G-L′) Activation of the BMP signalling pathway in the absence of Wnt signalling at ov stage. (G) Two beads, one soaked in the Wnt inhibitor WIF1 (white arrowhead) and one soaked in BMP7 (black arrowhead) were implanted into the ov. (H) One day later at stage 14/15, optic cup formation is not observed on the treated (arrowhead) and contralateral side (arrow). Note that the beads have moved towards the brain. (I-K′) MITF expression is downregulated or lost in the presumptive RPE of both the contralateral side (I-J′, arrows) and treated side (I,I′,K,K′, arrowheads). (L,L′) On the treated side, pSmad is weakly or is absent in the ov (white arrowheads), but strongly detected in the surface ectoderm (asterisks). (M-R′) In the absence of Wnt signalling, GSK3β inhibition is sufficient to stabilise pSmad and MITF expression. (M) Two beads, one soaked in the GSK3β inhibitor AP (white arrowhead) and one in WIF-1 (black arrowhead) were implanted into the ov. (N) One day later at stage 14, optic cup formation is not observed on the contralateral (arrow) and operated side (arrowhead). (O,O′) Following GSK3β inhibition, no nuclear accumulation of β-catenin is observed in the optic vesicle on the treated (arrowheads) and contralateral side that had been exposed to AP (arrows). Staining of β-catenin in the surface ectoderm appeared to be unaffected. (P,P′) The contralateral side that had been exposed to AP expresses MITF in the entire ov (arrows). (Q,Q′) Following WIF-1 mediated inhibition of Wnt signalling, GSK3β inhibition was sufficient to induce MITF expression (arrowheads) in the treated ov (compare with K,K′ and Fig. 4I′). (R,R′) Parallel section of Q shows that as a consequence of GSK3β inhibition pSmad is stabilised in the absence of Wnt signalling in both the dorsal and ventral region of the ov (arrowheads; compare with L,L′). Note that for clarity, all the embryos have been oriented, so that the treated side is always shown on the right side.

Expression of *Wnt2b* is detected in the dorsal surface ectoderm, dorsal ov and/or optic cup in several species (this study) (Zakin et al., 1998; Cho and Cepko, 2006; Müller et al., 2007; Veien et al., 2008; Grocott et al., 2011), and Wnt signalling can induce an RPE cell fate *in vitro* and *in vivo* (this study; Aoki et al., 2006; Eiraku et al., 2011). Targeting Wnt2b by electroporating Wnt2b siRNA at ov stages did not affect MITF expression (this study) and, although a large number of genes associated with Wnt signalling are expressed during vertebrate eye development, none of the single Wnt mutant mice, including the Wnt2b knockout mice, displays any eye phenotypes (van Amerongen and Berns, 2006; Tsukiyama and Yamaguchi, 2012). However, similar to BMP inhibition (Adler and Belecky-Adams, 2002; Müller et al., 2007) we show that Wnt signalling is required for RPE development. Targeting several Wnt ligands by

Development (2013) doi:10.1242/dev.096990

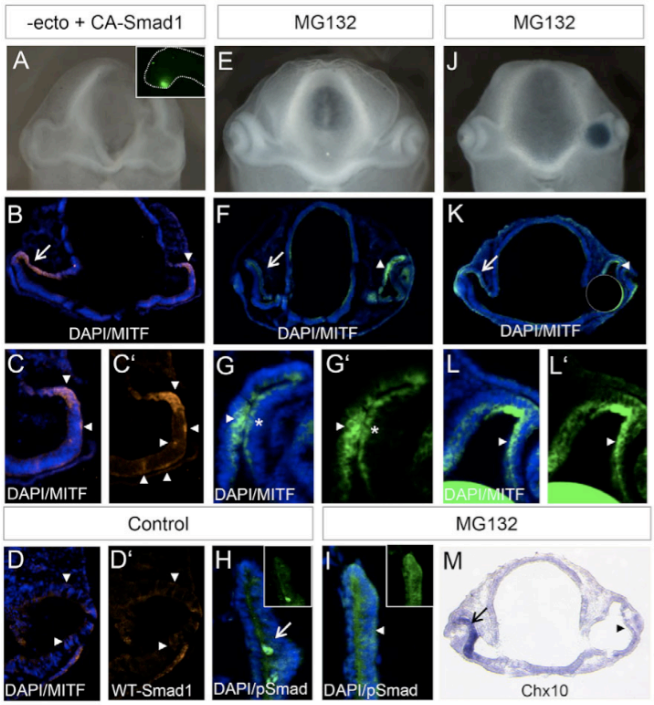

Fig. 7. pSmad1 signalling mediates RPE specification. (A) Chick embryo that developed one day after surface ectoderm removal and electroporation of a constitutively active form of Smad1 (CA-Smad1). The inset shows the GFP-positive ov. (B-C') Following surface ectoderm removal, pSmad signalling is sufficient to rescue MITF expression in both the dorsal and ventral ov (arrowheads). The arrow indicates MITF expression in the untreated eye. (D,D') Optic vesicle of a control experiment. Following surface ectoderm removal and electroporation of wild-type Smad1 (WT-Smad1), MITF expression is not maintained in the neuroepithelium (arrowheads). (E,J) Embryos that developed one day following implantation of the proteasomal inhibitor MG132 at ov stages. (F,K) Optic cup and lens formation is observed on both the treated (arrowheads) and untreated side (arrows). The bead is indicated by a white dashed line. (G,G',L,L') Higher magnification of the dorsal eye cup showing strong MITF expression in both the RPE (arrowheads in G,G') and NR (asterisks in G,G' and arrowheads in L,L'). (H) At stage 26, single positive pSmad cells are present in the ciliary margin zone (arrow). (I) In the MG132-treated embryo, pSmad labelling is detected throughout the ciliary margin zone (arrowhead). (M) Following proteasomal inhibition, expression of the NR-specific marker *Chx10/Vsx2* is lost (arrowhead), compared with the untreated eye (arrow).

inhibiting Wnt receptor-mediated signalling results in reduced pigmentation and downregulation of MITF expression (Fig. 4). Moreover, we show that during a narrow time window, the BMP- and Wnt- expressing surface ectoderm is required to mediate RPE specification. The loss of MITF expression following surface ectoderm removal can be rescued by the activation of the BMP or Wnt signalling pathways.

In the absence of the surface ectoderm BMP or Wnt signalling can rescue optic cup formation

During vertebrate development tissue interactions are required for proper organ formation. We confirm previous findings that the surface ectoderm is required for optic cup formation (Fig. 2) (Hyer et al., 1998; Hyer et al., 2003; Nguyen and Arnheiter, 2000). In the absence of the surface ectoderm, an optic cup fails to form, independently of whether mesenchymal cells remain dorsally or cover the entire ov. Interestingly, in the absence of the surface ectoderm, BMPs or Wnts can rescue optic cup and lens formation (Fig. 3). However, recent *in vitro* studies suggest that tissue interactions are not required for optic cup formation (reviewed by Sasai et al., 2012; Sasai, 2013). Embryonic stem cell (ESC) reaggregates cultured on matrigel are patterned into NR and RPE in a self-autonomous way (Eiraku et al., 2011; Nakano et al., 2012). It should be noted, that we observed optic cup formation only if optic vesicle explants were cultured on growth factor-containing matrigel, but not in the presence of collagen (Ichie Steinfeld, unpublished observations). It is possible that matrigel releases proteins (Hughes et al., 2010) that allow optic cup formation in the absence of the surface ectoderm. For example, during matrigel-induced hepatocyte differentiation, β-catenin undergoes multifactorial regulation (Monga et al., 2006). Interestingly, patterning into NR and RPE of ESC reaggregates is only observed in the presence of neuroectodermal epithelium or in the presence of both Wnt3a and high concentrations of matrigel (Eiraku et al., 2011). Further work is required to identify the exact cellular and molecular mechanisms that direct optic cup formation in vertebrates.

Wnt signalling, via a GSK3β-dependent but β-catenin-independent pathway, is involved in RPE specification

Wnt signals are context-dependently transduced via the noncanonical or canonical signalling pathways (reviewed by Kikuchi et al., 2007; Katoh and Katoh, 2007). Here, we show that RPE specification is mediated by a Wnt-signalling pathway that is GSK3β-dependent but β-catenin-independent. Firstly, in agreement with previous studies (see Introduction), we did not detect any nuclear β-catenin in the neuroepithelium at the time the RPE is specified (Fig. 1). Secondly, canonical Wnt/β-catenin signalling requires GSK3β inhibition. Following GSK3β inhibition the NR and optic stalk are respecified to develop into a strongly pigmented RPE, independent of nuclear β-catenin accumulation (Fig. 5). Thirdly, following inhibition of Wnt signalling, GSK3β inhibition is sufficient to rescue MITF expression, and this is again independent of nuclear β-catenin accumulation (Fig. 6). Lastly, specific inhibition of the Wnt/β-catenin signalling pathway at optic vesicle stages did not affect MITF expression and pigmentation (Fig. 4). In support of this, eye pigmentation appears normal in mutant mice, where the co-receptors of the Wnt/β-catenin signalling pathway, Lrp5 and 6, are mutated (Fujino et al., 2003; Zhou et al., 2008). Moreover, ectopic

activation of the Wnt/β-catenin signalling pathway alone is not sufficient to induce MITF expression (Westenskow et al., 2010) and instead eye development and optic cup formation is disrupted (Smith et al., 2005; Fu et al., 2006; Miller et al., 2006; Fujimura et al., 2009). In particular, β-catenin overexpression within the RPE itself results in a complete loss of pigmentation and *Mitf* expression (Fujimura et al., 2009). Dkk1, a specific antagonist of the Wnt/β-catenin signalling pathway, is expressed in the chick ov (GEISHA chicken embryo gene expression database: http://geisha.arizona.edu) and in *Dkk1* mutant mice, eyes or anterior head structures fail to develop (MacDonald et al., 2004; Mukhopadhyay et al., 2001). This suggests that at ov stages, repression of Wnt/β-catenin signalling is required for proper vertebrate eye development. Accordingly, during the process of stepwise differentiation of human or mouse ESCs towards a retinal cell fate, Dkk1 is initially supplemented to the medium (Osakada et al., 2009).

Initiation of MITF expression requires both the BMP and Wnt/GSK3β signalling pathways

The status of Wnt signalling regulates neural and epidermal cell fates in chick and frog embryos (Wilson et al., 2001; Fuentealba et al., 2007; Patthey et al., 2009). In *Xenopus*, the phosphorylation status of Smad1 determines whether a cell acquires an epidermal or neuronal cell fate (Fuentealba et al., 2007; Eivers et al., 2008). A neuronal cell fate is induced in the absence of Wnt signalling. Here, Smad-1 receives inhibitory phosphorylations by GSK3β and by the FGF/MAPK, which leads to proteasomal degradation of pSmad-1 (Fuentealba et al., 2007). By contrast, in the presence of Wnt signalling, GSK3β is inhibited and pSmad-1 can now induce an epidermal cell fate (Fuentealba et al., 2007). A similar mechanism appears to exist during ov patterning to restrict the RPE domain to the dorsal ov. On the one hand, activation of the Wnt signalling pathway at ov stages does not rescue MITF expression lost from BMP inhibition (Fig. 6). On the other hand, in the absence of Wnt signalling, activation of the BMP signalling pathway can no longer induce MITF expression in ov cells. In both cases, we observed no, or only weak, pSmad staining in ov cells. Following inhibition of Wnt signalling, GSK3β inhibition is sufficient to stabilise pSmad in ov cells and to rescue MITF expression and hence RPE development (Fig. 6). Moreover, overexpression of a constitutively active form of Smad1 rescues MITF expression in the absence of the surface ectoderm. Accordingly, inhibition of proteasomal pSmad degradation maintains MITF and results in the loss of *Vsx2* expression (Fig. 7).

Based on these findings, we propose a dorsoventral model for the initial stages of ov patterning. Members of the BMP, FGF and Wnt families are released from the surface ectoderm to pattern the ov transiently into a dorsal RPE and ventral NR domain. Initially, the BMP-expressing surface ectoderm initiates *Mitf* expression through pSmad in the entire distal ov (Fig. 8A). Wnt2b and as yet unidentified Wnt ligand(s) localised to the dorsal surface ectoderm and dorsal ov inhibit GSK3β, thereby stabilising pSmad and maintaining *Mitf* expression in the dorsal ov and optic cup. In the absence of Wnt signalling, pSmad is degraded through MAPK/ERK and GSK3β phosphorylation, which then leads to NR specification/*Vsx2* expression in the ventral ov (Fig. 8B). Once RPE and NR specification occurs, *Vsx2* expression is stabilised distally, whereas RPE development will continue in the dorso-proximal region, where mesenchymal cells now become involved in maintaining RPE-specific gene expression.

The molecular interplay between several pathways at the level of pSmad during cell fate specification in the ov may provide the basis for directed differentiation of human ESCs towards functional RPE cells that in the future could be used for cell replacement of RPE-mediated blinding diseases (reviewed by Clegg et al., 2008; Bharti et al., 2011).

MATERIALS AND METHODS

In vivo manipulations of the developing chick embryo

Fertilised chicken eggs (*Gallus gallus*, Linnaeus) were obtained from LSL Rhein-Main (Dieburg, Germany). For all experiments the eggs were incubated at 38°C and 60% humidity, until they reached the desired stages (stage 7 to 11) according to Hamburger and Hamilton (Hamburger and Hamilton, 1951). The eggs were then windowed and the embryonic membranes removed. A small incision was made into the midline of the forebrain, or temporally to the ov using sharpened tungsten needles. One bead (see below) was then transferred into the egg, inserted through the slit and positioned into the ov. The eggs were then sealed and left to develop at 38°C until they reached the desired stage. Owing to the turning of the chick embryo at stage 12/13, some

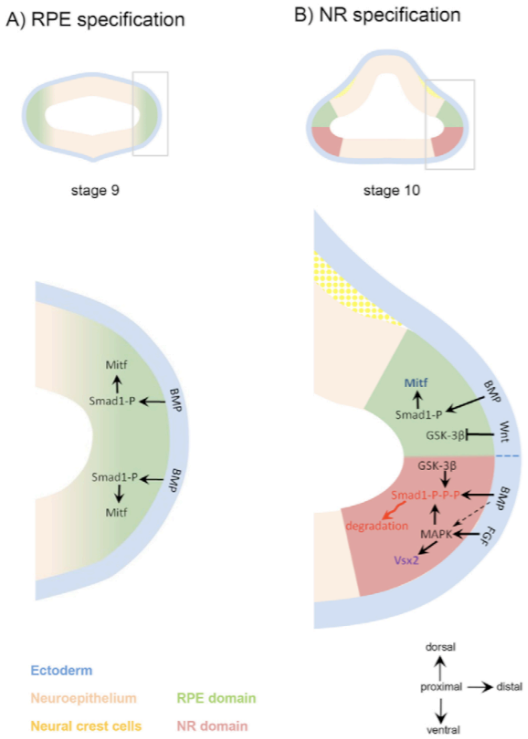

Fig. 8. Dorsoventral model of optic vesicle patterning in the chick embryo, integrating BMP and Wnt actions. (A,B) This model suggests that at stage 9 (A), BMPs released from the surface ectoderm initiate RPE specification through phosphorylation of Smad-1, -5 and/or -8, which leads to *Mitf* expression in distal ov cells. At stage 10 (B), Wnt signalling from the dorsal surface ectoderm inhibits GSK3β, which in turn stabilises BMP signalling. The transcription factor pSmad can translocate to the nucleus to initiate *Mitf* expression, thereby directing dorsal ov cells towards an epithelial cell fate (RPE). In the absence of Wnt ligands within the ventral surface ectoderm, Smad-1/5/8 is triple phosphorylated by BMPs released from the surface ectoderm, by GSK3β (not inhibited by Wnts) and possibly by FGF signalling (not studied here). This results in proteasomal degradation of Smad-1/5/8 in the ventral ov. The inhibition of BMP signalling now allows FGF/MAPK signalling to induce *Vsx2* expression, thereby directing the ventral region of the ov towards a neuronal cell fate.

beads placed into the right ov moved into the brain vesicle one day after the operation. The embryos were fixed in 4% paraformaldehyde (PFA) in PBS at 4°C for 2 to 48 hours. Embryos to be used for whole-mount *in situ* hybridisation (ISH) were dehydrated and stored in 100% methanol. Those intended for ISH on sections were cryoprotected overnight in 10% sucrose in diethylpyrocarbonate-H_2O at 4°C and transferred into 20% and 30% sucrose for at least 1 hour each. Consecutive 10-14 µm thick sections were analysed by ISH or immunohistochemistry. Control experiments were carried out by either implanting PBS- and/or DMSO-soaked beads into the ov of stage 9/10 chick embryos according to the protocol described above.

Bead preparation

A 2 µl drop of the designated protein or chemical was placed in a Petri dish and about eight drops (10 µl each) of PBS were placed around it. About 15 beads (see below) were added to the solution and incubated for a minimum of 1 hour. Agarose beads (AffiGel Blue Beads, Bio-Rad) were soaked either in 0.5 or 1 µg/µl BMP5 and BMP7 protein (R&D Systems), 0.5 or 1 µg/µl Wnt3a (R&D Systems), 1 µg/µl DKK1 (R&D Systems), 2 µg/µl sFRP1 (PreProTech) or 1 µg/µl human WIF-1 protein (R&D Systems), 1 µg/µl Noggin (R&D Systems). Alsterpaullone (Sigma-Aldrich) and MG132 (Merck) was dissolved in DMSO (Roth) and used at a concentration of 1 µg/µl using AG1-X2 resin beads (Bio-Rad).

Surface ectoderm removal

Two per cent Nile Blue A sulfate (Sigma-Aldrich) dissolved in agarose was used to support the removal of the surface ectoderm at stages 7 to 10 using fine glass needles (Geetha-Loganathan et al., 2010).

Transplantation experiments

The right ov was removed from stage 9 (nine somites) or stage 10 chick embryos (10-12 somites), treated with 0.05% collagenase for 30 minutes to loosen the surface ectoderm, which then was removed using sharpened tungsten needles. Using a glass pipette, the remaining ov was then transplanted back to the same chick embryo. Embryos were placed into the incubator and left to develop for another 72 hours, fixed in 4% PFA and processed as described above. *In vitro* experiments using chick explant cultures were carried out as described before (Kobayashi et al., 2010).

In vivo electroporation

The ov of stage 9-10 chick embryos were usually injected with a green fluorescent protein (GFP) expression construct (1-3 µM) mixed with 1.5-2 µg/µl plasmids or siRNA (see below) containing 0.01% Fast Green. Using a TSS20 Ovodyne Electroporator (Intracel), two pulses (7V, 30-msecond duration) in 970-msecond intervals were delivered, using 0.5 mm diameter, tungsten and platin electrodes. The anode was positioned lateral to the right ov and the cathode was placed into the brain. The DNA/RNA constructs used were Wnt2b siRNA and siRNA-A (both Santa Cruz), pC S2 hSmad1-WT (Addgene plasmid 22989) and pC S2 hSmad1-GM (Addgene plasmid 22992; Edward de Robertis; Pera et al., 2003; Fuentealba et al., 2007). The embryos were fixed 1 day later and assayed for MITF and GFP expression.

Assaying gene expression in chick embryos and ov explants by ISH and immunohistochemistry

RNA ISH on cryostat sections and whole mounts was performed as previously described (Müller et al., 2007). Antisense RNA probes specific for chicken *Rx* (T. Ogura, Tohoku University, Aoba, Japan), *Mitf* (M. Mochii, University of Hyogo, Japan), *Vsx2* and *Wnt3a*, *Wnt4*, *Wnt5*, *Wnt5b*, *Wnt7b*, *Wnt8b* (D. Schulte, Goethe University of Frankfurt/M., Germany) and *Wnt2b* (H. Roelink, University of Washington, Seattle, WA), were used.

In explant cultures of ov, MITF expression was carried out as previously described (Kagiyama et al., 2005; Kobayashi et al., 2010). Human MITF antibody (Sigma-Aldrich, HPA003259), PY489-β-catenin (DSHB), pSmad1/5, pSMAD1/5/8 (Cell Signaling, 9516, 9511S), Retinal pigment epithelial-specific protein 65 kDa (Novus Biologicals, 4018BD113D9) and mouse Pax7 (MAB1675) were used on cryostat sections.

Acknowledgements

We thank Ulrike Hoppe for excellent technical assistance and Anja Heselich, Dorothea Schulte and Hermann Rohrer for critical reading of the manuscript.

Competing interests

The authors declare no competing financial interests.

Author contributions

A.V.-H., P.G.L. and M.A. designed the experiments and gave advice. J.S., I.S. and N.C. carried out embryological manipulations and gain- and loss-of-function studies and analysed the data. M.-L.H. carried out the proteasomal inhibition experiment. J.S., P.G.L. and A.V.-H wrote the manuscript.

Funding

We thank the Deutsche Forschungsgemeinschaft [grant number Vo 685/4-1 to J.S. and N.C.] and Grant-in-Aid from the Ministry of Education, Culture, Sports, Science and Technology of Japan (MEXT KAKENHI) [grant number 23124506 to M.A. and I.S.] for funding and the Förderkreis der Freunde der TU Darmstadt for support.

Supplementary material

Supplementary material available online at
http://dev.biologists.org/lookup/suppl/doi:10.1242/dev.096990/-/DC1

References

Abdul-Ghani, M., Dufort, D., Stiles, R., De Repentigny, Y., Kothary, R. and Megeney, L. A. (2011). Wnt11 promotes cardiomyocyte development by caspase-mediated suppression of canonical Wnt signals. *Mol. Cell. Biol.* **31**, 163-178.

Abu-Khalil, A., Fu, L., Grove, E. A., Zecevic, N. and Geschwind, D. H. (2004). *Wnt* genes define distinct boundaries in the developing human brain: implications for human forebrain patterning. *J. Comp. Neurol.* **474**, 276-288.

Adler, R. and Belecky-Adams, T. L. (2002). The role of bone morphogenetic proteins in the differentiation of the ventral optic cup. *Development* **129**, 3161-3171.

Adler, R. and Canto-Soler, M. V. (2007). Molecular mechanisms of optic vesicle development: complexities, ambiguities and controversies. *Dev. Biol.* **305**, 1-13.

Aoki, H., Hara, A., Nakagawa, S., Motohashi, T., Hirano, M., Takahashi, Y. and Kunisada, T. (2006). Embryonic stem cells that differentiate into RPE cell precursors in vitro develop into RPE cell monolayers in vivo. *Exp. Eye Res.* **82**, 265-274.

Bharti, K., Nguyen, M. T., Skuntz, S., Bertuzzi, S. and Arnheiter, H. (2006). The other pigment cell: specification and development of the pigmented epithelium of the vertebrate eye. *Pigment Cell Res.* **19**, 380-394.

Bharti, K., Miller, S. S. and Arnheiter, H. (2011). The new paradigm: retinal pigment epithelium cells generated from embryonic or induced pluripotent stem cells. *Pigment Cell Melanoma Res.* **24**, 21-34.

Bharti, K., Gasper, M., Ou, J., Brucato, M., Clore-Gronenborn, K., Pickel, J. and Arnheiter, H. (2012). A regulatory loop involving PAX6, MITF, and WNT signaling controls retinal pigment epithelium development. *PLoS Genet.* **8**, e1002757.

Broun, M., Gee, L., Reinhardt, B. and Bode, H. R. (2005). Formation of the head organizer in hydra involves the canonical Wnt pathway. *Development* **132**, 2907-2916.

Cho, S. H. and Cepko, C. L. (2006). Wnt2b/beta-catenin-mediated canonical Wnt signaling determines the peripheral fates of the chick eye. *Development* **133**, 3167-3177.

Clegg, D. O., Buchholz, D., Hikita, S., Rowland, T., Hu, Q. and Johnson, L. V. (2008). RPE cells: development in vivo and derivation from human embryonic stem cells in vitro for treatment of age-related macular degeneration. In *Stem Cell Research and Therapeutics* (ed. D. O. Clegg and Y. Shi), Chapter 1, pp.1-24. Rotterdam: Springer.

Crossley, P. H., Martinez, S., Ohkubo, Y. and Rubenstein, J. L. R. (2001). Coordinate expression of Fgf8, Otx2, Bmp4, and Shh in the rostral prosencephalon during development of the telencephalic and optic vesicles. *Neuroscience* **108**, 183-206.

Eiraku, M., Takata, N., Ishibashi, H., Kawada, M., Sakakura, E., Okuda, S., Sekiguchi, K., Adachi, T. and Sasai, Y. (2011). Self-organizing optic-cup morphogenesis in three-dimensional culture. *Nature* **472**, 51-56.

Eivers, E., Fuentealba, L. C. and De Robertis, E. M. (2008). Integrating positional information at the level of Smad1/5/8. *Curr. Opin. Genet. Dev.* **18**, 304-310.

Fu, X., Sun, H., Klein, W. H. and Mu, X. (2006). Beta-catenin is essential for lamination but not neurogenesis in mouse retinal development. *Dev. Biol.* **299**, 424-437.

Fuentealba, L. C., Eivers, E., Ikeda, A., Hurtado, C., Kuroda, H., Pera, E. M. and De Robertis, E. M. (2007). Integrating patterning signals: Wnt/GSK3 regulates the duration of the BMP/Smad1 signal. *Cell* **131**, 980-993.

Fuhrmann, S. (2010). Eye morphogenesis and patterning of the optic vesicle. *Curr. Top. Dev. Biol.* **93**, 61-84.

Fuhrmann, S., Levine, E. M. and Reh, T. A. (2000). Extraocular mesenchyme patterns the optic vesicle during early eye development in the embryonic chick. *Development* **127**, 4599-4609.

Fujimura, N., Taketo, M. M., Mori, M., Korinek, V. and Kozmik, Z. (2009). Spatial and temporal regulation of Wnt/β-catenin signaling is essential for development of the retinal pigment epithelium. *Dev. Biol.* **334**, 31-45.

Fujino, T., Asaba, H., Kang, M. J., Ikeda, Y., Sone, H., Takada, S., Kim, D. H., Ioka, R. X., Ono, M., Tomoyori, H. et al. (2003). Low-density lipoprotein receptor-related protein 5 (LRP5) is essential for normal cholesterol metabolism and glucose-induced insulin secretion. *Proc. Natl. Acad. Sci. USA* **100**, 229-234.

Furuta, Y., Piston, D. W. and Hogan, B. L. (1997). Bone morphogenetic proteins (BMPs) as regulators of dorsal forebrain development. *Development* **124**, 2203-2212.
Garcia-Lopez, R., Vieira, C., Echevarria, D. and Martinez, S. (2004). Fate map of the diencephalon and the zona limitans at the 10-somites stage in chick embryos. *Dev. Biol.* **268**, 514-530.
Garcia-Lopez, R., Pombero, A. and Martinez, S. (2009). Fate map of the chick embryo neural tube. *Dev. Growth Differ.* **51**, 145-165.
Geetha-Loganathan, P., Nimmagadda, S., Christ, B., Huang, R. and Scaal, M. (2010). Ectodermal Wnt6 is an early negative regulator of limb chondrogenesis in the chicken embryo. *BMC Dev. Biol.* **10**, 32-40.
Gessert, S. and Kühl, M. (2010). The multiple phases and faces of wnt signaling during cardiac differentiation and development. *Circ. Res.* **107**, 186-199.
Grocott, T., Johnson, S., Bailey, A. P. and Streit, A. (2011). Neural crest cells organize the eye via TGF-β and canonical Wnt signalling. *Nat. Commun.* **2**, 265.
Hamburger, V. and Hamilton, H. (1951). A series of normal stages in the development of the chick embryo. *J. Morphol.* **88**, 49-92.
Hirashima, M., Kobayashi, T., Uchikawa, M., Kondoh, H. and Araki, M. (2008). Anteroventrally localized activity in the optic vesicle plays a crucial role in the optic development. *Dev. Biol.* **317**, 620-631.
Horsford, D. J., Nguyen, M. T., Sellar, G. C., Kothary, R., Arnheiter, H. and McInnes, R. R. (2005). Chx10 repression of Mitf is required for the maintenance of mammalian neuroretinal identity. *Development* **132**, 177-187.
Hughes, C. S., Postovit, L. M. and Lajoie, G. A. (2010). Matrigel: a complex protein mixture required for optimal growth of cell culture. *Proteomics* **10**, 1886-1890.
Hyer, J., Mima, T. and Mikawa, T. (1998). FGF1 patterns the optic vesicle by directing the placement of the neural retina domain. *Development* **125**, 869-877.
Hyer, J., Kuhlman, J., Afif, E. and Mikawa, T. (2003). Optic cup morphogenesis requires pre-lens ectoderm but not lens differentiation. *Dev. Biol.* **259**, 351-363.
Ishii, Y., Weinberg, K., Oda-Ishii, I., Coughlin, L. and Mikawa, T. (2009). Morphogenesis and cytodifferentiation of the avian retinal pigmented epithelium require downregulation of Group B1 Sox genes. *Development* **136**, 2579-2589.
Kagiyama, Y., Gotouda, N., Sakagami, K., Yasuda, K., Mochii, M. and Araki, M. (2005). Extraocular dorsal signal affects the developmental fate of the optic vesicle and patterns the optic neuroepithelium. *Dev. Growth Differ.* **47**, 523-536.
Katoh, M. and Katoh, M. (2007). WNT signaling pathway and stem cell signaling network. *Clin. Cancer Res.* **13**, 4042-4045.
Kawano, Y. and Kypta, R. (2003). Secreted antagonists of the Wnt signalling pathway. *J. Cell Sci.* **116**, 2627-2634.
Kikuchi, A., Yamamoto, H. and Kishida, S. (2007). Multiplicity of the interactions of Wnt proteins and their receptors. *Cell. Signal.* **19**, 659-671.
Klaus, A. and Birchmeier, W. (2008). Wnt signalling and its impact on development and cancer. *Nat. Rev. Cancer* **8**, 387-398.
Kobayashi, T., Yasuda, K. and Araki, M. (2010). Coordinated regulation of dorsal bone morphogenetic protein 4 and ventral Sonic hedgehog signaling specifies the dorso-ventral polarity in the optic vesicle and governs ocular morphogenesis through fibroblast growth factor 8 upregulation. *Dev. Growth Differ.* **52**, 351-363.
Layer, P. G., Araki, M. and Vogel-Höpker, A. (2010). New concepts for reconstruction of retinal and pigment epithelial tissues. *Expert Rev. Ophthalmol.* **5**, 523-543.
Lee, D. H. and Goldberg, A. L. (1998). Proteasome inhibitors: valuable new tools for cell biologists. *Trends Cell Biol.* **8**, 397-403.
Liu, W., Lagutin, O., Swindell, E., Jamrich, M. and Oliver, G. (2010). Neuroretina specification in mouse embryos requires Six3-mediated suppression of Wnt8b in the anterior neural plate. *J. Clin. Invest.* **120**, 3568-3577.
MacDonald, B. T., Adamska, M. and Meisler, M. H. (2004). Hypomorphic expression of Dkk1 in the doubleridge mouse: dose dependence and compensatory interactions with Lrp6. *Development* **131**, 2543-2552.
MacDonald, B. T., Tamai, K. and He, X. (2009). Wnt/β-catenin signaling: components, mechanisms, and diseases. *Dev. Cell* **17**, 9-26.
Miller, L. A., Smith, A. N., Taketo, M. M. and Lang, R. A. (2006). Optic cup and facial patterning defects in ocular ectoderm beta-catenin gain-of-function mice. *BMC Dev. Biol.* **6**, 14.
Monga, S. P. S., Micsenyi, A., Germinaro, M., Apte, U. and Bell, A. (2006). beta-Catenin regulation during matrigel-induced rat hepatocyte differentiation. *Cell Tissue Res.* **323**, 71-79.
Monteiro, R. M., de Sousa Lopes, S. M., Korchynskyi, O., ten Dijke, P. and Mummery, C. L. (2004). Spatio-temporal activation of Smad1 and Smad5 in vivo: monitoring transcriptional activity of Smad proteins. *J. Cell Sci.* **117**, 4653-4663.
Mukhopadhyay, M., Shtrom, S., Rodriguez-Esteban, C., Chen, L., Tsukui, T., Gomer, L., Dorward, D. W., Glinka, A., Grinberg, A., Huang, S. P. et al. (2001). Dickkopf1 is required for embryonic head induction and limb morphogenesis in the mouse. *Dev. Cell* **1**, 423-434.
Müller, F., Rohrer, H. and Vogel-Höpker, A. (2007). Bone morphogenetic proteins specify the retinal pigment epithelium in the chick embryo. *Development* **134**, 3483-3493.
Nakano, T., Ando, S., Takata, N., Kawada, M., Muguruma, K., Sekiguchi, K., Saito, K., Yonemura, S., Eiraku, M. and Sasai, Y. (2012). Self-formation of optic cups and storable stratified neural retina from human ESCs. *Cell Stem Cell* **10**, 771-785.
Nakayama, A., Nguyen, M. T., Chen, C. C., Opdecamp, K., Hodgkinson, C. A. and Arnheiter, H. (1998). Mutations in microphthalmia, the mouse homolog of the human deafness gene MITF, affect neuroepithelial and neural crest-derived melanocytes differently. *Mech. Dev.* **70**, 155-166.
Nguyen, M.-T. and Arnheiter, H. (2000). Signaling and transcriptional regulation in early mammalian eye development: a link between FGF and MITF. *Development* **127**, 3581-3591.
Nishihara, D., Yajima, I., Tabata, H., Nakai, M., Tsukiji, N., Katahira, T., Takeda, K., Shibahara, S., Nakamura, H. and Yamamoto, H. (2012). Otx2 is involved in the regional specification of the developing retinal pigment epithelium by preventing the expression of sox2 and *fgf8*, factors that induce neural retina differentiation. *PLoS ONE* **7**, e48879.
Ohkubo, Y., Chiang, C. and Rubenstein, J. L. (2002). Coordinate regulation and synergistic actions of BMP4, SHH and FGF8 in the rostral prosencephalon regulate morphogenesis of the telencephalic and optic vesicles. *Neuroscience* **111**, 1-17.
Ohta, K., Ito, A., Kuriyama, S., Lupo, G., Kosaka, M., Ohnuma, S., Nakagawa, S. and Tanaka, H. (2011). Tsukushi functions as a Wnt signaling inhibitor by competing with Wnt2b for binding to transmembrane protein Frizzled4. *Proc. Natl. Acad. Sci. USA* **108**, 14962-14967.
Osakada, F., Ikeda, H., Sasai, Y. and Takahashi, M. (2009). Stepwise differentiation of pluripotent stem cells into retinal cells. *Nat. Protoc.* **4**, 811-824.
Ou, J., Bharti, K., Nodari, A., Bertuzzi, S. and Arnheiter, H. (2013). *Vax1/2* genes counteract *Mitf*-induced respecification of the retinal pigment epithelium. *PLoS ONE* **8**, e59247.
Patthey, C., Edlund, T. and Gunhaga, L. (2009). Wnt-regulated temporal control of BMP exposure directs the choice between neural plate border and epidermal fate. *Development* **136**, 73-83.
Pera, E. M., Ikeda, A., Eivers, E. and De Robertis, E. M. (2003). Integration of IGF, FGF, and anti-BMP signals via Smad1 phosphorylation in neural induction. *Genes Dev.* **17**, 3023-3028.
Pombero, A. and Martinez, S. (2009). Telencephalic morphogenesis during the process of neurulation: an experimental study using quail-chick chimeras. *J. Comp. Neurol.* **512**, 784-797.
Qiu, W., Chen, L. and Kassem, M. (2011). Activation of non-canonical Wnt/JNK pathway by Wnt3a is associated with differentiation fate determination of human bone marrow stromal (mesenchymal) stem cells. *Biochem. Biophys. Res. Commun.* **413**, 98-104.
Qu, F., Wang, J., Xu, N., Liu, C., Li, S., Wang, N., Qi, W., Li, H., Li, C., Geng, Z. et al. (2013). WNT3A modulates chondrogenesis via canonical and non-canonical Wnt pathways in MSCs. *Front. Biosci.* **18**, 493-503.
Quinlan, R., Graf, M., Mason, I., Lumsden, A. and Kiecker, C. (2009). Complex and dynamic patterns of Wnt pathway gene expression in the developing chick forebrain. *Neural Dev.* **4**, 35.
Ramel, M. C., Buckles, G. R., Baker, K. D. and Lekven, A. C. (2005). WNT8 and BMP2B co-regulate non-axial mesoderm patterning during zebrafish gastrulation. *Dev. Biol.* **287**, 237-248.
Rossi, E., Siwiec, F. and Yan, C. Y. I. (2007). Pattern of Wnt ligand expression during chick eye development. *Braz. J. Med. Biol. Res.* **40**, 1333-1338.
Rowan, S., Chen, C. M., Young, T. L., Fisher, D. E. and Cepko, C. L. (2004). Transdifferentiation of the retina into pigmented cells in ocular retardation mice defines a new function of the homeodomain gene Chx10. *Development* **131**, 5139-5152.
Sasai, Y. (2013). Cytosystems dynamics in self-organization of tissue architecture. *Nature* **493**, 318-326.
Sasai, Y., Eiraku, M. and Suga, H. (2012). In vitro organogenesis in three dimensions: self-organising stem cells. *Development* **139**, 4111-4121.
Smith, A. N., Miller, L. A., Song, N., Taketo, M. M. and Lang, R. A. (2005). The duality of beta-catenin function: a requirement in lens morphogenesis and signaling suppression of lens fate in periocular ectoderm. *Dev. Biol.* **285**, 477-489.
Szeto, D. P. and Kimelman, D. (2004). Combinatorial gene regulation by Bmp and Wnt in zebrafish posterior mesoderm formation. *Development* **131**, 3751-3760.
Teraoka, M. E., Paschaki, M., Muta, Y. and Ladher, R. K. (2009). Rostral paraxial mesoderm regulates refinement of the eye field through the bone morphogenetic protein (BMP) pathway. *Dev. Biol.* **330**, 389-398.
Tsukiyama, T. and Yamaguchi, T. P. (2012). Mice lacking Wnt2b are viable and display a postnatal olfactory bulb phenotype. *Neurosci. Lett.* **512**, 48-52.
van Amerongen, R. and Berns, A. (2006). Knockout mouse models to study Wnt signal transduction. *Trends Genet.* **22**, 678-689.
Van Raay, T. J. and Vetter, M. L. (2004). Wnt/frizzled signaling during vertebrate retinal development. *Dev. Neurosci.* **26**, 352-358.
Veien, E. S., Rosenthal, J. S., Kruse-Bend, R. C., Chien, C.-B. and Dorsky, R. I. (2008). Canonical Wnt signaling is required for the maintenance of dorsal retinal identity. *Development* **135**, 4101-4111.
Westenskow, P., Piccolo, S. and Fuhrmann, S. (2009). β-catenin controls differentiation of the retinal pigment epithelium in the mouse optic cup by regulating Mitf and Otx2 expression. *Development* **136**, 2505-2510.
Westenskow, P. D., McKean, J. B., Kubo, F., Nakagawa, S. and Fuhrmann, S. (2010). Ectopic Mitf in the embryonic chick retina by co-transfection of β-catenin and Otx2. *Invest. Ophthalmol. Vis. Sci.* **51**, 5328-5335.
Wilson, S. I., Rydström, A., Trimborn, T., Willert, K., Nusse, R., Jessell, T. M. and Edlund, T. (2001). The status of Wnt signalling regulates neural and epidermal fates in the chick embryo. *Nature* **411**, 325-330.
Zakin, L. D., Mazan, S., Maury, M., Martin, N., Guénet, J.-L. and Brûlet, P. (1998). Structure and expression of Wnt13, a novel mouse Wnt2 related gene. *Mech. Dev.* **73**, 107-116.
Zechner, D., Müller, T., Wende, H., Walther, I., Taketo, M. M., Crenshaw, E. B., 3rd, Treier, M., Birchmeier, W. and Birchmeier, C. (2007). Bmp and Wnt/beta-catenin signals control expression of the transcription factor Olig3 and the specification of spinal cord neurons. *Dev. Biol.* **303**, 181-190.
Zhou, C. J., Molotkov, A., Song, L., Li, Y., Pleasure, D. E., Pleasure, S. J. and Wang, Y. Z. (2008). Ocular coloboma and dorsoventral neuroretinal patterning defects in Lrp6 mutant eyes. *Dev. Dyn.* **237**, 3681-3689.

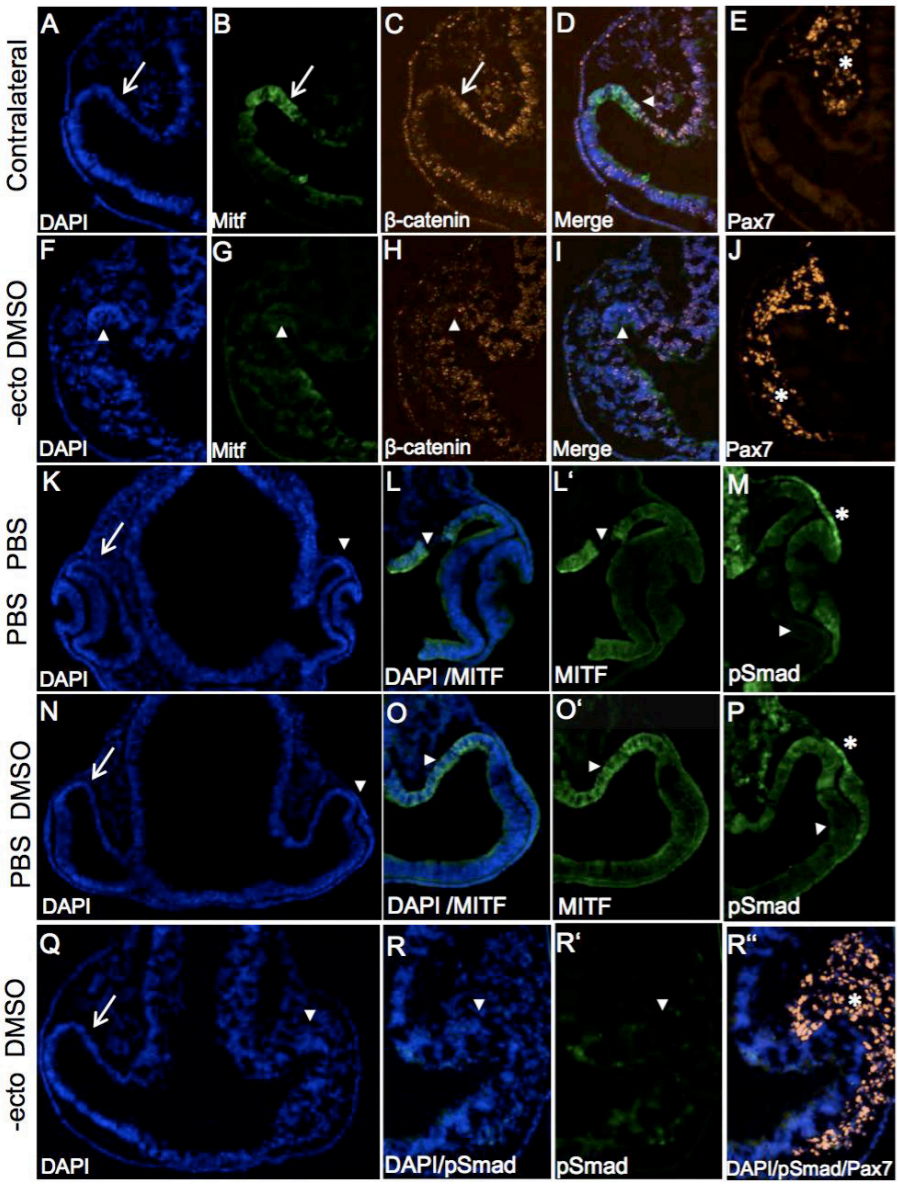

Fig. S1. Expression of proteins following implantation of PBS- and/or DMSO-soaked beads in the presence or absence of the surface ectoderm. (A-E) Contralateral ov (arrows) at stage 12/13, showing MITF (B), β-catenin (C) and Pax7 (E) expression following removal of the surface ectoderm and implantation of a DMSO-soaked bead. The overlay shown in (D) shows that at this stage nuclear staining of β-catenin starts to co-localise with a few MITF-positive cells (arrowhead). (E) In a parallel section Pax7 marks the neural crest-derived mesenchyme dorsally to the ov (asterisk). (F-J) Expression of MITF (G), β-catenin (H), and overlay (I) following surface ectoderm removal and implantation of a DMSO-soaked bead. MITF expression is lost (arrowhead in G), although in this case Pax-7 positive mesenchymal cells are surrounding the entire ov (asterisk in J). (K-P) Effects on protein expression at early optic cup stages, following implantation of two beads soaked in PBS (K-M), or one in PBS and one in DMSO (N-P). MITF expression is detected in the dorsal RPE (arrowheads in L, L′; O, O′) and pSmad1 labelling is not detected ventrally (arrowheads in M and P). Note that pSmad labelling is detected in the presumptive RPE, dorsal NR and dorsal surface ectoderm (asterisks). (Q-R") Effect on protein expression following surface ectoderm removal and implantation of two beads, one soaked in PBS and one soaked in DMSO. In the absence of the surface ectoderm, pSmad is not detected in the ov (arrowheads in R-R"), although Pax-7 positive mesenchymal cells (asterisk) are surrounding the optic vesicle.

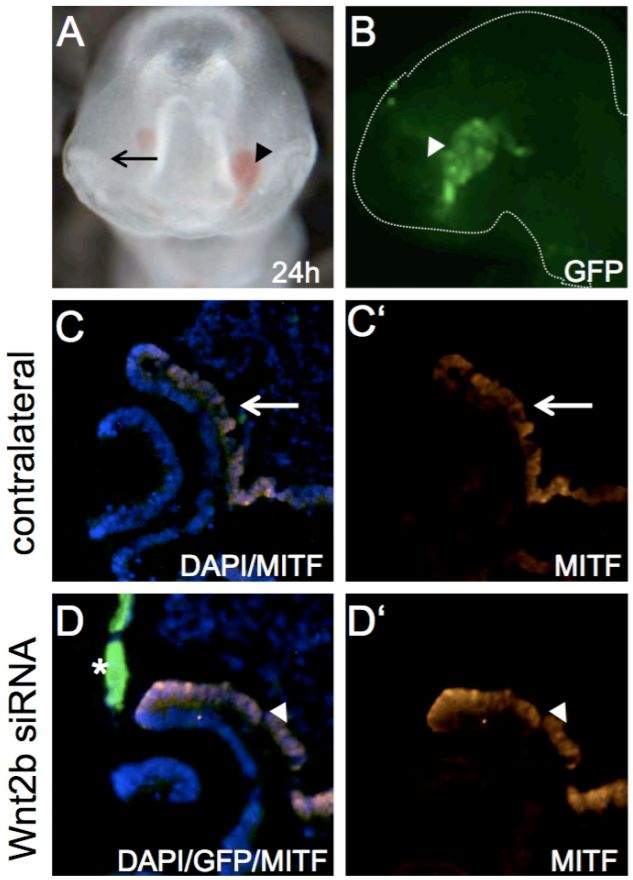

Fig. S2. Electroporation of Wnt2b siRNA does not affect MITF expression. (A) Frontal view of an embryo one day following electroporation of Wnt2b siRNA at ov stages. On the treated (arrowhead) and untreated (arrow) side an eye cup developed. (B) The electroporated ov of this embryo is GFP-positive (arrowhead). (C, C′) MITF expression in the RPE of the untreated side (arrow). (D, D′) MITF expression (arrowheads) appears to be unaffected following electroporation of Wnt2b siRNA at ov stages. The asterisk marks the GFP-positive surface ectoderm.

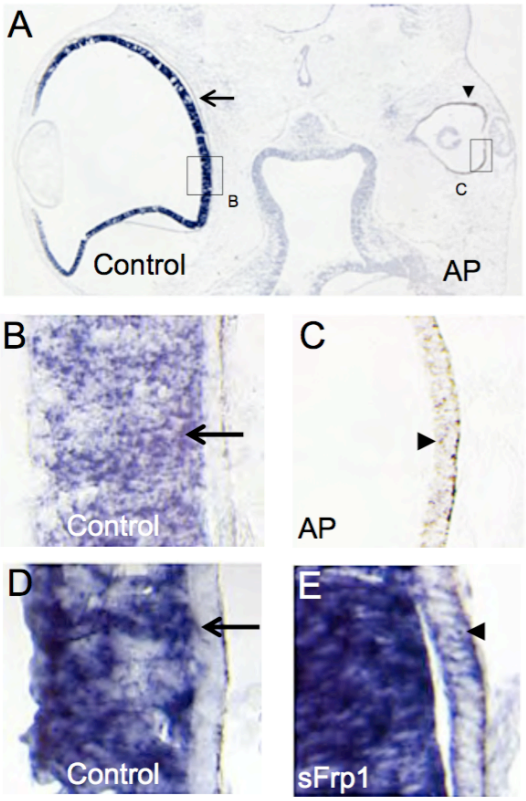

Fig. S3. Effects on *Vsx2* expression following activation and inhibition of Wnt signalling at ov stages. (A) Expression of *Vsx2*, 3 days following GSK-3β inhibition at ov stages. On the Alsterpaullone (AP)-treated side, a small microphthalmic and pigmented eye vesicle (arrowhead) develops with decreased *Vsx2* expression, when compared to the untreated side (arrow). (B) Higher magnification of the untreated eye showing *Vsx2* expression in the NR (arrow). (C) Following GSK-3β inhibition, *Vsx2* expression is dramatically downregulated and the distal ov is pigmented and has got RPE-like morphology (arrowhead). (D) *Vsx2* expression of a stage 25 chick eye. *Vsx2* expression is restricted to the NR and expression is not detected in the RPE (arrow). (E) Following implantation of beads soaked with the Wnt inhibitor sFrp1, faint *Vsx2* expression is detected in the RPE (arrowhead).